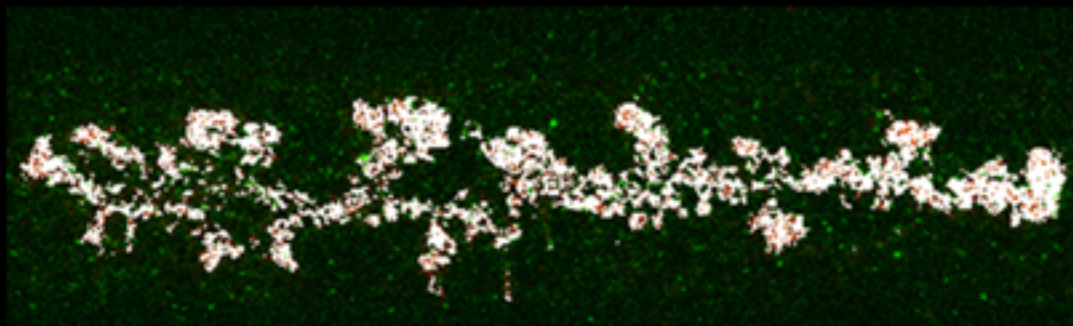


Caracterización molecular de las placas  
periaxoplásmicas en axones  
mielínicos de vertebrados.



José R. Sotelo Silveira  
Diciembre 2003

**PROGRAMA DE DESARROLLO DE CIENCIAS BASICAS  
(PEDECIBA)**

**TESIS PRESENTADA PARA ACCEDER AL DOCTORADO EN  
CIENCIAS BIOLÓGICAS**

**CARACTERIZACIÓN MOLECULAR DE LAS  
PLACAS PERIAXOPLÁSMICAS EN AXONES  
MIELÍNICOS DE VERTEBRADOS.**

Magíster José R. Sotelo Silveira

Tribunal

Dr. Francisco Morales (Presidente)

Dr. Luis Barbeito (Vocal)

Dr. Otto Pritsch (Vocal)

Orientador: Dr. Ricardo Ehrlich

Diciembre del 2003.

La opción que hemos seleccionado para presentar el presente trabajo de tesis esta basada en las comunicaciones científicas de los resultados obtenidos, agrupados de acuerdo a unidades temáticas en diferentes capítulos. Complementando una introducción general, los diferentes capítulos serán precedidos por una introducción específica para cada uno de los mismos. Los resultados serán discutidos luego en una discusión general al final del manuscrito. A su vez, al final de cada capítulo se realizará una breve discusión que abarcará los principales hallazgos de cada unidad y aspectos que no serán incluidos en la discusión general. Las mencionadas comunicaciones, que se enumeran a continuación, serán referidas en el texto por el numeral romano correspondiente (trabajos I-V)

- I. Koenig E., Martin R., Titmus M., Sotelo Silveira J.R. Cryptic peripheral ribosomal domains distributed intermittently along mammalian myelinated axons. (2000) *J. Neurosci.*, 20: 8390-8400.
- II. Sotelo Silveira, J.R., Calliari A., Kun A, Benech JC, Sanguinetti C, Chalar C, Sotelo JR. Neurofilament mRNAs are present and translated in the normal and severed sciatic nerve. (2000) *J. Neurosci. Res.* 62: 65-74.
- III. Sotelo Silveira, J.R., Koenig E.  $\beta$ -actin is localized in ribosomal domains of myelinated axons. Manuscrito.
- IV. Calliari A., Sotelo Silveira J.R., Costa M.C., Nogueira J., Cameron L.C., Kun A., Benech J., Sotelo J.R. (2002). Myosin Va is locally synthesized following nerve injury. *Cell Motyl Cytoskeleton* 51: 169-176.
- V. Sotelo Silveira J.R., Calliari A., Cardenas M., Koenig E., Sotelo J.R. Myosin Va and kinesin motor proteins are enriched in ribosomal domains (periaxoplasmic plaques) of myelinated axons. Manuscrito. aceptado para su publicación en *Journal of Neurobiology*.

## **Agradecimientos.**

**A mi esposa Maria Ana, por atreverse a caminar juntos y compartir sueños conmigo.**

**A mi padre y mi madre, por el apoyo constante y todo el amor que me han dado.**

**A mis hermanos: Mariana, Juan Manuel, Claudio Ignacio y Mercedes.**

**Al Prof. Edward Koenig, quien me orientó y apoyo durante mis estadias en su laboratorio y también a la distancia, desde Búfalo Nueva York.**

**Al Prof. Ricardo Ehrlich, por creer en esta propuesta y por todo el apoyo que me ha dado en estos años.**

**A todos los amigos entrañables del laboratorio de Biofísica del Instituto de Investigaciones Biológicas Clemente Estable.**

**A todos los amigos entrañables de la sección Bioquímica de la Facultad de Ciencias.**

**A todos los amigos entrañables de la sección Biología Celular de la Facultad de Ciencias.**

**Al tribunal, por sus comentarios, apoyo y una lectura detallada y crítica de esta tesis.**



<b>Contenidos.</b>	<b>Página</b>
Introducción.	6
El modelo “centralista” que propone al soma neuronal como única fuente de proteínas axonales.	7
Síntesis proteica en axones y terminales nerviosas.	8
Localización y transporte de ARN mensajeros en el territorio axonal.	9
Los procesos de traducción local en el crecimiento axonal, la regeneración y la plasticidad neuronal.	12
Localización de la maquinaria traduccional en axones.	14
Los axones desnudos “in toto” como modelo para la búsqueda y caracterización de dominios ribosomales.	16
Dominios corticales de ribosomas en axones de la neurona de Mauthner: las placas periaxoplasmicas.	16
Hipótesis de trabajo	19
Objetivos.	20
<b>Material y métodos</b>	<b>21</b>
Estrategias experimentales	22
Material y métodos	25
Índice de metodologías empleadas.	26
Métodos no descritos en los capítulos siguientes.	27
Generación de Expressed Séquence Tags (EST) a partir de ARN total extraído de axón de Mauthner.	27
Contribución específica en los diferentes trabajos presentados.	29
<b>Capítulo 1.</b>	
<b>Estructura de las placas periaxoplásmicas.</b>	<b>30</b>
Trabajo I: Cryptic peripheral ribosomal domains distributed intermittently along mammalian myelinated axons.	33
Comentarios sobre el trabajo I.	34
<b>Capítulo 2.</b>	
<b>Presencia de ARNm en los axones de vertebrados y las placas periaxoplásmicas.</b>	<b>37</b>
Trabajo II: Neurofilament mRNAs are present and translated in the normal and severed sciatic nerve.	40
Trabajo III: $\beta$ -actin is localized in ribosomal domains of myelinated axons. Manuscrito.	41
Generación de ESTs a partir de ARN total de axón de Mauthner.	66
Comentario sobre los trabajos II y III.	68
<b>Capítulo 3.</b>	
<b>Sistemas de transporte celular asociados a las placas periaxoplásmicas.</b>	<b>72</b>
Trabajo IV: Myosin Va is locally synthesized following nerve injury.	75
Trabajo V: Myosin Va and kinesin motor proteins are enriched in ribosomal domains (periaxoplasmic plaques) of myelinated axons. Manuscrito.	76
Comentarios sobre artículos IV y V.	106

<b>Capítulo 4.</b>	
<b>Discusión General y Perspectivas.</b>	<b>109</b>
Estructura de las PARPs	111
Localización intra-axonal y sub-axolemal de las PARPs	113
Los componentes de la maquinaria traduccional y el ARNm de la $\beta$ -actina se localizan en las PARPs.	115
Estudios sobre el repertorio de ARN mensajeros axonales.	118
Etiquetado y transporte selectivo de la maquinaria traduccional	121
Sistemas de transporte subcelular asociados a las PARPs	127
Modelo del funcionamiento de las placas ribosomales periaxoplásmicas	130
<b>Perspectivas</b>	<b>134</b>
Ultraestructura y composición de las placas periaxoplásmicas.	134
Etiquetado y transporte de ARNm y ribosomas.	135
Función de las placas periaxoplásmicas	137
Regulación de la actividad de síntesis proteica en el dominio axonal.	137
Formación de las placas periaxoplásmicas en el proceso de diferenciación neuronal.	138
Futuro de la temática estudiada.	139
Referencias Generales	141

Abreviaciones utilizadas.

DTT, dithiothreitol

EDTA, ethylenediamine-tetraacetic acid

EGTA, ethylene glycol bis( $\beta$ -aminoethyl ether) N,N,N',N'-tetraacetic acid

ESI, electrón spectroscopic imaging

EST, expressed sequence tags

H2, anticuerpo monoclonal anti Kinesina KIF5

HIS, hibridización *in situ*

IBII, anticuerpo monoclonal pan específico anti Kinesina

IHQ, inmuno-histoquímica

KIF, kinesina

mAb, anticuerpo monoclonal

MET, microscopia electrónica de transmisión

pAb, anticuerpo policlonal

PARP, peri-axoplasmic ribosomal plaque

PCR, reacción en cadena de la polimerasa

PMSF, phenylmethylsulfonyl fluoride.

RT, transcripción reversa

# **Introducción.**

La existencia de sistemas de traducción génica localizados en los axones fue propuesta hace más de 40 años (Edstrom and Sjostrand, 1969). Durante este tiempo, se ha ido generando un conjunto de evidencias creciente en apoyo de esta idea, contra la opinión que durante largo tiempo prevaleció de que el soma neuronal es la única fuente de proteínas axonales. Aún hoy esta posición es preferida por numerosos autores. La presente tesis discurre entorno de la contraposición de estos dos puntos de vista: a) el territorio axonal considerado estrictamente dependiente del soma neuronal, y b) la neurona como una célula altamente polarizada con diferentes niveles de autonomía metabólica y fisiológica.

A continuación se resumen las principales evidencias experimentales a favor de la síntesis proteica axonal.

### **El modelo “centralista” que propone al soma neuronal como única fuente de proteínas axonales.**

El modelo clásico, al que nosotros llamamos “centralista”, establece que el mantenimiento y renovación de todas las proteínas neuronales dependen de su síntesis en el soma neuronal. Diferentes estudios han demostrado que dicho modelo presenta inconsistencias que sugieren que en los diferentes territorios neuronales existen formas de renovación localizada de proteínas. Seguidamente, se resumen algunas de las objeciones que presenta el modelo “centralista”.

La principal objeción para este modelo (Alvarez & Torres, 1985), nace del postulado de que las proteínas citoesqueléticas citoplásmicas alcanzan su destino final en el axón mediante el transporte axoplásmico lento (Black & Lasek, 1980). En axones normales de mamíferos grandes, que se extienden

por distancias muy largas (por ejemplo 1 metro), viajando a pocos milímetros por día, estas proteínas tardarían 1 año para llegar a los extremos axonales distales en las terminales sinápticas. Los requerimientos de estabilidad metabólica para estos lapsos de serían irreales. En efecto, la hipótesis *ad hoc* de estabilidad sostenida durante tiempos largos de transporte (Black & Lasek, 1980), fue refutada por evidencias de degradación de las proteínas transportadas lentamente (Nixon, 1998). A su vez se ha demostrado que la vida media típica de una proteína citoesquelética, medida en tejido nervioso, se encuentra en el rango de pocos días a semanas (Hemminiki, 1973, Forgue & Dahl, 1978, Safaei & Fisher, 1990). Hoy en día, aunque se ha identificado que elementos tradicionalmente considerados transportados en el componente lento pueden moverse de forma rápida (Wang et al., 2000), éstos sólo representarían un 10% de toda la población que permanece estacionaria por largos periodos. Aunque estos recientes hallazgos podrían reforzar la base teórica del modelo del transporte lento, las inconsistencias generales motivaron la búsqueda durante décadas, de mecanismos que permitan el mantenimiento axonal de formas diferentes. Así se han propuesto alternativas para el recambio de proteínas del citoesqueleto, ya que el soma neuronal, como fuente exclusiva de proteínas axonales, no puede explicar el mantenimiento y variaciones locales de la masa axoplásmica, ni la plasticidad exhibida en sitios de ramificación y arborizaciones terminales (Alvarez & Torres, 1985, Alvarez 1992).

### **Síntesis proteica en axones y terminales nerviosas.**

Los primeros estudios llevados a cabo en axones gigantes (peces y calamar), demostraron que el axoplasma era capaz de incorporar

aminoácidos radioactivos a proteínas, mediante un mecanismo sensible a diversos inhibidores de la síntesis de proteica ribosomal eucariótica (por revisiones ver Koenig, 1984, Van Minen, 1994, Koenig & Giuditta 1999, Alvarez y cols 2000). Más adelante se realizaron observaciones similares en diferentes tipos de axones adultos, incluyendo axones de la médula del pez dorado, raíces espinales de mamíferos y axones de nervios periféricos, así como distintos axones inmaduros en cultivo (Alvarez y cols 2000).

### **Localización y transporte de ARN mensajeros en el territorio axonal.**

Las primeras comunicaciones sobre la presencia de ARN mensajeros en territorios axonales, provienen del estudio del axoplasma del axón gigante de calamar. Mediante la extrusión y posterior colección del axoplasma se caracterizó una familia heterogénea de ARNm, identificándose algunos de ellos (Perrone Capano y cols, 1987). Estos incluyeron los codificantes para la beta actina y beta tubulina (Chun y cols 1996), los neurofilamentos (Giuditta y cols 1991), enolasa neuronal (Chun y cols 1995), kinesina (Gioio y cols 1994) y una proteína de integral de membrana con cierto parecido al receptor de rianodina (Chun y cols 1997). La comparación de los niveles relativos de estos ARNm en el axón con los niveles en los somas neuronales mostraron diferencias, indicando la acción de mecanismos de transporte selectivos (Chun y cols 1996). Sumado a esto, ya existían comunicaciones previas sobre la presencia de ARN de transferencia en esos axones (Ingoglia y cols 1983) y de cofactores proteicos necesarios para la síntesis de proteínas (Giuditta y cols 1977) Recientemente, utilizando marcado metabólico de proteínas de sinaptosomas presinápticos (purificados de sinapsis axo-

axónicas) y espectrometría de masas de las proteínas separadas por electroforesis bidimensional, se identificaron 18 proteínas de un grupo de aproximadamente 80 que habían sido sintetizadas *de novo* (Jiménez y cols 2002). A su vez, estos estudios confirmaron la síntesis de proteínas citoesqueléticas, varias enzimas citoplásmicas y la proteína HSP70. Curiosamente, se encontraron también proteínas mitocondriales codificadas por el genoma nuclear, indicando que la mitocondria podría renovar sus proteínas localmente.

Consistente con los mencionados hallazgos, los análisis de transcritos o sus productos de traducción en axones de vertebrados sugieren, en la mayoría de los casos estudiados, la existencia de procesos de transporte selectivo de ARN. Aunque se ha comunicado que los ARNm codificantes para los neurofilamentos liviano y medio se encuentran en axones maduros como el de Mauthner (Weiner y cols 1996) y en los axones del tracto hipotálamo hipofisario (Mohr y cols, 1991), la mayoría de los avances se han dado utilizando axones inmaduros provenientes de explantos o neuronas disociadas en cultivo. Ha sido establecido en forma clara que las neuritas y los conos de crecimiento contienen los ARNm codificantes para la beta actina, pero la alfa tubulina y la gama actina son excluidas de los mismos (Bassell y cols 1994, Olink-Coux & Hollenbeck, 1996, Bassell y cols 1998). A su vez, cuando se aíslan polisomas a partir de axones regenerantes (*in vitro*) se constata la asociación con los mismos de ARNm codificantes para NF-L y beta actina (Bassell y cols 1994). Las primeras indicaciones, observadas por Koenig (1989), de que tanto la beta actina como la beta tubulina, pero no la alfa tubulina eran sintetizadas localmente en axones inmaduros, han sido confirmadas recientemente utilizando



inmunoprecipitación de productos de traducción en axones simpáticos en cultivos in vitro (Eng y cols 1999). En axones inmaduros, los ARNm son detectados en estructuras que forman pequeños puntos en estrecha asociación con los microtúbulos (Bassell y cols 1994, 1998) y transportados asociados a ellos (Olink-Coux & Hollenbeck, 1996). Es importante resaltar que lo que sucede en axones inmaduros en cultivo, en lo que concierne a la síntesis de proteínas, es posible que no represente totalmente lo que sucede en axones maduros. Así lo indican resultados obtenidos en los axones de Mauthner y axones de las raíces espinales ventrales de rata (Koenig, 1991) donde se observó la síntesis de alfa y beta tubulina. Esto último resalta la necesidad continuar estudios en animales adultos.

Con el fin de responder preguntas concernientes a la funcionalidad y regulación de la síntesis proteica local en axones, Zheng y cols (1999) demostraron que la localización selectiva del ARNm codificante para la beta actina, es modulada por la acción de la neurotrofina NT-3 por medio de un mecanismo dependiente del AMPc. Estos ARNm utilizan los microtúbulos como forma de transporte dentro de los conos de crecimiento axonal en cultivo.

## **Los procesos de traducción local en el crecimiento axonal, la regeneración y la plasticidad neuronal.**

En axones adultos, se ha propuesto que la síntesis local de proteínas es necesaria para contribuir con el mantenimiento y renovación de las estructuras que soportan la organización del axón (Alvarez y cols 2000). Pero en situaciones donde el axón se encuentra en activo crecimiento, la síntesis de proteínas en forma independiente del soma neuronal cumple funciones importantes en la guía del crecimiento axonal, su regeneración y la plasticidad sináptica. Observaciones realizadas por Campbell y Holt (2001), indican que axones descentralizados en cultivo, cuando la síntesis proteica es inhibida, no responden a un gradiente quimiotrófico de Netrina-1 o Sem3a pero preservan su capacidad de crecimiento. Estos fenómenos indicarían la activación de factores de traducción y estimulación de la síntesis de proteínas por parte de estas neurotrofinas. Por otro lado, en estudios realizados por Zheng y cols (2001), la aplicación de inhibidores de la traducción provoca la retracción del cono de crecimiento en axones donde previamente se había interrumpido el transporte de material entre el soma y dicha región. Este grupo de resultados ha sido extendido por el trabajo de Brittis y cols (2002), utilizando la transfección *in vitro* en médulas espinales, de genes indicadores fluorescentes fusionados al receptor de Efrina3a. Estos investigadores han logrado demostrar la regulación positiva, dependiente de la síntesis de proteínas e independiente del soma neuronal, de dicho receptor en conos de crecimiento *in vivo* luego de cruzar la línea media de la médula espinal en desarrollo. Estos resultados indicarían que el potencial de crecimiento axonal y su direccionalidad, dependerían de la síntesis axónica de ciertas proteínas,

cuyos ARNm serían traducidos cuando la neurona interacciona con señales extracelulares locales en el tejido circundante.

La regeneración de axones en el sistema nervioso periférico, es otro fenómeno donde una fuente de proteínas sintetizadas localmente puede ser de utilidad para abastecer en forma rápida el crecimiento de los axones regenerantes. Utilizando el nervio ciático como modelo se ha observado, por autoradiografía de cortes histológicos, que los axones son capaces de incorporar aminoácidos y uridina marcados radioactivamente, en una forma dependiente de inhibidores de la traducción y la transcripción (Benech y cols 1982). Entre las proteínas marcadas durante la regeneración se encontró la subunidad menor de los neurofilamentos (Sotelo y cols 1992). Estos resultados fueron ampliados al analizar en mayor detalle el patrón de expresión de las tres subunidades de los neurofilamentos durante la regeneración temprana (Sotelo Silveira, JR. 1998), confirmándose la síntesis de *novο* del triplete citoesquelético durante la regeneración. Estos resultados sugerirían que en momentos de profunda remodelación del nervio ciático y crecimiento axonal, la síntesis de neurofilamentos formaría parte de dichos procesos plásticos.

¿Cuán necesario es el aporte de la síntesis de proteínas para el crecimiento axonal durante la regeneración? Esto fue estudiado al analizar la dependencia del crecimiento de los brotes axonales luego de un aplastamiento en el nervio ciático en la presencia de inhibidores de la síntesis de proteínas (Gaete y cols 1998). En este estudio, la inhibición local de la traducción redujo hasta en un 60% la velocidad de regeneración, en forma independiente de la presencia o no de las células gliales en el extremo distal al corte. Dicho efecto era claramente local ya que la aplicación de

cicloheximida en la zona proximal al sitio de la lesión no tenía efecto sobre la capacidad regenerativa. Esto coincide con los trabajos previos donde se constataba el aumento de la síntesis de proteínas en la extremidad de los axones en regeneración (Tobías & Koenig, 1975).

Es interesante mencionar, que se ha propuesto que ciertos procesos plásticos relacionados a la memoria y aprendizaje, también requerirían de la neosíntesis de proteínas en los terminales presinápticos. Esto ha sido demostrado para cultivos neuronales primarios de *Aplysia*, donde la formación de facilitación a largo plazo es altamente dependiente de la síntesis de proteínas en la presinapsis (Martin y cols 1997, Casadio y cols 1999). Más aún, los axones de estas neuronas, separados de sus cuerpos neuronales, son capaces de crecer durante períodos de tres días y establecer sinapsis, siendo estas propiedades afectadas, de manera reversible, por la presencia de anisomicina (Schacher & Wu, 2002). Fenómenos similares han sido observados para la inducción de facilitación a largo plazo en el langostino (Beaumont y cols, 2001). Estos resultados apoyan la participación de un sistema de traducción de proteínas local en la plasticidad sináptica.

### **Localización de la maquinaria traduccional en axones.**

La búsqueda de la maquinaria traduccional mediante aproximaciones morfológicas ultraestructurales fue infructuosa durante largos períodos. Exceptuando las comunicaciones en cierta forma preliminares de Zelená (1972) y Panese & Leda (1991), que identificaban ribosomas en los segmentos proximales de axones del sistema nervioso periférico, este problema no fue resuelto hasta hace pocos años cuando se observaron por

primera vez los dominios ribosomales periaxoplásmicos (Koenig & Martín, 1996).

Como se ha mencionado antes, el axón gigante de Mauthner ha sido uno de los modelos donde se han realizado las primeras investigaciones en que se analizó el contenido de RNA mediante la micro-disección de axones fijados en paraformaldehído (Edstrom, 1969). Más tarde se demostró que el axón de Mauthner tenía ARN ribosomal intacto (Koenig, 1979). Las especies identificadas, incluían el 26 S, 18 S, y una especie en mayor cantidad correspondiente al RNA 4S. Un hecho llamativo, era que el ARN de 15 S no era visto en extractos de la mielina que recubría el axón, indicando especies únicamente presentes en el axoplasma. Utilizando otras aproximaciones experimentales, la presencia de ARNr y ribosomas, fue demostrada en el axoplasma del axón gigante de calamar (Giuditta y cols 1980) y luego fue demostrado que estaban activos (Giuditta y cols 1991).

Los primeros esfuerzos realizados para buscar estructuras ribosomales en secciones ultrafinas de axón gigante de Mauthner generadas al azar, fueron infructuosos (Koenig, 1979). Más adelante, utilizando Electrón Spectroscopic Imaging (ESI) (Martin y cols 1989) y técnicas inmunohistoquímicas (Sotelo y cols 1999, Bleher & Martín 2001) al nivel de resolución de MET se reconocieron perfiles compatibles con imágenes ribosomales, distribuidos homogéneamente en el axoplasma del axón gigante de calamar. Pero la presencia y ubicación exacta de los ribosomas en axones de vertebrados permanecía sin caracterizarse. Si los ribosomas en axones de vertebrados no se encontrasen distribuidos homogéneamente (como ocurre en calamar), sino localizados discretamente en la periferia del volumen axoplásmico, la probabilidad de encontrarlos con métodos de búsqueda

aleatoria a nivel de MET, sería muy reducida. Para solucionar este problema de muestreo, Koenig desarrolló una técnica de micro-disección para observar axones *in toto* sin su envoltura miélnica a nivel de microscopía fotónica (Koenig, 1965, 1979 y 1986).

*Los axones desnudos “in toto” como modelo para la búsqueda y caracterización de dominios ribosomales.*

Debido a su alto contenido de neurofilamentos el citoesqueleto del axoplasma del axón de Mauthner, es capaz de resistir la tracción, comportándose como un sólido-elástico, al ser extraído de su envoltura miélnica mediante el uso de pinzas de micro-disección. Es posible extraer axones de menor diámetro utilizando tratamientos desnaturalizantes leves, que transforman al axón en una estructura más sólida y resistente a la tracción generada por la disección. Los axones así extraídos, desprovistos ya de su vaina de mielina, son colocados en un cubreobjetos para su posterior procesamiento mediante diversas técnicas histoquímicas.

*Dominios corticales de ribosomas en axones de la neurona de Mauthner: las placas periaxoplásmicas.*

En la corteza axonal de axoplasmas en estado nativo, aislados como se describe en el párrafo anterior, se describieron inicialmente la presencia de dominios restringidos de ribosomas en la fibra de la célula de Mauthner del pez dorado (Koenig y Martín, 1996). Dichos dominios fueron denominados por los autores como “placas periaxoplásmicas”.

Los dominios corticales de ARN son visibles en la superficie de los axones *in toto* luego de una tinción con YOYO-1, un colorante de alta afinidad para el ARN. Las áreas teñidas están claramente delimitadas espacialmente, son sensibles a la digestión con RNAsa y están distribuidas en forma azarosa en intervalos intermitentes a lo largo de la corteza del axón (Koenig y Martín, 1996). Fueron llamadas placas periaxoplásmicas porque poseían correlatos estructurales distintivos, que son capaces de ser observados mediante microscopia de contraste de fases u óptica de Nomarski. Estas estructuras, son observadas solamente en condiciones ideales de aislamiento y en esos casos se superpone claramente con las tinciones fluorescentes para ARN. Cuando la estructura de las placas se ha alterado durante el aislamiento, se observa frecuentemente la presencia de puntos fluorescentes periféricos, llamados *puncta* por los autores. Es posible que los *puncta* sean correlatos de las imágenes obtenidas por microscopía electrónica combinada con ESI (ver más adelante), de agrupamientos de poliribosomas. Cuando los axones fueron teñidos con faloidina conjugada a rodamina, para marcar la actina F, y además YOYO-1 para evidenciar los dominios ribosomales, el análisis de microscopía confocal mostraba una íntima asociación entre estos dominios (y los “*puncta*” circundantes) y la corteza axonal rica en actina. La asociación entre ribosomas y citoesqueleto ha sido estudiada en detalle en otros tipos celulares (Hesket y Prime, 1991; Hovland y cols, 1996) e implicaría que el citoesqueleto jugaría un papel importante en la organización de estos dominios.

La localización a nivel ultra estructural de ribosomas en estos dominios fue estudiada utilizando Electrón Spectroscopic Imaging (ESI). Esta técnica se basa en la medición de la pérdida de energía de los electrones que

colisionan con el material biológico, para detectar la presencia de elementos químicos, en el presente caso los átomos de fósforo. Las imágenes obtenidas de esta manera indicarían que un dominio tipo placa periaxoplásmica estaría constituido por una matriz estructural, de características aún no determinadas, a la cual estarían asociadas las señales de fósforo correspondientes a estructuras que por su tamaño y riqueza en átomos de fósforo corresponderían a poliribosomas. Estos se asociarían a la cara interna de la matriz así como otros estarían en regiones circundantes. La matriz se correspondería con las estructuras observadas por microscopía fotónica utilizando contraste de fases o óptica de Nomarski. Por otro lado, los poli ribosomas encontrados en la periferia de la matriz y los circundantes podrían ser el correlato ultraestructural de los *puncta* fluorescentes observados por epifluorescencia.

Es importante resaltar que la distribución y agrupación de ribosomas en el axón gigante de calamar y otros invertebrados difiere de la distribución recién descrita. Los ribosomas se encuentran distribuidos aleatoriamente a lo largo del axón y frecuentemente cercanos a mitocondrias. Esto quizá refleje una estructuración diferente del axoplasma, como sucede con las diferencias de organización de la polaridad neuronal, en vertebrados e invertebrados. Esta última es mayor en vertebrados que en invertebrados.

Un aspecto todavía no resuelto es si existe o no retículo endoplásmico asociado a los ribosomas observados y por ende la capacidad de sintetizar proteínas integrales de membrana. Resultados que discutiremos más adelante, obtenidos en axones del caracol limnea (Spencer y cols, 2000) y axones en desarrollo de pollo (Brittis y cols 2002) indicarían que la síntesis de proteínas de membrana pueda realizarse en el propio axón.



### **Hipótesis de trabajo.**

Como lo hemos resumido más arriba, la existencia de actividad traduccional en axones fue propuesta hace más de 40 años. A pesar de que se ha ido generando un bloque de evidencias creciente en apoyo de la misma, siguen existiendo grupos de investigadores que aún consideran que el soma neuronal es la única fuente de proteínas axonales. Nuestra tesis se va a inscribir en este contexto.

Basándome en esta propuesta y a las evidencias presentadas en la sección precedente se propone la siguiente hipótesis de trabajo:

***Las placas periaxoplásmicas, ubicadas en la corteza axonal, serían dominios especializados en la traducción de proteínas axonales. Si esta hipótesis es correcta, en las mismas deberían encontrarse localizados los componentes de la maquinaria traduccional, incluyendo entre otros los ARNm, los ARN ribosomales y las proteínas ribosomales. Al mismo tiempo, en dicho dominio deberían encontrarse los sistemas de transporte que asegurasen el ensamblado del aparato traduccional y el transporte de las proteínas neosintetizadas a sus destinos axonales.***

## **Objetivos.**

La presente tesis tiene como objetivo general el contribuir a entender los mecanismos moleculares del crecimiento, mantenimiento y regeneración de los axones.

Los objetivos específicos son los siguientes:

1. El estudio morfológico de las placas periaxoplásmicas en axones mielínicos de vertebrados.
2. La demostración de la presencia y el estudio de la distribución de la maquinaria traduccional en relación con estos dominios.
3. El análisis de los ARN mensajeros presentes en el dominio axonal y en las placas periaxoplásmicas.
4. El análisis de la relación entre las placas periaxoplásmicas y el entorno axonal.

## **Materiales y Métodos**

## **Estrategias Experimentales.**

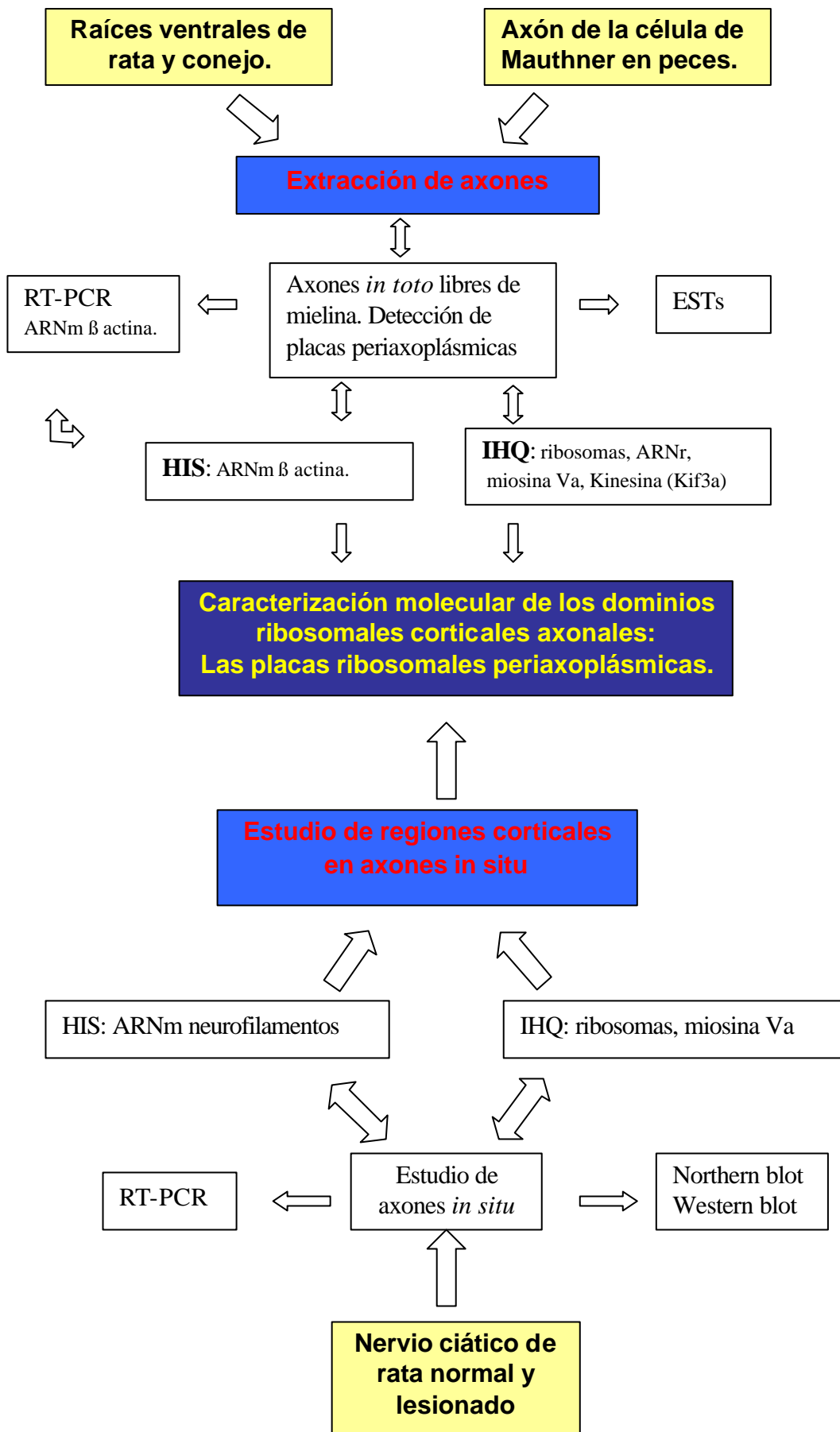
En esta sección se describirán las estrategias experimentales utilizadas para abordar los temas de estudio propuestos. Como se observa en el esquema adjunto (ver pág. 23), el estudio de los dominios ribosomales periaxoplásmicos se realizó principalmente utilizando dos aproximaciones: el estudio de las placas periaxoplásmicas en axones *in toto*, y el estudio en axones *in situ* en el nervio ciático.

La primera aproximación utiliza la preparación de axones desnudos sin vaina de mielina desarrollada por E. Koenig y utilizada en diferentes ocasiones previamente para analizar la composición de ARN (Koenig, 1965, 1979), para estudio de proteínas marcadas radioactivamente (Tobias y Koenig, 1975, Frankel y Koenig, 1978, Koenig, 1991), para estudiar el transporte axoplásmico (Koenig, 1986) y para estudios inmunohistoquímicos de la proteína spectrina (Repasky y Koenig, 1986). Representa una preparación que ha sido definida citológicamente como axoplasma carente en su mayoría de la membrana axónica y sin mielina de su célula glial circundante y fue la que se utilizó cuando por primera vez se describieron las placas periaxoplásmicas (Koenig & Martín, 1996).

Esta preparación puede obtenerse a partir de las fibras de Mauthner en el pez dorado o raíces ventrales de mamíferos como la rata o el conejo. Es especialmente útil ya que ofrece una visión global, sin obstrucciones de la mielina, del compartimiento axonal y donde se puede realizar una caracterización morfológica y molecular de las placas periaxoplásmicas mediante diferentes aproximaciones histoquímicas. En especial, la búsqueda de antígenos proteicos mediante el uso de anticuerpos específicos y la

búsqueda de ARNm específicos mediante hibridización *in situ* sobre estos “wholemounds” han sido de mucha utilidad para una primera caracterización de estos dominios ribosomales. También pueden utilizarse aproximaciones bioquímicas, como la micro-extracción de ARN para analizar, mediante métodos de alta sensibilidad como RT-PCR, la presencia de diferentes ARNm en el compartimiento axonal.

La otra aproximación utilizada para estudiar las moléculas presentes en los axones y su corteza, es el estudio de los mismos *in situ*, donde todas las interrelaciones axón-glía se encuentran conservadas. El modelo experimental seleccionado fue el nervio ciático de la rata. Mediante el estudio de la expresión de ARNm neuro-específicos (trabajo II) o de moléculas encontradas en las placas periaxoplásmicas, como la miosina V, en el nervio ciático (trabajo IV), se pretende investigar sobre la función y regulación de esta proteínas en procesos donde la síntesis de proteínas en el compartimiento axonal sea necesaria. Uno de estos procesos sería la regeneración en el sistema nervioso periférico, siendo el nervio ciático un modelo para investigar el comportamiento de estas moléculas en el tejido intacto o estimulado por lesiones que generan la secuencia de eventos de la regeneración.



## **Material y Métodos.**

Los materiales y métodos específicos para cada trabajo publicado o presentado como manuscrito en preparación, se encuentran incluidos en los mismos. Se incluye a continuación un índice para encontrarlos en los trabajos mencionados.

### **Índice de metodologías empleadas.**

I) Estudio de las placas periaxoplásmicas en Axones *in toto*.

- 1) Aislamiento de axoplasmas a partir de fibras mielínicas de raíces espinales. Capítulo 1, trabajo I, pág específica 8390.
- 2) Aislamiento de axoplasma de axón gigante de la célula de Mauthner. Capítulo 2, trabajo III, pág 29.
- 3) Tinción con YOYO-1 de los axones *in toto*. Capítulo I, trabajo I, pág. Específica 8391.
- 4) Inmuno fluorescencia:
  - Anti ARNr (Y10B): Cap. I, trabajo I, pagina 8391.
  - Anti proteínas ribosomales (anti-p), Cap. I, trabajo I, pagina 8391.
  - Anti Miosina Va y anti kinesina: Cap. III, trabajo V, págs. 49-50.
- 5) Hibridización *in situ* para detectar el ARNm de la beta actina. Cap. II, trabajo III, pag 30.
- 6) Extracción de ARN y RT-PCR a partir de extractos axonales. Cap II, trabajo III, págs. 32, 33.
- 7) Generación de ESTs y análisis de los mismos. Sección material y métodos. Página 26.

- 8) Microscopía y análisis de imagen de placas periaxoplásmicas en axones mielínicos. Cap I, trabajo I, pág. 8391.
- 9) Western blots para miosina Va y kinesinas: cap. 3, trabajo V, pag. 51.

II) Estudios de axones, *in situ*, en el nervio ciático de la rata.

1) Tratamientos quirúrgicos.

Para el análisis de la expresión del ARNm codificante para la subunidad mayor de los neurofilamentos. Cap 2, trabajo II, pag. específica 66.

Para el análisis de la expresión de la proteína miosina Va, Cap. 3, trabajo IV, pag. específica, 170.

2) Extracción de ARN a partir de nervio ciático. Cap 2, trabajo II, pag. específica 66-67. Cap. 3. trabajo IV pág. Específica 171.

3) RT-PCR

Análisis de la expresión de los ARNm codificantes para neurofilamentos: cap. 2, trabajo II, pag. específica 67.

Análisis de la expresión del ARNm codificantes para la miosina Va: cap 3, trabajo IV, pag. específica 171.

4) Inmunohistoquímica.

Detección de ribosomas: cap 2, trabajo II, pag. específica 67.

Detección de miosina Va: cap. 3, trabajo IV, pag. específica 172.

5) Electroforesis y Western blots.

Detección de neurofilamentos neo sintetizados: cap. 2, trabajo II, pág. específica 67.

Detección de miosina Va: cap 3, trabajo IV, pag. 171.



## **Métodos no descritos en los capítulos siguientes.**

### **Generación de Expressed Sequence Tags (EST) a partir de ARN total extraído de axón de Mauthner.**

Las EST fueron generadas gracias a la combinación del uso de sistemas de transcripción reversa capaces de sintetizar ADNc a partir de picogramos de ARNtotal (ver Cap II, trabajo III, pags. 32, 33.) y el uso de un protocolo de amplificación por PCR de los extremos 3' de los ARNm, llamado "Three Prime End Amplification" (TPEA) (Dixon y cols., 1998).

El método TPEA fue diseñado para amplificar ADNc mediante PCR a partir de muestras pequeñas (1 sola célula). El protocolo utilizado es el siguiente. El ARN total extraído a partir de 1 a 2 axones, fue retro transcripto utilizando 1 U de la transcriptasa reversa RiboAmp (Epicentre, CA, USA) en el buffer suministrado por el fabricante, adicionando 250 µM de cada nucleótido, en un total de 10µl. El cebador utilizado (0.5ng) consistió de un segmento poli T seguido de un "ancla" (5'CTCTCAAGGATCTTACCGC TTTTTTTTTTTTTTTTTT3'). La síntesis de la primera hebra se llevo a cabo por 60' a 37°C. La segunda hebra se sintetizó utilizando la actividad ADN polimerasa de la enzima Retroamp y adicionando 1ng de cebador con un segmento aleatorio en el centro de su secuencia y un ancla hacia el 5' del mismo (CTGCATCTATCTAATGCTCCNNNNNCGAGA) en el buffer proporcionado por el fabricante. La síntesis de la segunda hebra fue llevada a cabo por 15' a 50°C para permitir hibridización y por 10' a 72°C para la extensión del primer.

Una vez obtenido el ADNc doble cadena se realizaron 3 etapas de amplificación por PCR, utilizando como cebador un oligonucleótido idéntico al

ancla del cebador poli T (REV A) y otro cebador idéntico al extremo 5' del cebador (FOR A), utilizado para sintetizar la segunda hebra de ADNc. Para los primeros 10 ciclos se adicionan 0.4ng de cebador REV A. Las temperaturas y tiempos del ciclado fueron las siguientes: 10 ciclos a 92°C por 2.5', 60°C por 1.5', 72°C por 1'. Para los siguientes 15 ciclos se adicionó 125ng FOR A y 50ng de REV A. Para los siguientes y últimos 15 ciclos se adicionó nuevamente las cantidades de cebadores mencionadas. Los parámetros de ciclado fueron los utilizados para los 10 primeros ciclos.

Los fragmentos generados fueron clonados en vector T de acuerdo con las instrucciones del fabricante (Promega). Para la transformación se utilizaron células competentes E.coli XL1 con una eficiencia de transformación de  $10^{8-9}$  ufc/ $\mu$ g de ADN plasmídico.

Los plásmidos obtenidos fueron analizados utilizando enzimas de restricción y los que presentaron insertos mayores a 150 pares de bases fueron secuenciados mediante secuenciación automática en el servicio CTAG de la Facultad de Ciencias.

La identidad de las secuencias fue determinada mediante el uso del programa BLAST en el sitio web del National Center for Biotechnology and Information, National Institute of Health.

### **Contribución específica en los diferentes trabajos presentados.**

La realización de esta tesis implicó fecundas y numerosas asociaciones y colaboraciones. En los siguientes párrafos quisiéramos dejar constancia de nuestra participación formal en cada una de las diferentes etapas.

**TRABAJO I.** En esta comunicación se colaboró con el Dr. Koenig en el desarrollo de métodos para lograr una mejor recuperación de PARPs en axones de raíces ventrales de rata y conejo y el diseño de estrategias para identificar componentes moleculares de las mismas. Se realizó la búsqueda de anticuerpos necesarios para la identificación de ribosomas en las PARPs (anti P e Y10B) y la primera caracterización del anticuerpo Y10B anti ARNr sobre esta preparación y la del axón de Mauthner, contribuyendo en la figuras 2 y 4. Los primeros análisis morfométricos de las PARPs, fueron llevados adelante en axones de conejo mediante el análisis de imágenes mediante el uso del programa IPLAB, contribuyendo a la construcción de la tabla 1. Finalmente colaboramos en la corrección del manuscrito final.

**TRABAJO II.** Diseñamos y realizamos los experimentos que dan origen a las figuras 1, 2, 3, 4 y 7 a,b y c. Se redactó en colaboración con J.R. Sotelo el manuscrito de este trabajo.

**TRABAJO III.** Diseñamos, pusimos a punto y realizamos los experimentos que dan origen a las figuras 1, 2, 3, 4, 5. Redacción completa del manuscrito.

**TRABAJO IV.** Realización y puesta a punto de las metodologías de biología molecular utilizadas en el trabajo y experimentos que dan origen a la figura 5. Preparación del material histológico para realizar las inmunohistoquímicas presentadas en la figura 2. Colaboración en la redacción del manuscrito.

**TRABAJO V.** Puesta a punto y realización de los experimentos presentados en la figura 2, 3, 4. Colaboración en la realización de los experimentos de la figura 1, 5 y 6, con A. Calliari. Redacción del manuscrito, corrección en colaboración con A. Calliari, E. Koenig y J.R. Sotelo.

# **Capítulo 1.**

## **Estructura de las placas periaxoplásmicas.**

La caracterización inicial de las placas periaxoplasmicas en los axones de la célula de Mauthner efectuada por primera vez en 1996 (Koenig & Martín, 1996), sugirió inmediatamente los caminos posibles para avanzar en el conocimiento de esta estructura. Uno de ellos era investigar cuáles eran los componentes moleculares de las mismas, en particular determinar si los acúmulos de ARN y partículas ricas en átomos de fósforo podían corresponder realmente a ribosomas. Por otro lado, si esta estructura poseía funciones importantes en el territorio axonal, debería verificarse su presencia en otro tipo de axones, en particular en axones de mamíferos.

La preparación de axones *in toto* tenía ventajas claras para aproximarse hacia el primer objetivo, ya que incrementaba las posibilidades de observación de las zonas corticales del axón subyacentes a la membrana axónica. En cuanto a la preservación de los antígenos proteicos, los tratamientos utilizados para obtener dicha preparación podían variar. Los más sencillos implicaban disecar los axones en soluciones fisiológicas, otros involucraban la desnaturalización del axoplasma en soluciones que contenían cantidades reducidas de cloruro de zinc (en torno a 10 mM), para facilitar su posterior extracción. En las primeras el axoplasma se encontraría nativo y en la segunda estaría levemente desnaturalizado. En estas condiciones, era muy probable que las proteínas componentes de las placas periaxoplásmicas se conservaran en buena forma para estudios inmunohistoquímicos.

Los anticuerpos que fueron utilizados para investigar la presencia de ribosomas fueron dos, uno monoclonal que reacciona contra el ARN ribosomal mayor (cedido generosamente por Joan Steitz, Yale University) y otro policlonal que reacciona cruzado con tres proteínas de la subunidad

menor de los ribosomas. Ambos fueron empleados con éxito en los axones de pez dorado y de mamíferos.

En el caso de mamíferos, antes del estudio de la presencia de ribosomas en los axones, era necesario primero constatar la presencia de las placas periaxoplásmicas en estos los mismos. Trabajos realizados por el grupo de Koenig ya habían utilizado modificaciones de la metodología empleada para preparar los axones de Mauthner *in toto*, con el objetivo de analizar la incorporación de aminoácidos marcados radiactivamente a proteínas axonales. Teniendo en cuenta esa información, hemos colaborado con Koenig en desarrollar una metodología similar que logra maximizar la recuperación de las zonas corticales del axón, sus placas periaxoplásmicas y las proteínas en ellas (trabajo I). De esta forma, se realizaron estudios morfométricos, inmunohistoquímicos y de microscopía electrónica de las placas periaxoplásmicas encontradas en los axones de las raíces ventrales de rata y conejo.

**Trabajo I:** Koenig E., Martin R., Titmus M., Sotelo Silveira J.R. Cryptic peripheral ribosomal domains distributed intermittently along mammalian myelinated axons. (2000) J. Neurosci., 20: 8390-8400.

# Cryptic Peripheral Ribosomal Domains Distributed Intermittently along Mammalian Myelinated Axons

Edward Koenig,<sup>1</sup> Rainer Martin,<sup>2</sup> Margaret Titmus,<sup>1</sup> and José R. Sotelo-Silveira<sup>3</sup>

<sup>1</sup>Department of Physiology and Biophysics, University at Buffalo School of Medicine, Buffalo, New York 14214, <sup>2</sup>Universität Ulm, Sektion Elektronenmikroskopie, D-89081 Ulm, Germany, and <sup>3</sup>Biofísica, Instituto de Investigaciones Biológicas Clemente Estable, Montevideo, Uruguay

A growing body of metabolic and molecular evidence of an endogenous protein-synthesizing machinery in the mature axon is a challenge to the prevailing dogma that the latter is dependent exclusively on slow axoplasmic transport to maintain protein mass in a steady state. However, evidence for a systematic occurrence of ribosomes in mature vertebrate axons has been lacking until recently, when restricted ribosomal domains, called “periaxoplasmic plaques,” were described in goldfish CNS myelinated axons. Comparable restricted RNA/ribosomal “plaque” domains now have been identified in myelinated axons of lumbar spinal nerve roots in rabbit and rat on the basis of RNase sensitivity of YOYO-1-binding fluorescence, immunofluorescence of ribosome-specific antibodies, and ribosome phosphorus mapping by electron spectroscopic imaging (ESI). The findings were derived from examination of the axoplasm isolated

from myelinated fibers as axoplasmic whole mounts and delipidated spinal nerve roots. Ribosomal periaxoplasmic plaque domains in rabbit axons were typically narrow (~2  $\mu\text{m}$ ), elongated (~10  $\mu\text{m}$ ) sites that frequently were marked by a protruding structure. The domain complexity included an apparent ribosome-binding matrix. The small size, random distribution, and variable intermittent axial spacing of plaques around the periphery of axoplasm near the axon–myelin border are likely reasons why their systematic occurrence has remained undetected in ensheathed axons. The periodic but regular incidence of ribosomal domains provides a structural basis for previous metabolic evidence of protein synthesis in myelinated axons.

**Key words:** axoplasm; myelinated axons; ribosomes; RNA; YOYO-1; electron spectroscopic imaging; ESI; spinal nerves

The structural continuity of the extended axon depends on the steady-state maintenance of its protein mass. Goldscheider in the late nineteenth century was probably the first to postulate that the axon was maintained by “autochthonous metabolism” (see Barker, 1899). However, later in the twentieth century, axons were characterized ultrastructurally as lacking ribosomes (Palay and Palade, 1955; Peters et al., 1970). By default, axoplasmic transport (Grafstein and Foreman, 1980) appeared to afford the only means by which the axon compartment could be supplied with requisite proteins. The concept rapidly gave rise to a prevailing dogma. The principal tenets were that *all* axoplasmic proteins were synthesized in cognate cell bodies, that they were supplied to the axon via two slow transport rate groups, and that they were assumed to be metabolically stable during transport, irrespective of axon length (Lasek and Hoffman, 1976; Black and Lasek, 1980).

Prevailing views notwithstanding, some studies during this time indicated that mature axons may contain an endogenous protein-synthesizing machinery (see Giuditta, 1980; Koenig, 1984). Moreover, it also became apparent that slowly transported proteins were not metabolically stable (Nixon, 1980; Nixon and Logvinenko, 1986) and that amino acid residues released during breakdown in the axon were reused locally (Nixon, 1980). A review of the current evidence for an endogenous machinery (Koenig and Giuditta, 1999; Alvarez et al., 2000) and a critique of slow transport theory (Alvarez et al., 2000) indicate that slow transport as a sole mechanism to explain maintenance and some aspects of the biology of long axons is not tenable.

In general, there have been only occasional reports of ribosomes in mature axons (Zelená, 1972; Martin et al., 1989; Pannese and

Ledda, 1991; Sotelo et al., 1999). Recent experiments, however, performed on “axoplasmic whole mounts” isolated from myelinated fibers of goldfish CNS revealed a systematically organized distribution of *restricted* RNA-containing domains (Koenig and Martin, 1996). These restricted RNA domains were sites that often were identified in phase or DIC microscopy by a protruding structural correlate localized in the periphery of axoplasm of whole mounts and were called, therefore, “periaxoplasmic plaques.” Electron spectroscopic imaging (ESI) of rRNA phosphorus confirmed that ribosomes were present in plaque domains and further indicated that polyribosomes probably corresponded to large fluorescent “puncta” in axoplasm after RNA staining by YOYO-1. ESI also revealed that ribosomes were attached to the inner zone of a matrix, comprising the overlying structural correlate of the domain.

The present report focuses on experiments conducted on axoplasmic whole mounts isolated from mammalian myelinated fibers in lumbar spinal nerve roots. Such preparations reveal restricted ribosome-containing domains that lie near the axolemma and have a random intermittent longitudinal distribution, similar to those referred to as periaxoplasmic plaques in myelinated axons of the goldfish CNS (Koenig and Martin, 1996). These domains are likely the focal centers of local translational activity that can account for protein synthesis in Mauthner and spinal root axons (Koenig, 1991) and may well be ubiquitous to myelinated axons as a class.

## MATERIALS AND METHODS

**Isolation of axoplasmic whole mounts from myelinated spinal root fibers.** Lumbar spinal nerve roots that were used in the present study were dissected from dead rabbits or rats. The tissues were suspended in a modified gluconate-substituted calcium-free Cortland salt solution (Koenig and Martin, 1996) containing (in mM) 132 Na-gluconate, 5 KCl, 20 HEPES, 10 glucose, 3.5 MgSO<sub>4</sub>, and 2 EGTA, pH 7.2, stored at 4°C. Recovery of periaxoplasmic plaques on isolated axoplasmic whole mounts is best with fresh tissue and becomes increasingly variable and less likely from nerves stored for >1 d.

Compared with peripheral nerves, lumbar spinal nerve roots were nerves of choice in the present study because they are long, lack an epineurium, and have less interfascicular connective tissue that improves

Received May 26, 2000; revised Aug. 25, 2000; accepted Aug. 28, 2000.

This work was supported by Grant IBN-9604841 from the National Science Foundation to E.K. We thank Dr. Joan A. Steitz for her generous supply of Y-10B antibodies.

Correspondence should be addressed to Dr. Edward Koenig, Department of Physiology and Biophysics, Cary Hall 321, University at Buffalo, Buffalo, NY 14214. E-mail: ekoenig@acsu.buffalo.edu.

Copyright © 2000 Society for Neuroscience 0270-6474/00/208390-11\$15.00/0



the efficiency of isolating axoplasm from multiple fibers simultaneously. A nerve root/rootlet, 3–5 mm, was immersed in a solution of 30 mM zinc acetate, 0.1 M *N*-tris[hydroxymethyl]methylglycine (Tricine; Sigma, St. Louis, MO), and 0.1 M *N,N*-bis[hydroxyethyl]-2-aminoethane-sulfonic acid (Bes; Sigma), pH 4.8, for 10 min and then was placed in a 35 mm plastic culture dish containing 2 ml of a “pulling” solution, pH 5.5, and a “critical permissive concentration” (CPC) of aspartic acid, neutralized by arginine. The CPC usually was sharply defined for a given animal, in which the best recovery of ribosomal plaque domains varied within a limited range of concentrations of 35–45 mM, but it could be as low as 30 or as much as 50 mM aspartate. The CPC was determined by making up test “pulling” solutions. The “pulling” solution contained an appropriate arginine aspartate concentration from a stock, 50 mM Bes, and 5 mM Mg-acetate, pH 5.5. The stock solution contained 0.2 M aspartic acid (Sigma), 0.22 arginine (free base), 5 mM Na<sub>3</sub>, and 0.1% Tween 20 (Bio-Rad, Hercules, CA) to reduce surface tension, pH 5.5, and was stored at 4°C. For each test, plaque occurrence was evaluated after staining with YOYO-1 (see below); two or three sprays were isolated at each of three concentrations that were separated by increments of 5 mM with respect to aspartate.

**YOYO-1 staining of axoplasmic whole mounts.** YOYO-1 iodide (491/509; Molecular Probes, Eugene, OR) was stored in DMSO as a 1:10 stock solution at –15°C. After whole-mount sprays were attached to a coverslip, 1 μl of stock YOYO-1 was added to the pulling medium (final concentration, 1:5000) for 15 min. The YOYO-1 was washed out by brief immersion in acidified 0.15 M ammonium acetate (i.e., NH<sub>4</sub>OAc; pH-adjusted to 4.5 with acetic acid) and 0.1% Tween 20. For fluorescence microscopy the coverslip with axoplasmic sprays was mounted on a flow-thru chamber. The chamber was constructed by inverting the coverslip over spacers (0.5–1 mm thick) made of Silastic elastomer (Dow Corning, Midland, MI) attached to a large glass coverslip (35 × 50 mm) taped to a thin “U”-shaped metal plate, and the well was filled with acidified NH<sub>4</sub>OAc solution.

**Immunofluorescence staining.** Axoplasmic whole mounts attached to a coverslip were fixed by immersion in 3.75% paraformaldehyde in 0.1 M sodium diethylmalonate [0.1 M diethylmalonic acid (Aldrich, Milwaukee, WI), pH-adjusted to 7.2 with NaOH] and 0.1% Tween 20, pH 7.2, for 15 min. They were washed in 0.15 M ammonium acetate and 0.1% Tween 20, pH 6.7, three times for 5 min each and then immersed in an immunoblocking solution, composed of 25 mM Tris HCl, 0.9% NaCl, 3.75% glycine, 1% of normal goat and/or donkey serum, 0.05% Tween 20, and 5 mM Na<sub>3</sub> for 15 min. Incubation with primary antibody was for 1 hr on a rocker. Coverslips were washed three times with a working buffer (i.e., blocking buffer with 0.1% serum) and incubated for 45 min with a secondary antibody conjugated to one of two Alexa fluorophores (Molecular Probes) having an excitation maximum at either 488 or 546 nm. The immunostained specimens were washed further three times for 5 min each before being mounted over spacers of the flow-thru chamber for microscopic examination (see above).

The immunoreagents that were used were monoclonal antibody (mAb) Y-10B (a generous gift of Dr. Joan A. Steitz, Yale University, New Haven, CT) and human autoantibodies against ribosomal P antigen, purchased from ImmunoVision (Springdale, AR). Y-10B is a monoclonal antibody specific for the large ribosomal subunit RNA (Lerner et al., 1981), and human ribosomal P antigen autoantibodies react with a complex of three specific proteins associated with the large ribosomal subunit (Chu et al., 1991). Ribonuclease (RNase) digestion of axoplasmic whole mounts (see below) completely eliminated immunoreactivity of Y-10B (see below). Primary antibodies were used at 1:200 in a working buffer of the same composition.

**Ribonuclease digestion of axoplasmic whole-mount sprays.** Two sets of axoplasmic whole-mount sprays attached to coverslips, in which the presence of periaxoplasmic plaques was confirmed by YOYO-1 staining, were fixed with 3.75% paraformaldehyde and 0.1 M diethylmalonic acid, pH-adjusted to 7.2 with NaOH. One spray set was incubated with 0.4 mg of ribonuclease (RNase)/ml (Worthington Biochemical, Freehold, NJ) in 0.15 M NH<sub>4</sub>OAc and 0.1% Tween 20, pH 6.8, at 37°C for 45 min, and the second was incubated with buffer alone. Axoplasmic whole mounts then were stained again with YOYO-1 or processed for mAb Y-10B immunofluorescence to evaluate periaxoplasmic plaque occurrence.

**Microscopy.** For routine epifluorescence, DIC, or phase-contrast microscopy the specimens were examined with an Olympus BHS microscope with 25× (numerical aperture, NA, 0.60), 40× (NA, 0.70), and 100× oil immersion (NA, 1.25) objectives. Computer-assisted (Power Macintosh G3) gray scale video images were acquired with an air-cooled CCD MTI camera (model 3001-RC) mounted on the Olympus microscope, using a Scion LG-3 framegrabber (Scion, Frederick, MD) and a Dage DSP-2000 image processor (Dage-MTI, Michigan City, IN).

**Image analysis of periaxoplasmic plaques.** Fluorescent images of whole-mount sprays after staining by YOYO-1 or immunostaining by Y-10B were captured at 40× power, and single whole-mount segments of variable lengths in the plane of focus were selected for image processing and analysis. Acquired images were analyzed with IPLab (Scanalytics, Fairfax, VA) software. To analyze in-focus images of plaques in some cases, we captured the image of the same whole-mount segment in more than one focal plane. A single out-of-focus plaque image acquired in one focal plane was cut and replaced by pasting in the corresponding in-focus image from the second focal plane. Analysis of fluorescent plaques was highlighted and selected by thresholding. This also eliminated from analysis the weaker

punctate staining of mitochondria in axoplasm. The following geometrical variables were analyzed: plaque length, plaque width, plaque area, axial interplaque distance, axoplasmic whole-mount diameter, and the length of the whole-mount segment from which plaques had been selected for analysis.

**Whole-mount bundle and delipidated nerve root preparations for ESI.** Use of heavy metals is precluded for energy loss elemental mapping by ESI. Therefore, it was necessary to use either bundles of isolated axoplasmic whole mounts or lipid-extracted nerve specimens. Axoplasmic whole-mount sprays were isolated from a ventral nerve rootlet. Each spray was condensed into a compact bundle by briefly drawing the spray out of solution except for one end, resubmerging it, and attaching the condensed bundle at both ends to a coated coverslip (see above). Several whole-mount bundles attached to a coverslip in this manner were fixed by immersion in 2.5% glutaraldehyde in 0.1 M sodium diethylmalonate, pH 7.2, for 1 hr, dehydrated by an ethanol series, and embedded in Epon 812.

In the delipidation procedure a segment of ventral nerve root was fixed by immersion in 2.5% glutaraldehyde and 0.1 M Na-diethylmalonate, pH 7.2, for 3 hr. Then the nerve was removed, blotted lightly, and immersed in chloroform–methanol (2:1, v/v) for 15 min; the organic solvent mixture was replaced by absolute methanol for 10 min. The nerve was rehydrated in 0.15 M ammonium acetate, pH 6.8, dehydrated through an ethanol series, equilibrated in propylene oxide, and embedded in an Epon 812 mixture on a coverslip.

The glass coverslip was removed from the embedded specimen by immersion in 49% hydrofluoric acid in an ice bath, and the plastic wafer was washed in tap water (20 min). The whole-mount bundle or nerve specimen was cut out, and acceptable portions were divided into ~1 mm segments and mounted on individual blocks for sectioning. Ultrathin sections (10–20 nm) were cut from selected blocks. They were collected on uncoated 700-mesh grids and examined in a Zeiss CEM 902 transmission microscope equipped with an integrated electron energy spectrometer (Zeiss, Oberkochen, Germany) and an image analysis system from Kontron (Munich, Germany).

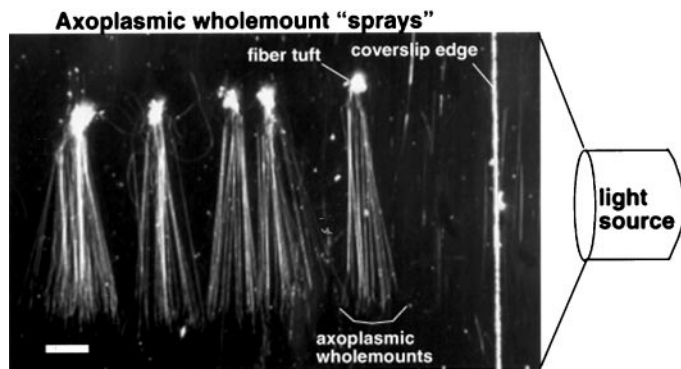
## RESULTS

Axoplasmic whole mounts were isolated from both dorsal and ventral nerve root fibers of the rabbit and rat to evaluate plaque occurrence, morphology, and distribution. Because gross morphological features and distribution of periaxoplasmic plaques appeared qualitatively similar in both dorsal and ventral nerve fibers, and in the two species, most of the findings reported below are based on the generally larger rabbit axons of ventral root fibers unless otherwise noted.

### Conditions for isolating axoplasmic whole-mount preparations with periaxoplasmic plaques

Native axoplasm behaves as a viscoelastic solid, in which the tensile strength that is required for isolation depends on axon diameter and the content of neurofilaments (Gilbert et al., 1975; E. Koenig, unpublished observations). Although periaxoplasmic plaques initially were discovered in native axoplasm of a whole mount translated from the large goldfish myelinated Mauthner fiber (Koenig and Martin, 1996), there was a significant likelihood that the cortical layer of the whole mount would be disrupted during translation. Axoplasm of smaller axons, such as those isolated from myelinated fibers of mammalian cranial (Koenig, 1965) or lumbar spinal nerve roots (Koenig, 1991), requires increased tensile strength to withstand the axial stress and frictional forces that are generated during translation. Zinc denaturation increases tensile strength, and such treatment increases the efficiency of isolation by allowing multiple axoplasmic whole mounts to be removed and then attached to a coverslip as a “spray” under low magnification (e.g., 12×; see Materials and Methods). Whole mounts can be viewed in a dark microscopic field by light scattering, using a horizontally oriented halogen light source (Fig. 1).

Although denatured axoplasm is easy to isolate by translation, conditions that favor the recovery of plaques cannot be defined precisely. In the goldfish Mauthner axon, plaque formations are associated closely with or are actual inclusions of the cortical F-actin layer (Koenig and Martin, 1996). This is a thin cytoskeletal layer subjacent to the plasma membrane that surrounds an axoplasmic core, made up mainly of axially oriented cross-bridged neurofilaments and microtubules (Hirokawa, 1991). The translation technique produces an abrupt shearing of interactions that normally cross-link the F-actin layer to the membrane and potential transmembrane elements in the intact myelinated fiber. As axo-



**Figure 1.** A dark-field view through a dissecting microscope of five axon sprays isolated from rabbit ventral nerve root fibers that were attached to a coverslip surface. A spray is defined as multiple isolated axoplasmic whole mounts originating in a nerve fiber tuft remnant that was used to grasp the spray. Scale bar, 1 mm.

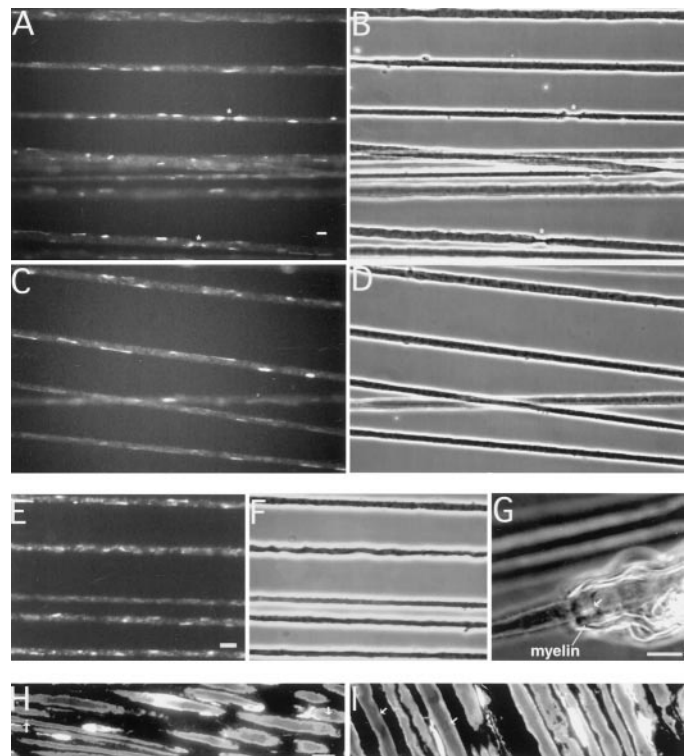
plasm slides along the lumen formed by the myelin sheath, there is further shearing by frictional forces, depending on stiffness and compression of the sheath. Although the present protocol (see Materials and Methods) promotes the recovery of plaques, the CPC, the incidence of whole mounts with plaques, the frequency of plaque occurrence on individual whole mounts, and the structural integrity of plaques that have been recovered (see below) are all affected by biological variation and the amount of time that tissue is stored at 4°C.

#### RNA and ribosomes in periaxoplasmic plaque domains located on axoplasmic whole mounts isolated from ventral root fibers

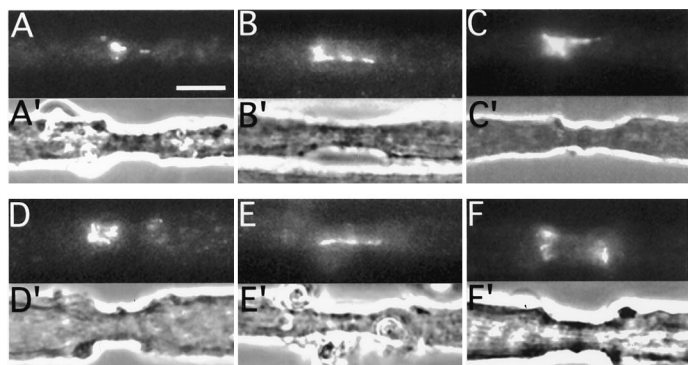
When axoplasmic whole mounts are isolated under permissive conditions (i.e., at the CPC of aspartate), periaxoplasmic plaques become visible at the surface of whole mounts after fluorescence staining with a high-affinity nucleic acid-binding dye such as YOYO-1. Typically, plaques are sharply defined, elongated fluorescent domains (Fig. 2) in which background fluorescence in axoplasm is low, except for weak punctate fluorescence because of staining of mitochondria (see Fig. 4D). Uptake of dye by mitochondria and fluorescence intensity are variable, depending on incubation time and treatments that affect mitochondrial permeability. Spatially discrete plaque domains are restricted to the surface boundary of the whole mount and are readily distinguishable from the weaker, punctate fluorescence of mitochondria dispersed throughout the volume of axoplasm (see also Koenig and Martin, 1996).

At a concentration of 5–10 mM above or below the CPC of aspartate, stained plaques may be absent entirely, or there may be only a few whole mounts with scattered plaques that appear “skeletonized,” in which only fluorescent remnants are apparent. At concentrations moderately above the CPC, whole-mount axoplasm also may exhibit an overall diffuse, nonspecific bright background fluorescence. Because sprays isolated over a range of aspartate concentrations that includes the CPC are stained at the same time by YOYO-1, the abrupt nonspecific increase in background fluorescence of sprays isolated above the CPC would appear to reflect an indeterminate change in properties of axoplasm.

Figure 2 shows typical examples of whole-mount sprays isolated from rabbit and rat ventral root fibers with plaques in acquired images. Plaques appear randomly distributed at intermittent intervals along the whole mount, and staining is eliminated by incubation with RNase (data not shown; see below). Their dimensions as well as interplaque spacing vary considerably (see below). The morphological features and distributional patterns characteristic of whole mounts isolated from myelinated ventral root fibers are also typical of whole mounts isolated from dorsal root fibers (data not shown) and similar to whole mounts isolated from ordinary myelinated fibers of the goldfish spinal cord (Koenig and Martin,



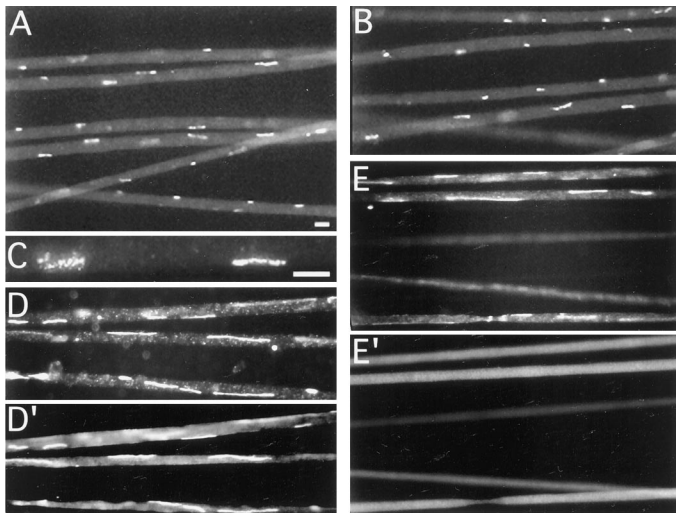
**Figure 2.** Periaxoplasmic plaques distributed along axoplasmic whole mounts isolated from rabbit and rat ventral root nerve fibers. *A, C*, Low-power micrographs of randomly selected portions of rabbit whole-mount sprays in which periaxoplasmic plaque domains are revealed by fluorescence staining with YOYO-1. Note that plaques are distributed around the surface of the whole mount and may appear indistinct because they are out of the plane of focus, either on the same whole mount or on another whole mount. *B, D*, Phase-contrast images corresponding to those shown in *A* and *C*. Nodes of Ranvier are indicated by an asterisk. *E, F*, Plaque domains associated with axoplasmic whole mounts on a portion of a spray isolated from rat ventral root fibers (note higher magnification). *G*, An isolated rat axoplasmic whole mount with a partially myelinated segment in which a plaque (arrow) that was stained fluorescently by YOYO-1 is shown near the border of the ensheathed portion (the image was acquired by simultaneous phase and epifluorescence microscopy). *H, I*, Representative examples of 0.5  $\mu\text{m}$  sections of Epon-embedded rabbit ventral root fibers stained with YOYO-1 in which putative plaques are identified (arrows). Scale bars: *A–G*, 10  $\mu\text{m}$ ; *H, I*, 15  $\mu\text{m}$ .



**Figure 3.** Examples of plaque-like YOYO-1 fluorescence in nodal/paranodal regions of axoplasmic whole mounts isolated from rabbit ventral root fibers. *A–F*, Fluorescence images show variations in RNA fluorescence patterns within nodal and paranodal regions. *A'–F'*, Corresponding phase images. Scale bar, 10  $\mu\text{m}$ .

1996). Although most periaxoplasmic plaques are located along internodes, fluorescent plaque-like domains also are seen occasionally within nodal and/or paranodal regions (Fig. 3). Occasionally, an isolated whole mount may have a segment to which myelin may still adhere. Axoplasm within the ensheathed portion usually does





**Figure 4.** Immunofluorescence staining of ribosomes in periaxoplasmic plaques by monoclonal antibody Y-10B distributed along axoplasmic whole mounts isolated from rabbit ventral root nerve fibers and RNase sensitivity. *A, B*, Randomly selected portions of rabbit whole-mount sprays in which periaxoplasmic plaque domains are revealed at low magnification by immunofluorescence staining with Y-10B, a monoclonal antibody (mAb) that binds to the large ribosome subunit RNA (Lerner et al., 1981). *C*, High-resolution images of periaxoplasmic plaques reveal the discrete, large, punctate character of immunofluorescence staining by Y-10B. *D*, A region of a spray from one spray set showing fluorescence staining of plaques by YOYO-1 ( $\lambda_{\text{max}}$ , 509 nm). Note that the weak punctate fluorescence after YOYO staining is associated with mitochondria within axoplasm. *D'*, The corresponding region imaged in *D* after fixation and immunofluorescence staining by mAb Y-10B ( $\lambda_{\text{max}}$ , 575 nm) showing a direct correspondence in plaque staining between YOYO-1 and mAb Y-10B. Out-of-focus fluorescence originates from plaques located on opposite surfaces. *E*, A region of a spray from a second spray set showing fluorescence staining of plaques by YOYO-1. *E'*, The corresponding region imaged in *E* after fixation, RNase digestion, and immunofluorescence cytochemistry showing the absence of plaque immunofluorescence staining by mAb Y-10B. YOYO-1 did not retain plaques after RNase (data not shown). Scale bars: *A–E'*, 10  $\mu\text{m}$ .

not stain during a short incubation with YOYO-1; however, a plaque domain may become stained if it is located near the border of the myelinated segment, as illustrated in Figure 2*G* (arrow). Examples such as the latter provide confirmation of the occurrence of periaxoplasmic plaques in the myelin-ensheathed state.

Finally, our experience in testing standard histological sections as an optional means for studying periaxoplasmic plaques leads us to conclude that a conventional approach offers little merit. Representative examples of 0.5  $\mu\text{m}$  sections of Epon-embedded rabbit ventral root fibers stained with YOYO-1 are shown in Figure 2, *H* and *I*, in which a few putative plaques are identified (arrows). The principal problem with this approach is the ambiguity inherent in identifying very small elongated domains, distributed randomly at the periphery of the axon (see below), in which domain exposure depends on the plane of section and usually is truncated to a variable extent. In addition, the bright fluorescence of nuclei and the RNA-rich cytoplasm of adjacent Schwann cells can obscure the comparatively weak fluorescence signal originating from a small discrete source such as a plaque domain located close to the axon–myelin interface. At present, therefore, isolation of axoplasmic whole mounts, notwithstanding the limitations of the technique from the standpoints of recovery and structural preservation, still appears to provide the best mode of studying periaxoplasmic plaques in myelinated axons.

YOYO-1 is a high-affinity dye that binds to RNA and DNA, and its nonspecific binding properties provide no information about ribosomes. Monoclonal antibody Y-10B, however, binds to the large ribosomal subunit RNA (Lerner et al., 1981) and was used to probe for the occurrence of ribosomes in periaxoplasmic plaque domains by immunofluorescence microscopy. Immunofluorescence staining yielded stereotypical plaque domains (Fig. 4). Although

the fluorescence staining at low magnification appeared diffuse, it was consistently punctate at higher optical resolution (Fig. 4*C*). Human autoantibodies against ribosomal P antigen also produced similar punctate immunofluorescence staining of plaque domains (data not shown). In the Mauthner axon the larger fluorescent puncta, which spatially define the plaque domain, correlated with polyribosomal clusters at the electron microscopic level (Koenig and Martin, 1996). Mitochondria were not stained by the mAb Y-10B.

Inasmuch as mAb Y-10B immunoreacts with the RNA of the large ribosomal subunit (Lerner et al., 1981), immunoreactivity should be sensitive to RNase. To test mAb Y-10B immunospecificity, we prepared two sets of sprays on separate coverslips and identified plaques by YOYO-1 fluorescence staining (Fig. 4*D, E*). One set of sprays was incubated with RNase, and the second one was incubated with buffer alone (see Materials and Methods). Then the two sets of sprays were processed for mAb Y-10B immunocytochemistry. The results showed that (1) immunofluorescence staining of plaques by mAb Y-10B corresponded to fluorescence staining of the same plaque domains by YOYO-1 (Fig. 4*D, D'*), and (2) immunofluorescence staining of plaques previously identified by YOYO-1 fluorescence was eliminated completely after RNase digestion (Fig. 4*E, E'*) and was not restained by YOYO-1 (data not shown). The findings indicate, therefore, that plaque domains contain RNA and that the discrete punctate immunoreactivity of mAb Y-10B is probably attributable to rRNA. The identification of ribosomes in plaque domains by mAb Y-10B and by anti-human ribosomal P antigen (data not shown) is consistent with ESI mapping of rRNA phosphorus at an electron microscopic level (see below).

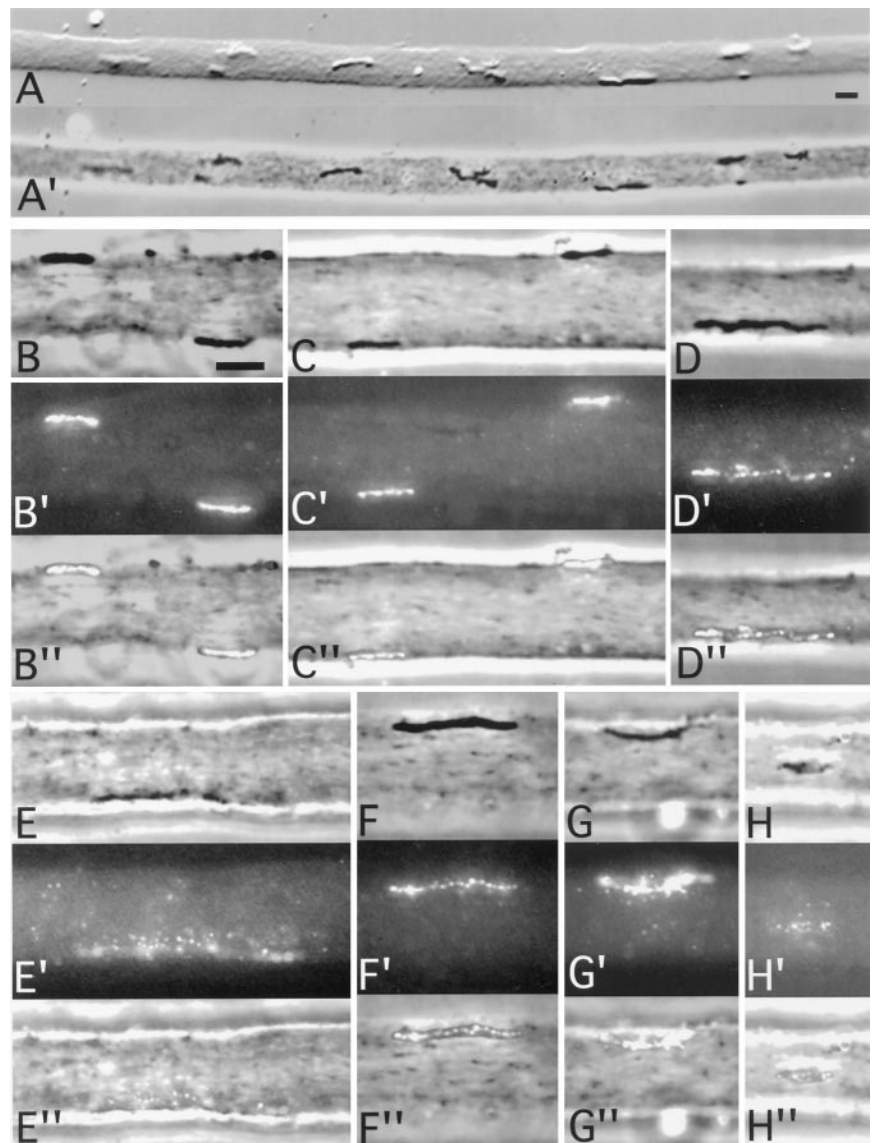
#### Phase structural correlates of periaxoplasmic plaque domains

Well preserved periaxoplasmic plaques, identified by fluorescence staining on whole mounts, frequently are marked by structural correlates protruding at the surface of the whole mount (Fig. 5*A, A1*). At low magnification the entire plaque domain, including the phase correlate, is fluorescent. As revealed by mAb Y-10B immunofluorescence at higher optical resolution, however, there is a distinction between the structural correlate and fluorescent putative polyribosomal puncta, as seen by comparing corresponding phase and fluorescence images (Fig. 5). The configuration of structural correlates generally appears to correspond to the distribution of underlying fluorescent “puncta,” but the overlying structure usually extends beyond the boundary of the puncta distribution. Structural correlates of plaque domains in the goldfish Mauthner axon are made up of a nondescript matrix to which ribosomes are attached at the inner zone (Koenig and Martin, 1996), and the possibility of matrix–ribosome interactions in mammalian plaques also is suggested by findings at the electron microscopic level (see below).

Preservation of structural correlates during isolation of axoplasmic whole mounts shows biological variability in that the latter are more resistant to disruption in some animals than in others. Thus, they may appear intact, as remnants (i.e., “skeletonized”) because of disruption, or they may be absent entirely because they were “excavated” during translation. With some exceptions, the frequency of recovery of structural correlates usually diminishes with the storage of tissue at 4°C.

#### Morphological and distributional features of periaxoplasmic plaques in whole mounts from rabbit ventral nerve root fibers

Axoplasmic whole-mount sprays were isolated from rabbit ventral nerve root fibers in which periaxoplasmic plaques were visualized by either YOYO-1 fluorescence staining or by mAb Y-10B immunofluorescence staining. The sprays were deemed to have normal plaque abundance and distribution. A limited series of in-focus images of single whole-mount segments, each ranging from 200 to 250  $\mu\text{m}$  in length, was selected from a set of acquired images of



**Figure 5.** Structural correlates of periaxoplasmic plaques and a comparison of their shapes with distributions of fluorescent putative polyribosomal puncta immunostained by mAb Y-10B. *A*, Differential interference contrast (DIC) and corresponding phase-contrast images (*A'*) of plaque structural correlates protruding at the surface of an axoplasmic whole mount. *B–H*, Phase-contrast images of overlying plaque structural correlates and corresponding mAb Y-10B immunofluorescence images (*B'–H'*) of underlying putative polyribosomal “puncta.” *B''–H''*, Phase (*B–H*) and corresponding fluorescence images (*B'–H'*) were positioned in registration, and transparencies of the superimposed images were adjusted to reveal both structural and fluorescence distributions. Most plaque domains show a close correspondence between the shape of structural correlates and underlying fluorescent puncta distributions. Scale bars: *A–H''*, 10  $\mu\text{m}$ .

whole-mount sprays, and several size and distributional variables of periaxoplasmic plaques were measured (see Materials and Methods). From 3 to 22 plaques per segment were analyzed in 42 whole-mount segments after staining with YOYO-1 and in 10 whole-mount segments after immunostaining with mAb Y10-B. Most of the whole mounts that were examined ranged between 4 and 12  $\mu\text{m}$  in diameter (Fig. 6*A*).

Table 1 contains a summary of size characteristics of periaxoplasmic plaques as determined by image analysis of the larger YOYO-1 fluorescence series and the smaller mAb Y-10B immunofluorescence series. Although there was an apparent difference in the mean plaque length between the two groups, the difference

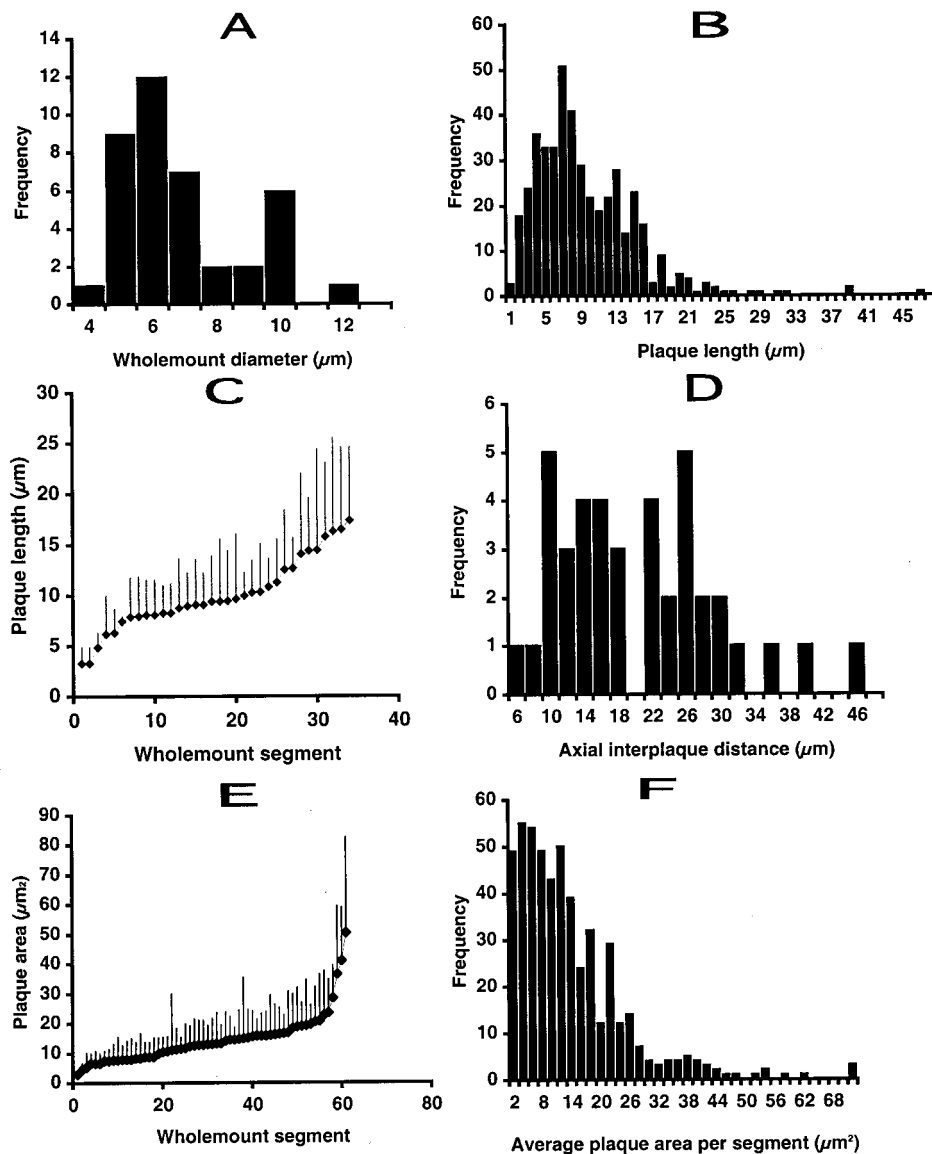
did not reach statistical significance ( $p < 0.07$ ; two-tailed Student's *t* test). The average plaque width, which is based on the average of the means of plaque widths per segment in each series, and the average plaque area for all measured plaques were quite similar between the groups.

The data sets from the YOYO-1 and mAb Y-10B series were pooled, and several parameters were evaluated graphically in Figure 6. Although plaque length averaged  $\sim 10 \mu\text{m}$  (see Table 1), the distribution of plaque lengths in the population was asymmetric (Fig. 6*B*), with lengths varying considerably within individual whole-mount segments (Fig. 6*C*). Similarly, the distribution of plaque areas was skewed also (Fig. 6*F*), and areas varied as well within whole-mount segments (Fig. 6*E*). Finally, the average axial interplaque distance per segment ( $n = 50$ ) was  $23.0 \pm 12.3 \mu\text{m}$ ; the overall distribution is shown in Figure 6*D*.

Summation of individual plaque areas per whole-mount segment yielded a mean ( $\pm$  SD) that composed  $2.4 \pm 1.4\%$  of the surface area of the segment. However, the mean total plaque area per whole-mount segment correlated neither with the nominal surface areas of whole-mount segments nor with the nominal volumes of whole-mount segments. Potential systematic differences in the size and/or distributional characteristics of periaxoplasmic plaques that were based on age or weight of the animals were not investigated. The possibility that there could be differences, as in plaque lengths—for example, can be inferred from a comparison of the spray

**Table 1.** Size characteristics of periaxoplasmic plaques in axoplasmic whole amounts isolated from rabbit ventral root fiber

Mode of staining	Overall average plaque length (mean $\pm$ SD)	Average plaque width/segment (mean $\pm$ SD)	Overall average plaque area (mean $\pm$ SD)
YOYO-1	9.9 $\pm$ 5.9 $\mu\text{m}$	2.1 $\pm$ 0.7 $\mu\text{m}$	13.1 $\pm$ 11.3 $\mu\text{m}^2$
<i>n</i>	305	39	508
Y-10B	8.5 $\pm$ 5.7 $\mu\text{m}$	2.1 $\pm$ 0.3 $\mu\text{m}$	13.0 $\pm$ 8.1 $\mu\text{m}^2$
<i>n</i>	73	10	73



**Figure 6.** Analysis of axoplasmic whole mounts isolated from rabbit ventral root fibers and selected geometric variables related to periaxoplasmic plaque domains. The data in *A*, *B*, *D*, and *F* are binned values from pooled measurements of specimens stained with YOYO-1 and Y-10B (see Results). *A*, A frequency distribution histogram of diameters of whole mounts used in the two series for analysis. *B*, A frequency histogram distribution showing the range of periaxoplasmic plaque lengths encountered in the combined series. *C*, A scatter plot of mean  $\pm$  SD plaque length per segment, ranked in order of increasing length. *D*, A frequency histogram of axial distances between periaxoplasmic plaques. *E*, A scatter plot of mean plaque area  $\pm$  SD per whole-mount segment, ranked in order of increasing area. *F*, A frequency distribution histogram showing the range of plaque areas per whole-mount segment.

regions shown in Figure 4, *A* and *B*, from a young 2 kg rabbit with those shown in Figure 4, *D* and *E*, from an older 5 kg rabbit.

#### ESI examination of periaxoplasmic plaque domains in axoplasmic whole mounts

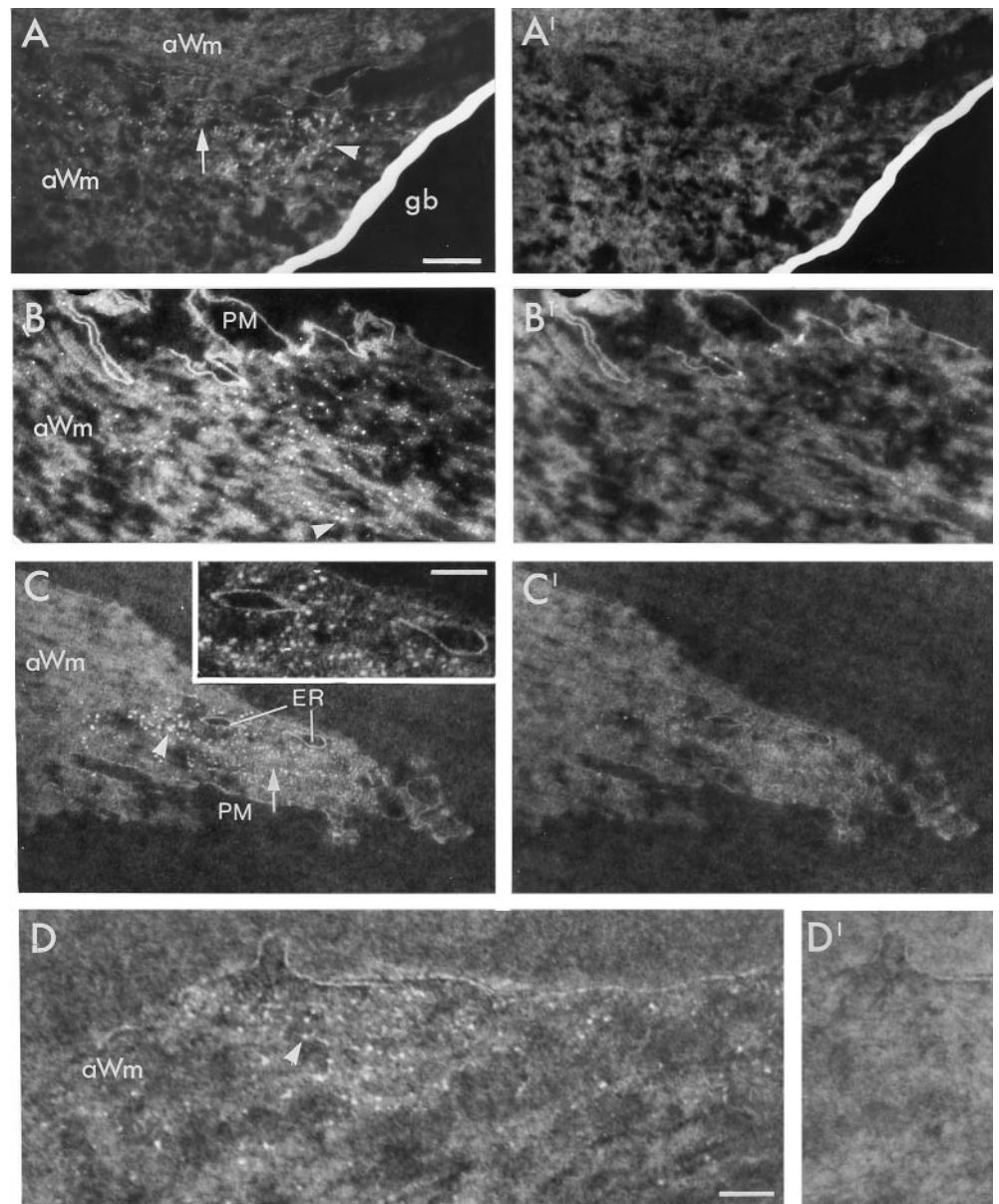
Generally, electron density, enhanced by heavy metal staining, and size provide the criteria for identifying ribosomes by conventional transmission electron microscopy (CTEM). When there is a search for ribosomes in cross-sectional profiles of axoplasm, however, the density of axially oriented cytoskeletal elements can give rise to structural ambiguities that contribute to uncertainty in identifying ribosomes (our unpublished observations). On the other hand, the high phosphorus content of nucleic acids lends itself to the use of ESI, a physical method in which the mapping of ribosomal phosphorus (P) signals is based on energy loss spectroscopy (Korn et al., 1983; Ottensmeyer, 1986). ESI requires an electron microscope equipped with an energy spectrometer and appropriate energy filters. When an ultrathin section ( $<25$  nm) is imaged in an energy window above the P absorption edge (e.g.,  $\Delta E = 155$  eV), electrons inelastically scattered from ribosomal P produce a bright signal of  $\sim 25$  nm in diameter (Martin et al., 1993) in a low-contrast microscopic field. Bright phosphorus-specific signals fade when the energy window that has been selected is below the P absorption edge (e.g.,  $\Delta E = 110$  eV). ESI images of the rough endoplasmic reticulum (ER) of a cell above and below the phosphorus absorption

edge may be found elsewhere (e.g., see Fig. 3; Koenig and Giuditta, 1999).

Because osmium fixation is required to stabilize myelin but is precluded for ESI examination, the available options are to use either bundles of axoplasmic whole mounts or delipidated nerve fibers (see Materials and Methods). Each of these approaches was tried for ESI on specimens prepared from rabbit ventral nerve roots. Ultrathin sections of Epon-embedded whole-mount bundles were prepared (see Materials and Methods) for examination by ESI. Figure 7 is a gallery containing examples of plaque domains, in which images were mapped above and below the phosphorus absorption edge. The whole-mount specimen images were brighter than normal both in energy loss windows above (e.g.,  $\Delta E = 155$  eV; Fig. 7*A–D*) and below the P edge ( $\Delta E = 110$  eV; Fig. 7*A'–D'*) because of nonspecific electron scattering. This may have been caused by an increased compaction of axoplasmic mass during the preparative procedure (see Materials and Methods). Nonetheless, specific ribosome-like P signals (*arrowheads*) are visible above the nonspecific background brightness and fade in the energy window below the P absorption edge.

In longitudinal sections the plaque domains are localized in a peripheral zone of axoplasm near the surface boundary (i.e., membrane; Fig. 7*A–D*). In addition to P signals typical of ribosomes (*arrowheads*), there are clusters of smaller P signals (*arrow*) that are





**Figure 7.** A gallery of selected ESI images of plaque domains in the peripheral zone of axoplasmic whole mounts isolated from rabbit ventral root fibers. *A* contains two axoplasmic whole mounts; there is a plaque domain only in the lower whole mount. All other panels have a single whole mount exhibiting a plaque domain. *A–D*, Photomicrographs of plaque domains that were mapped in energy windows above the phosphorus absorption edge (e.g.,  $\Delta E = 155$  eV). *A'–D'*, Corresponding plaque domains mapped below the phosphorus absorption edge (e.g.,  $\Delta E = 110$  eV). Nonspecific electron scattering of embedded whole mounts generally increased the brightness of axoplasm in the two energy windows (see Results); nonetheless, bright P-specific signals visible in the 155 eV energy window faded in the 110 eV energy window. In addition to ribosomal P signals (arrowheads) in plaque domains, there are also distributions of smaller, nonribosomal P signals (arrows), especially evident in *A* and *C*. Profiles of ER cisterns in *C*, with which ribosomal P signals appear to be in close contact (inset), are also visible. The significance of the protuberance in *D* is unknown. *aWm*, Axoplasmic whole mount; *gb*, grid bar; *ER*, endoplasmic reticulum; *PM*, plasma membrane. Scale bars: *A–C'*, 0.30  $\mu\text{m}$ ; *C*, inset, 0.14  $\mu\text{m}$ ; *D*, *D'*, 0.20  $\mu\text{m}$ .

present in some instances (Fig. 7*A,C*), which also fade in the energy window below the P absorption edge (Fig. 7*A',C'*). The smaller P signals could comprise partial ribosomes because the section thickness is less than that of a single ribosome; however, a cluster or delimited distribution of P signals of uniform size is more likely to represent a subpopulation of ribonucleoprotein particles (RNPs), which may include mRNAs (Martin et al., 1998) (also see below).

The plaque domain shown in the ultrathin section of Figure 7*C* contains two intact membranous inclusions to which ribosome-like P signals appear to be attached (see Fig. 7*C*, inset). Such membrane profiles in the plaque domain suggest that they may represent ribosome-bound cisterns of an ER.

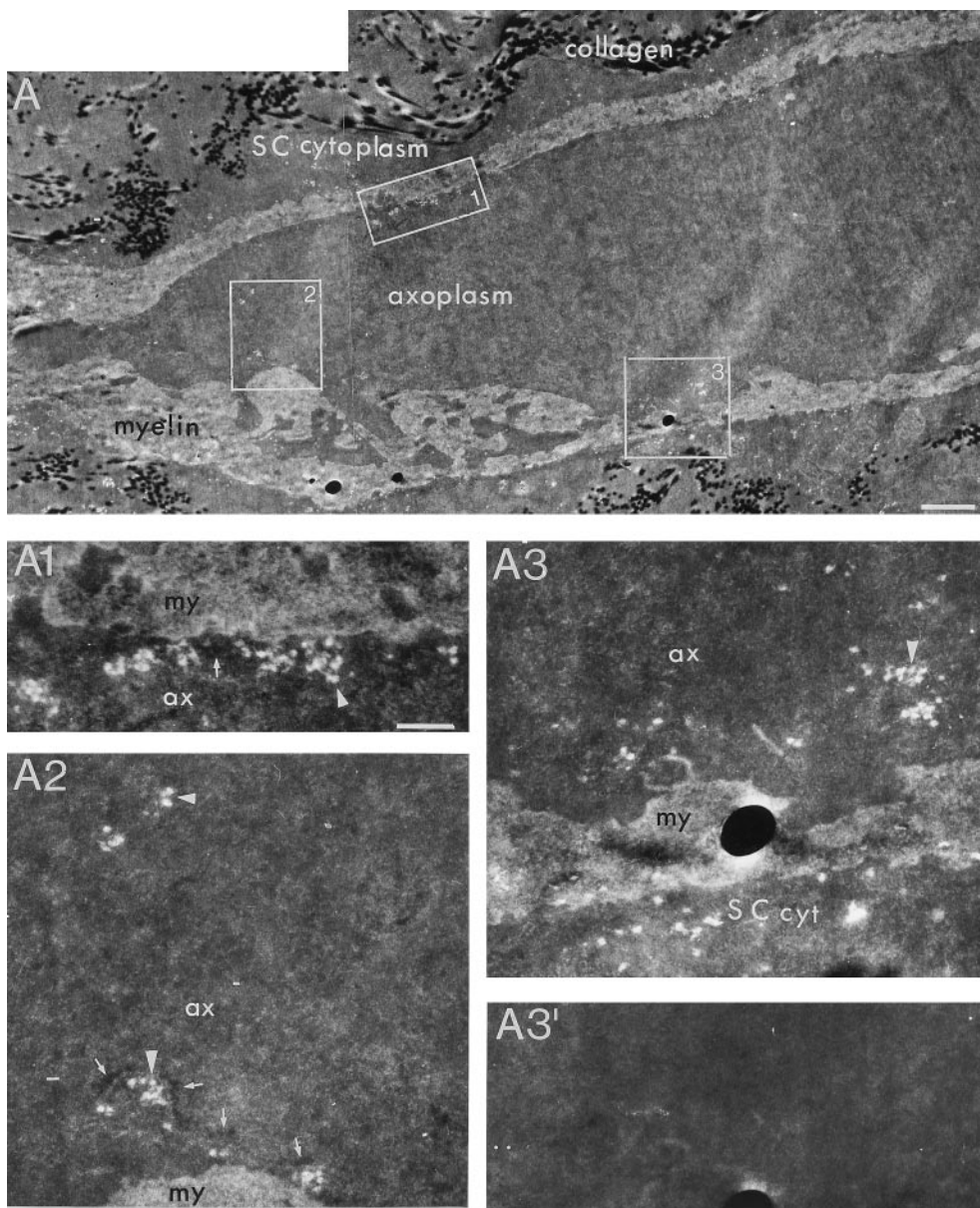
Structures that mark the plaque domain sites noted in phase microscopy (see above) were not encountered in whole-mount specimens during ESI examination of ultrathin sections. This may have been attributable to loss by disruption during preparation of the whole mounts or may have been inherent in the adventitious nature of the sampling process (however, see below).

#### ESI examination of delipidated myelinated ventral root fibers

Another option tested for ESI examination was to extract nerve lipids to obviate the need for osmium fixation that ordinarily is used

to stabilize myelin lipids. Several organic solvents and/or procedural options that were tested proved to be unsatisfactory because of poor image contrast and quality. One procedure that offered some measure of success was the insertion of chloroform–methanol extraction and methanol washout steps after glutaraldehyde fixation, followed by rehydration before standard processing for embedding (see Materials and Methods).

Figure 8 is a low-magnification montage of a myelinated ventral root fiber shown in longitudinal profile after the delipidation procedure. Membranous components, including the axolemma, mitochondrial, and ER membranes, were not evident, and vacant spaces interspersed within the remnants of the myelin sheath made the latter appear “Swiss cheese-like.” In Figure 8, the longitudinal plane of section was off axis and was so angled as to pass from the axon interior to the surface of the latter. Clusters of ribosomal P signals appear in three framed locations at the periphery of axoplasm, which are shown at higher magnification (Fig. 8*A1–A3*, arrowheads). The P signals in the 155 eV energy window, which fade in the 110 eV energy window (Fig. 8*A3'*), are typically ribosomal in size and appearance. Also noteworthy are high-contrast linear structures near ribosome distributions at some locations (Fig. 8*A1,A2*, arrows). Such structures near ribosomes are



**Figure 8.** Ribosome distributions in a myelinated ventral nerve root fiber shown in longitudinal profile after the delipidation procedure (see Materials and Methods). Vacant spaces in the myelin sheath render it “Swiss cheese-like” in appearance. *A*, A low-magnification montage of ESI micrographs mapped in the P energy window (e.g.,  $\Delta E = 155$  eV), in which three areas with ribosome distributions are framed and identified by numbers. The plane of section was so angled as to pass from the interior of the axon (right) to the surface of the axon (left). Thus, framed area 2 is near the lateral surface of the axon. Each of the framed areas (1–3) containing ribosomes is magnified in corresponding panels (A1–A3). Note that ribosomes (arrowheads) are distributed at the periphery (i.e., near axon surface). In addition, high-contrast linear structures (arrows) in A1 and A2 are located near ribosome distributions and are reminiscent of a matrix (see Results). A3', A portion of framed area 3 shows that P signals in A3 fade when they are mapped in an energy window below the P absorption edge (e.g.,  $\Delta E = 110$  eV). SC, Schwann cell; ax, axoplasm; cyt, cytoplasm; my, myelin. Scale bars: *A*, 0.74  $\mu\text{m}$ ; A1–A3', 0.14  $\mu\text{m}$ .

reminiscent of a matrix described in Mauthner axoplasmic whole mounts (Koenig and Martin, 1996). More direct evidence of ribosome-binding properties of matrix in a plaque domain is presented below.

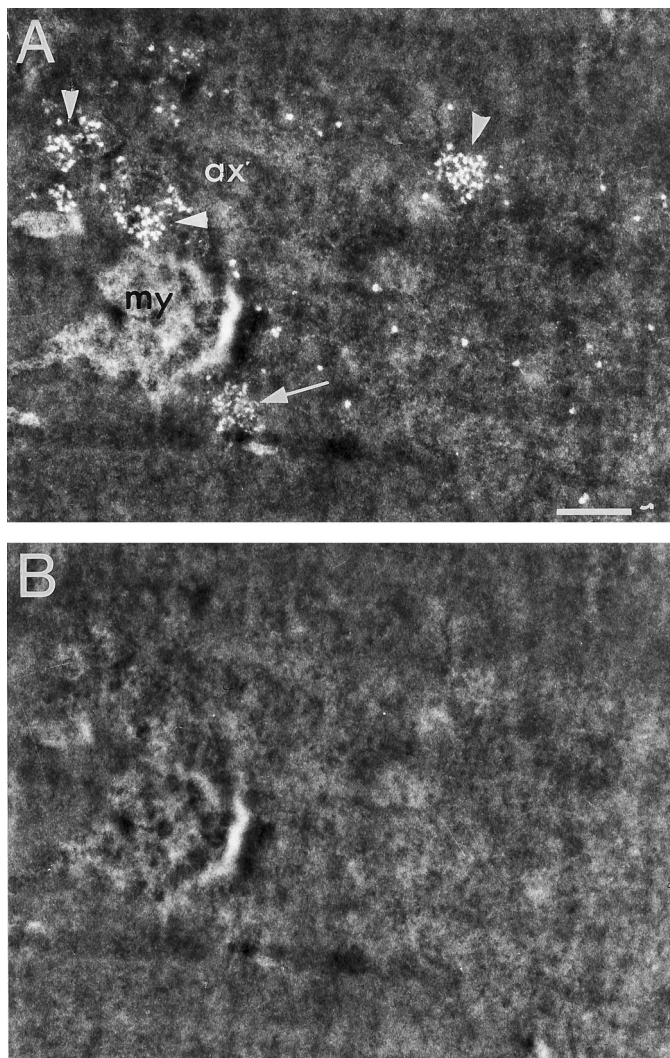
Portions of two ultrathin sections, cut tangential to the surface of a putative plaque domain in one block of a delipidated nerve fiber, provide additional examples of a nonribosomal RNP P signal distribution and of a ribosome-binding matrix. The inner plane of the plaque domain is shown in Figure 9. In addition to three large clusters of ribosomes in the phosphorus energy window (arrowheads) and some scattered single ribosomes, there is a cluster of smaller nonribosomal P signals (arrow) similar to those noted above in axoplasmic whole mounts (see Fig. 7). Such delimited distributions suggest that the plaque domain may contain one or more subdomains in which putative RNP particles may be enriched.

Figure 10 shows a portion of the outer plane of the same plaque domain in which a ribosome-binding matrix was identified also. As noted previously, a protruding structure marking the domain site was not encountered in rabbit whole mounts sampled by ESI (see above). Nonetheless, a ribosome-binding matrix became readily discernible in the plaque domain of the delipidated fiber when it

was examined in an energy window above the carbon absorption edge (e.g.,  $\Delta E = 300$  eV; Fig. 10B). In this energy window the contrast of the matrix was enhanced greatly because of its much lower electron-scattering properties in comparison to those of the surrounding plastic-embedding material. The clustered and scattered single P signals (Fig. 10A) appearing in an energy window above the P absorption edge ( $\Delta E = 155$  eV; Fig. 10A) were typical of ribosomes, and they also faded below the P absorption edge (data not shown). Unlike the matrix, however, ribosomes are not identified uniquely in the carbon energy window, presumably because inelastic electron scattering is not different from that of Epon.

From an inspection of ESI images in the two energy windows, the distributions of ribosomes and matrix were similar. To evaluate a potential overlap of the two, we digitized, inverted, and pseudocolored the relevant region of the 155 eV micrograph as green; we digitized and pseudocolored the corresponding portion of the 300 eV micrograph as red. The two pseudocolored images were positioned in register, using fiduciary micrograph markings against a black background. The yellow/orange pixels (Fig. 10C) of most ribosomes, including many scattered ones, indicate common areas of overlap with matrix. It seems likely, therefore, that ribosomes and matrix do form a distinctive structural complex.





**Figure 9.** The inner plane of a putative plaque domain in a grazing ultrathin surface section of a delipidated ventral root nerve fiber. *A*, An ESI micrograph mapped in the P energy window (e.g.,  $\Delta E = 155$  eV) shows distributions of ribosome P signals (arrowheads) and a cluster of smaller, nonribosomal P signals (arrow). *B*, An ESI micrograph corresponding to *A*, mapped in an energy window below the P absorption edge (e.g.,  $\Delta E = 110$  eV), shows that the P signals fade. *ax*, Axoplasm; *my*, myelin. Scale bar, 0.26  $\mu\text{m}$ .

## DISCUSSION

The complexity in the biology of the axon has long been underestimated as a result of prevailing views about the apparent lack of an endogenous protein-synthesizing machinery, despite biochemical and molecular biological evidence to the contrary (Koenig and Giuditta, 1999; Alvarez et al., 2000). The view was predicated by the inability to verify the systematic occurrence of ribosomes with conventional electron microscopic techniques. It was not until very recently that earlier reports of rRNA in the Mauthner axon (Koenig, 1979) and in the squid giant axon (Giuditta et al., 1980) could be confirmed by documenting the *systematic* occurrence of ribosomes in these model axons at an ultrastructural level (Koenig and Martin, 1996; R. Martin and R. Bleher, unpublished observations). The present report extends the findings to mammalian myelinated axons.

Immunofluorescence that is based on rRNA-specific mAb Y-10B (Lerner et al., 1981) and ribosomal P antigen (Chu et al., 1991) antibodies and energy loss spectroscopic (ESI) mapping of ribosome phosphorus signals (Martin et al., 1989) provide the principal line of evidence for identifying ribosomes in spinal root axons at the light and electron microscopic levels, respectively. Unlike most

cells in which ribosomes usually are distributed within the bulk volume of cytoplasm, ribosomes in axons of myelinated fibers in rabbit and rat spinal nerve roots and in the goldfish CNS (Koenig and Martin, 1996) are localized in restricted domains, distributed intermittently around the periphery of axoplasm. These restricted ribosomal domains are called periaxoplasmic plaques because of their peripheral location and an overlying structure that marks the domain sites. The structural component appears to be a matrix to which the ribosomes are attached (Koenig and Martin, 1996).

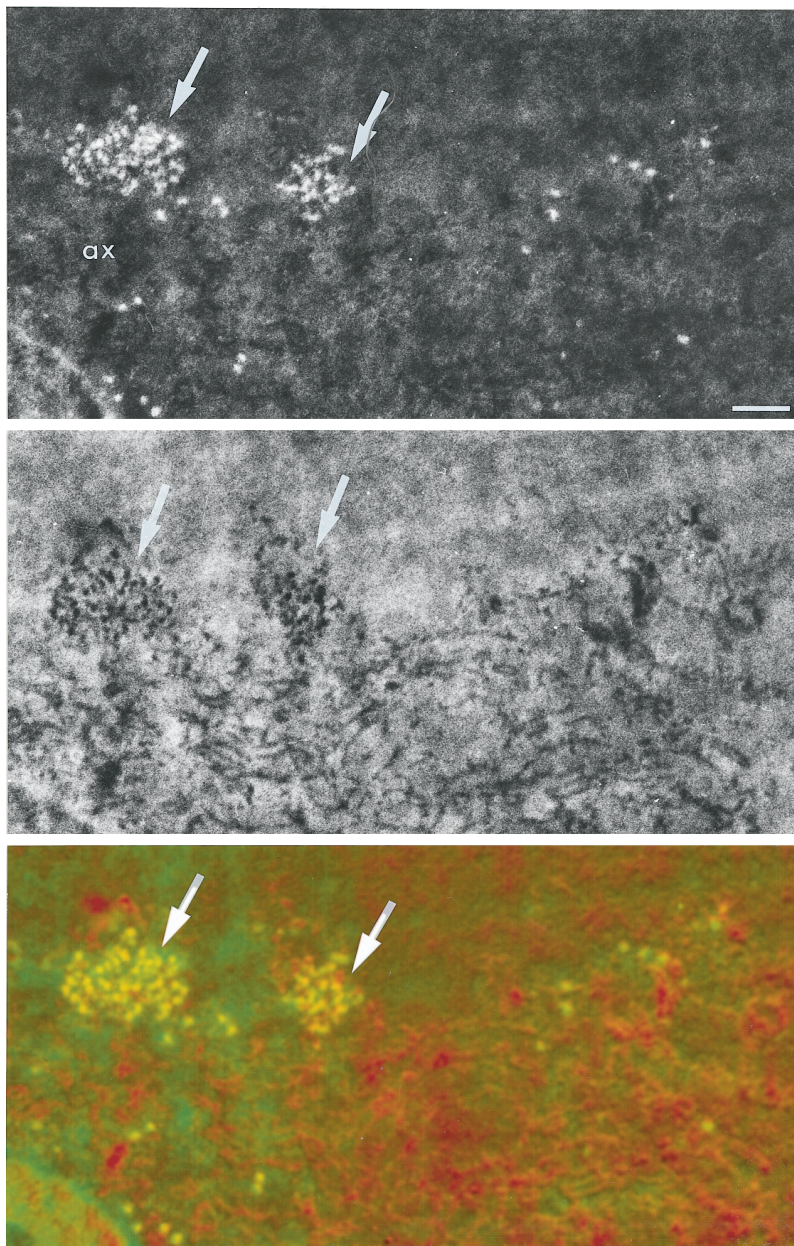
In the younger adult rabbit an average ribosomal plaque domain is  $\sim 10$   $\mu\text{m}$  long and  $\sim 2$   $\mu\text{m}$  wide (see Table 1); it appears from inspection to be shorter in the smaller-diameter rat axons (see Fig. 2) and perhaps longer in older rabbits (see Fig. 4). The dispersed random distribution of structures of such small dimensions near the membrane offers a challenge for detection by random sampling and sectioning techniques that are used in conventional light and electron microscopy. It is not surprising, therefore, that the systematic distribution of periaxoplasmic ribosomal domains remained undetected in ensheathed axons.

The principal findings at a light microscope level and partly at an EM level are based on the use of the axoplasmic whole-mount preparation, in which axoplasm is translated out of its myelin ensheathment for experimental observation and analysis. This preparation was used previously to analyze RNA composition (Koenig, 1965, 1979), metabolic radiolabeling of proteins (Tobias and Koenig, 1975; Frankel and Koenig, 1978; Koenig, 1991), particle transport (Koenig, 1986), and spectrin immunocytochemistry (Koenig and Repasky, 1985) of cytologically defined axoplasm. It offers an unobstructed global overview of the extended axonal compartment in which morphological and distributional features of periaxoplasmic plaques along axons can be visualized readily after appropriate staining (see Figs. 2–5). When conventional histological techniques were tested, the approach was judged to lack merit for studying plaque domains for several reasons, included among which were a low incidence of occurrence associated with the random sampling technique and the ambiguity inherent in identifying partially exposed domains with low-fluorescence intensity.

The technique of isolating axoplasm as a whole mount does have limitations, however, because the periaxoplasmic location of plaque domains makes the latter vulnerable to disruptive shear forces during translation out of the myelin sheath (see Materials and Methods, Results). Subtle variations in mechanical properties (e.g., plasticity, stiffness, compliance) of denatured axoplasm and the myelin sheath very likely play a role in the variability related to the CPC, efficacy in recovering plaques, and structural integrity of plaque domains.

Although it remains to be demonstrated that proteins are synthesized in periaxoplasmic plaque domains, their systematic occurrence provides a ready explanation for the radiolabeling of axoplasmic proteins in mature myelinated axons sensitive to inhibitors of cytoribosomal-dependent protein synthesis (Edström, 1966; Koenig, 1967, 1991; Edström and Sjöstrand, 1969; Tobias and Koenig, 1975; Frankel and Koenig, 1978). Some of the radiolabeled polypeptides appear to be proteins identified as constituents of slow transport rate groups and include actin and tubulin in rat spinal root axons, as well as neurofilament (NF) proteins in the case of the Mauthner axon (Koenig, 1991). Such findings are also consistent with reports of mRNAs coding for NF-L in rat neurohypophyseal axons (Mohr and Richter, 1992) and NF-M in Mauthner axon (Weiner et al., 1996) as well as  $\beta$ -actin,  $\beta$ -tubulin (Kaplan et al., 1992), kinesin heavy chain (Gioio et al., 1994), enolase (Chun et al., 1995), and a calcium channel protein (Chun et al., 1997) in squid axoplasm. *In situ* hybridization (ISH) of  $\beta$ -actin mRNA in plaque domains of Mauthner axoplasmic whole mounts (J. Sotelo-Silveira, M. Crispino, and E. Koenig, unpublished observations) provides additional support for the idea that periaxoplasmic plaques are likely to be discrete centers of local translational activity in the myelinated axon. Inasmuch as they are in close proximity to the plasma membrane, there is also a potential for local regulation of protein synthesis in axons by membrane-signaling pathways.





**Figure 10.** A portion of an outer plane of the same plaque domain shown in Figure 9, in which a ribosome-binding matrix is evident. *A*, An ESI micrograph mapped in the P energy window (e.g.,  $\Delta E = 155$  eV) shows two large ribosomal clusters (arrows) in addition to scattered single ribosomes. *B*, An ESI micrograph corresponding to the same area in *A*, mapped in an energy window above the carbon absorption edge (e.g.,  $\Delta E = 300$  eV). Note that the brightness of the background, because of electron scattering of the embedding plastic, enhances the contrast of the two large clusters of matrix (arrows). *C*, Digitized images of the 155 eV ESI ribosome map, shown in *A*, were inverted and pseudocolored green, and the 300 eV ESI matrix map, shown in *B*, was pseudocolored red and positioned in register (see Results for details). The yellow/orange pixels correspond to areas of common overlap and indicate that ribosomes and matrix may represent components of a distinctive structural complex. ax, Axoplasm. Scale bar, 0.15  $\mu\text{m}$ .

If proteins are synthesized in plaque domains to satisfy requirements for local turnover of axoplasmic proteins, then the question arises as to whether the ribosome content of an axon segment is related in any way to the protein mass of that segment. Total area occupied by plaques in a whole-mount segment did not correlate with the surface area nor with the volume of the cognate segment. This may be explained in part by inconsistent recovery of intact plaques in the whole mounts that were selected for analysis or by errors inherent in the measurements themselves. It is more likely, however, that plaque area is not a valid indicator of ribosome content in a domain because ribosomes are not distributed in a two-dimensional plane. Thus, immunofluorescence intensity of Y-10B per whole-mount segment may offer a better indirect quantitative measure with which to probe the relationship between ribosome content and axoplasmic volume/mass.

In a CTEM study of fibers in dorsal nerve root of the rat, Pannese and Ledda (1991) documented an example of ribosomes attached to the surface of tubular ER in peripheral axoplasm of sensory root axons. In one plaque domain (see Fig. 7C) ribosomal P signals were also in close contact with putative ER cisterns. Currently, there is no evidence that ER-dependent translation or

post-translational glycosylation, which has been documented in dendrites (Torre and Steward, 1996), occurs in the axon compartment. However, the calcium channel protein mRNA identified in the squid giant axon (Chun et al., 1997) is an example of at least one RNA transcript coding for an integral membrane protein in the giant squid axon. In addition, ISH evidence of 7 SL RNA and immunofluorescence of SRP 54 in axoplasmic whole mounts (I. Muslimov, M. Titmus, H. Tiedge, and E. Koenig, unpublished observations) suggests that there may be signal recognition particles (SRPs) in the axon compartment. The question of whether there is a local capability for translating membrane protein mRNA merits further investigation (see Note Added in Proof).

The occasional distinct distributions of ribosomal and small RNP-like phosphorus signals (see Figs. 7, 9) suggest a novel partitioning of the plaque domain into ribosome- and RNP-enriched subdomains. Although further work is needed to evaluate this question also, the potential significance of such a spatial segregation is unclear at present.

The protruding structure that marks the ribosomal domain in whole mounts is a singular feature that seems to characterize many plaques observed in Mauthner (Koenig and Martin, 1996), rabbit,

and rat whole mounts (see Fig. 5). It comprises a matrix to which ribosomes appear to be bound (see Koenig and Martin, 1996) (see Fig. 10). In the squid giant axon there are ribosomal “ovoid aggregates” of  $\sim 1 \mu\text{m}$  in size, based on Y-10B immunofluorescence staining and ESI analysis (Martin and Bleher, unpublished data). These structural ribosomal entities are *not* located selectively in a periaxoplasmic zone, as in the case of myelinated axons, but they are distributed sparsely and randomly *within* bulk axoplasm of the giant fiber. Because ribosomal ovoid aggregates also contain a matrix and because ribosomes free of matrix were not observed (Martin and Bleher, unpublished data), they also can be considered to be “endoaxoplasmic” plaques. It would appear, therefore, that matrix and ribosomes may form a distinct structural complex in axons in which matrix could serve to anchor and/or govern the spatial distribution of ribosomes. Matrix thereby would localize translational machinery to discrete sites within the axon compartment. The notable correspondence between the shape of structural correlates and the distribution of ribosomes (see Fig. 5) supports the inference that the matrix may govern ribosome distribution in some manner.

In conclusion, the results of this report and other recent findings (see Koenig and Giuditta, 1999; Alvarez et al., 2000) indicate that traditional views of the axon as a metabolic compartment that is deficient in protein-synthesizing machinery need to be revised.

**Note added in proof.** The capacity to synthesize and express a functionally competent G-protein-coupled conopressin membrane receptor after microinjection of the cognate mRNA in surgically isolated axons of an identified invertebrate neuron in *Lymnaea* was reported recently (Spencer et al., 2000).

## REFERENCES

- Alvarez J, Giuditta A, Koenig E (2000) Protein synthesis in axons and terminals: significance for maintenance, plasticity, and regulation of phenotype. With a critique of slow transport theory. *Prog Neurobiol* 62:1–62.
- Barker L (1899) *The nervous system*, p 307. New York: Appleton.
- Black M, Lasek RJ (1980) Slow components of axonal transport: two cytoskeletal networks. *J Cell Biol* 86:616–623.
- Chu J-L, Brot N, Weissbach H, Elkon K (1991) Lupus antiribosomal P antisera contain antibodies to a small fragment of 28S rRNA located in the proposed ribosomal GTPase center. *J Exp Med* 507–514.
- Chun JT, Gioio AE, Crispino M, Giuditta A, Kaplan BB (1995) Characterization of squid enolase mRNA: sequence analysis, tissue distribution, and axonal localization. *Neurochem Res* 20:923–930.
- Chun JT, Gioio AE, Crispino M, Eyman M, Giuditta A, Kaplan BB (1997) Molecular cloning and characterization of a novel mRNA present in the squid giant axon. *J Neurosci Res* 49:144–153.
- Edström A (1966) Amino acid incorporation in isolated Mauthner nerve fibre of goldfish. *J Neurochem* 13:315–321.
- Edström A, Sjöstrand J (1969) Protein synthesis in isolated Mauthner nerve fibre components. *J Neurochem* 16:67–81.
- Frankel RD, Koenig E (1978) Identification of locally synthesized proteins in proximal stump axons of neurotomized hypoglossal nerve. *Brain Res* 141:67–76.
- Gilbert DS, Newby BJ, Anderton BH (1975) Neurofilament disguise, destruction and disciplines. *Nature* 256:586–589.
- Gioio AE, Chun JT, Crispino M, Capano CP, Giuditta A, Kaplan BB (1994) Kinesin mRNA is present in the squid giant axon. *J Neurochem* 63:13–18.
- Giuditta A (1980) Origin of axoplasmic protein in the squid giant axon. *Riv Biol (Italy)* 73:35–49.
- Giuditta A, Cupello A, Lazzarini G (1980) Ribosomal RNA in the axoplasm of the squid giant axon. *J Neurochem* 34:1757–1760.
- Grafstein B, Foreman DS (1980) Intracellular transport in neurons. *Physiol Rev* 60:1167–1283.
- Hirokawa N (1991) Molecular architecture and dynamics of the neuronal cytoskeleton. In: *The neuronal cytoskeleton* (Burgoyne RD, ed), pp 5–74. New York: Wiley.
- Kaplan BB, Gioio AE, Perrone Capano C, Crispino M, Giuditta A (1992)  $\beta$ -Actin and  $\beta$ -tubulin are components of a heterogeneous mRNA population present in the squid giant axon. *Mol Cell Neurosci* 3:133–144.
- Koenig E (1965) Synthetic mechanisms in the axon. II. RNA in myelin-free axons of the cat. *J Neurochem* 12:357–361.
- Koenig E (1967) Synthetic mechanisms in the axon. IV. *In vitro* incorporation into axonal protein and RNA. *J Neurochem* 14:437–446.
- Koenig E (1979) Ribosomal RNA in Mauthner axon: implications for a protein synthesizing machinery in the myelinated axon. *Brain Res* 175:95–107.
- Koenig E (1984) Local synthesis of axonal protein. In: *Handbook of neurochemistry*, Vol 7 (Lajtha A, ed), pp 315–340. New York: Plenum.
- Koenig E (1986) Isolation of native Mauthner cell axoplasm and an analysis of organelle movement in non-aqueous and aqueous media. *Brain Res* 398:288–297.
- Koenig E (1991) Evaluation of local synthesis of axonal proteins in the goldfish Mauthner cell axon and axons of dorsal and ventral roots of the rat *in vitro*. *Mol Cell Neurosci* 2:384–394.
- Koenig E, Giuditta A (1999) Protein synthesizing machinery in the axon compartment. *Neuroscience* 89:5–15.
- Koenig E, Martin R (1996) Cortical plaque-like structures identify ribosome-containing domains in the Mauthner axon. *J Neurosci* 16:1400–1411.
- Koenig E, Repasky E (1985) A regional analysis of  $\alpha$ -spectrin in isolated Mauthner neuron and in isolated axons of the goldfish and rabbit. *J Neurosci* 5:705–714.
- Korn AP, Spitznik-Elson P, Elson D, Ottensmeyer FP (1983) Specific visualization of ribosomal RNA in the intact ribosome by electron spectroscopic imaging. *Eur J Cell Biol* 31:334–340.
- Lasek RJ, Hoffman PN (1976) The neuronal cytoskeleton, axonal transport, and axonal growth. In: *Cell motility: microtubules and related proteins* (Goldman R, Pollard T, Rosenbaum J, eds), pp 1021–1049. New York: Cold Spring Harbor.
- Lerner EA, Lerner MR, Janeway Jr CA, Steitz JA (1981) Monoclonal antibodies to nucleic acid-containing cellular constituents: probes for molecular biology and autoimmune disease. *Proc Natl Acad Sci USA* 78:2737–2741.
- Martin R, Fritz W, Giuditta A (1989) Visualization of polyribosomes in the postsynaptic area of the squid giant synapse by electron spectroscopic imaging. *J Neurocytol* 418:11–18.
- Martin R, Door R, Breitig D (1993) High resolution imaging of protein phosphorylation in the squid giant axon and synapse. *J Histochem Cytochem* 41:1133–1139.
- Martin R, Vaida B, Bleher R, Crispino M, Giuditta A (1998) Protein synthesizing units in presynaptic and postsynaptic domains of squid neurons. *J Cell Sci* 111:3157–3166.
- Mohr E, Richter D (1992) Complexity of mRNAs in the axonal compartment of peptidergic neurons in the rat. *Eur J Neurosci* 4:870–876.
- Nixon RA (1980) Protein degradation in the mouse visual system. I. Degradation of axonally transported and retinal proteins. *Brain Res* 200:69–83.
- Nixon RA, Logvinenko KB (1986) Multiple fates of newly synthesized neurofilament proteins: evidence for a stationary neurofilament network distributed nonuniformly along axons of retinal ganglion cell neurons. *J Cell Biol* 102:647–659.
- Ottensmeyer FP (1986) Elemental mapping by energy filtration: advantages, limitations, and compromises. *Ann NY Acad Sci* 483:339–353.
- Palay SL, Palade GE (1955) The fine structure of neurons. *J Biophys Biochem Cytol* 1:69–88.
- Pannese E, Ledda M (1991) Ribosomes in myelinated axons of the rabbit spinal ganglion neurons. *J Submicrosc Cytol Pathol* 23:33–38.
- Peters A, Palay SL, Webster HF (1970) *The fine structure of the nervous system*. New York: Harper and Row.
- Sotelo JR, Kun A, Benech JC, Giuditta A, Morillas J, Benech CR (1999) Ribosomes and polyribosomes are present in the squid giant axon: an immunocytochemical study. *Neuroscience* 90:705–715.
- Spencer GE, Syed NI, van Kesteren E, Lukowiak K, Geraets WPM, van Minnen J (2000) Synthesis and functional integration of a neurotransmitter receptor in isolated invertebrate axons. *J Neurobiol* 44:72–81.
- Tobias GS, Koenig E (1975) Axonal protein synthesizing activity during the early outgrowth period following neurotomy. *Exp Neurol* 49:221–234.
- Torre ER, Steward O (1996) Protein synthesis within dendrites: glycosylation of newly synthesized proteins in dendrites of hippocampal neurons in culture. *J Neurosci* 16:5967–5978.
- Weiner OD, Zorn AM, Krieg PA, Bittner GD (1996) Medium-weight neurofilament mRNA in goldfish Mauthner axoplasm. *Neurosci Lett* 213:83–86.
- Zelená J (1972) Ribosomes in myelinated axons of dorsal root ganglia. *Z Zellforsch Mikrosk Anat* 124:217–229.



## **Comentarios sobre el trabajo I.**

El principal hallazgo presentado en este capítulo se refiere a la presencia de dominios ribosomales en los axones de vertebrados superiores. Con la primera descripción de estos dominios en el axón gigante de Mauthner se provocaron diversas discusiones, una de ellas discurría sobre la incógnita de que estas formaciones fueran una característica común en diferentes tipos de axones. Los axones que fueron estudiados aquí podrían ser representativos de axones largos de neuronas del sistema nervioso, como los pertenecientes a motoneuronas. Al contrario de neuronas que poseen axones con dimensiones pequeñas (interneuronas), las motoneuronas podrían necesitar, dado el gran volumen de su axón, sistemas localizados de síntesis de proteínas. Por otro lado, se han observado ribosomas, retículo endoplásmico rugoso y aparato de Golgi en dendritas de muy corta longitud (Gardioli y cols, 1999, Burack y cols., 2000) o aparato traduccional en axones de neuritas en cultivo (Bassell y cols., 1998; Aronov y cols 2002), indicando quizás que los mismos puedan requerir de un aparato traduccional para su funcionamiento. La capacidad de estos modelos experimentales, para extraer conclusiones sobre axones maduros, diferenciados completamente, es limitada ya que se trata de modelos en cultivos. Esto resalta la importancia de utilizar un modelo de estudio que pueda responder si por lo menos algún tipo de axón en un animal adulto posee maquinaria traduccional. La preparación utilizada en la presente tesis cumple, en parte, estos requerimientos, pero la confirmación de los hallazgos realizados no necesariamente vendrá de la utilización de modelos más simples.

Ya que estos axones son trasladados desde su localización original, rodeados por su vaina de mielina, hacia la superficie de un cubre-objeto, la zona cortical del axón se encuentra sometida a fuerzas de fricción que pueden alterar la morfología y distribución de las placas periaxoplásmicas durante el proceso. Una forma de corroborar su localización fue el estudio *in situ* (Figura 2 G, H, I, trabajo I) del cual se puede concluir únicamente que se pueden encontrar zonas ricas en ARN en estrecha relación con la membrana axonal y la mielina circundante. La falta de correlación obtenida entre parámetros dimensionales de las placas periaxoplásmicas con el volumen o superficie axonal (figura 6, trabajo I) quizás reflejen lo variable del proceso de aislamiento de axones conteniendo placas periaxoplásmicas.

De los estudios morfométricos se concluye que el material YOYO-1 positivo coincide en su distribución con el Y10B (anti ARN ribosomal) positivo, demostrando la presencia de ribosomas en las placas periaxoplásmicas, sin revelar la compartimentalización que fue observada utilizando ESI, donde se observan partículas tipo ribosomas y otras más pequeñas (con alto contenido de fósforo) que se asemejan a partículas ribonucleoproteicas.

La distancia promedio entre placas periaxoplásmicas cuantificada en estos estudios se encontraba en el entorno de 23  $\mu\text{m}$ . Si a esto le agregamos que estas estructuras se encuentran en íntima relación con la membrana axónica, es más fácil de entender la falta de observaciones de ribosomas, a nivel de microscopía electrónica, utilizando secciones ultrafinas al azar. Ya que cada sección ultra-fina posee pocos nanómetros la probabilidad de encontrar estas estructuras mediante un estudio no sistemático es muy baja. Teniendo en cuenta estas observaciones y realizando un estudio sistemático de preparaciones axonales *in toto*, en las que previamente se encontraron

placas, R. Martin logró observar acúmulos ribosomales en regiones corticales de dichos axones (figuras 7, 8, 9, trabajo I).

Una característica en común entre las placas periaxoplásmicas de los axones de Mauthner y las encontradas en los axones de raíces ventrales fue la presencia de correlatos estructurales observables por microscopía de contraste de fase y también a nivel de microscopía electrónica. Estas últimas observaciones indican cierto grado de organización interna de estas estructuras, corroborando la presencia, ya descrita en el trabajo previo (Koenig & Martin, 1996) de una especie de “matriz estructural”. Para la misma se postulan funciones principalmente estructurales, pero ya que se desconoce su composición, atribuirle funciones es aún prematuro.

Los resultados discutidos aquí y en el capítulo 5 con mayor profundidad, con respecto a esta sección, refuerzan la hipótesis planteada en esta tesis ya que se demuestra que las placas periaxoplásmicas existen en axones de diferentes especies y poseen al menos ARN ribosomal y proteínas ribosomales. Estas observaciones nos hacen plantear las preguntas, abordadas mediante aproximaciones similares a las utilizadas en este capítulo, sobre cual podría ser la variedad de ARNm localizados en estos dominios y si podemos estudiar su distribución en tejidos intactos. En el siguiente capítulo se presentaran los resultados correspondientes a la búsqueda de ARNm en axones de vertebrados utilizando como modelo axones intactos de nervio ciático y preparaciones axonales *in toto*.

## **Capítulo 2**

**Presencia de ARNm en los axones de vertebrados y las placas periaxoplásmicas.**

Las observaciones presentadas en el capítulo anterior sugerían que en la periferia de la corteza axonal, más precisamente en las placas periaxoplásmicas, deberían de estar presentes ARNm codificantes para diversas proteínas. Los experimentos presentados en el presente capítulo han tenido como objetivo principal la caracterización de los ARNm presentes en el axón e investigar su asociación con las placas periaxoplásmicas.

Una de las aproximaciones experimentales utilizadas en un principio, fue la de analizar la expresión de ARNm codificantes para proteínas específicas de neuronas como los neurofilamentos en los axones del nervio ciático (Sotelo Silveira, 1998 y trabajo II). En este modelo, es posible realizar manipulaciones experimentales que eventualmente pueden provocar cambios en la expresión de local de ARN mensajeros, como por ejemplo el aplastamiento o corte del nervio.

Por otro lado, se utilizó la preparación de axones montados *in toto*, provenientes de la célula de Mauthner y de las raíces ventrales de rata y conejo (ver Capítulo 1 y trabajo I), para analizar *in situ* la localización y distribución del ARNm codificante para la beta actina. Una de las razones para buscar este ARNm en particular, fue que se verificó la presencia del mismo en prolongaciones neuronales en cultivo *in vitro* (Bassell y cols 1998) y que estudios de incorporación de aminoácidos marcados en proteínas axonales demostró que la actina era una de las proteínas sintetizadas *de novo* en axones de Mauthner y de raíces ventrales de rata (Koenig, 1991). Para cumplir con este objetivo se desarrollaron protocolos de hibridación *in situ* de alta sensibilidad combinados con el uso de microscopía láser confocal para lograr estudiar la asociación de dicho ARNm con las placas periaxoplásmicas (trabajo III).

A su vez, los ARNm presentes en la preparación de axones de Mauthner fue estudiada utilizando RT-PCR específico y aleatorio. El primero fue utilizado con el objetivo de confirmar la expresión axonal de la beta actina y el segundo para generar mini genotecas de segmentos de genes expresados (Expressed Sequences Tags, "EST") provenientes de ARNm axonal. Utilizando esta ultima técnica se podría ampliar el conocimiento del repertorio de ARN presente en el territorio axonal. Debe destacarse que para ambos casos se diseñaron estrategias utilizadas por primera vez en estos modelos, que permitían maximizar la detección de ARNm a partir de muestras axonales, combinando la micro extracción de ARN cuantitativa, con métodos de transcripción reversa de alta sensibilidad y amplificación por PCR.



**Trabajo II:** Sotelo Silveira, J.R., Calliari A., Kun A, Benech JC, Sanguinetti C, Chalar C, Sotelo JR. Neurofilament mRNAs are present and translated in the normal and severed sciatic nerve. (2000) J. Neurosci. Res. 62: 65-74.

# Neurofilament mRNAs Are Present and Translated in the Normal and Severed Sciatic Nerve

José R. Sotelo-Silveira,<sup>1,3,4</sup> Aldo Calliari,<sup>1,2</sup> Alejandra Kun,<sup>1,2,5</sup> Juan Claudio Benech,<sup>1,2</sup> Carlos Sanguinetti,<sup>3</sup> Cora Chalar,<sup>3</sup> and José R. Sotelo<sup>1\*</sup>

<sup>1</sup>Departamento de Biofísica, Instituto de Investigaciones Biológicas Clemente Estable, Montevideo, Uruguay

<sup>2</sup>Área Biofísica, Departamento de Biología Molecular y Celular, Facultad de Veterinaria, Universidad de la República, Montevideo, Uruguay

<sup>3</sup>Sección Bioquímica, Facultad de Ciencias, Universidad de la República, Montevideo, Uruguay

<sup>4</sup>Sección Biología Celular, Facultad de Ciencias, Universidad de la República, Montevideo, Uruguay

<sup>5</sup>Unidad Asociada Biofísica, Facultad de Ciencias, Universidad de la República, Montevideo, Uruguay

Local protein synthesis within axons has been studied on a limited scale. In the present study, several techniques were used to investigate this synthesis in sciatic nerve, and to show that it increases after damage to the axon. Neurofilament (NF) mRNAs were probed by RT-PCR, Northern blot and in situ hybridization in axons of intact rat sciatic nerve, and in proximal or distal stumps after sciatic nerve transection. RT-PCR demonstrated the presence of NF-L, NF-M and NF-H mRNAs in intact sciatic nerve, as well as in proximal and distal stumps of severed nerves. Northern blot analysis of severed nerve detected NF-L and NF-M, but not NF-H. This technique did not detect the three NFs mRNAs in intact nerve. Detection of NF-L and NF-M mRNA in injured nerve, however, indicated that there was an up-regulation in response to nerve injury. In situ hybridization showed that NF-L mRNA was localized in the Schwann cell perinuclear area, in the myelin sheath, and at the boundary between myelin sheath and cortical axoplasm. RNA and protein synthesizing activities were always greater in proximal as compared to distal stumps. NF triplet proteins were also shown to be synthesized de novo in the proximal stump. The detection of neurofilament mRNAs in nerves, their possible upregulation during injury and the synthesis of neurofilament protein triplet in the proximal stumps, suggest that these mRNAs may be involved in nerve regeneration, providing a novel point of view of this phenomenon. *J. Neurosci. Res.* 62:65–74, 2000.

© 2000 Wiley-Liss, Inc.

**Key words:** neurofilament; cytoskeleton; RNA; regeneration

Axonal transport of proteins synthesized in cell bodies has been intensively studied for decades. Only recently has it become clear that not all axonal proteins are synthesized in the soma (Koenig and Giuditta, 1999; Van Minnen et al., 1997, Alvarez et al., 2000). Axonal proteins were proposed to be synthesized in the periaxonal glial cell

of the squid giant axon and to be transferred thereafter to the axon (Lasek et al., 1977; Gainer et al., 1977). It is, however, increasingly clear that there is also de novo protein synthesis within the axoplasm of squid giant axon. Evidence for this includes the finding of tRNA, elongation factors, aminoacyl tRNA synthetases (Giuditta et al., 1977), rRNA (Giuditta et al., 1980), a set of mRNAs (Giuditta et al., 1986), transference of RNAs from glia cells to axons (Rapallino et al., 1988), as well as active polyribosomes in the giant axon (Giuditta et al. 1991). To date, axonal mRNAs that were identified, include those coding for  $\beta$ -actin and  $\beta$ -tubulin (Kaplan et al., 1992), kinesin (Gioio et al., 1994), and neuron specific enolase (Chun et al., 1995). There is also evidence that the neurofilament light mRNA (NF-L) is present in the squid giant axon (Giuditta et al., 1991). Finally, ribosomes and polysomes have been identified in the squid giant axon, both by Electron Spectroscopic Imaging (ESI) (Martin et al., 1989), and by Electron Microscope immunocytochemistry, using a polyclonal antibody against ribosomes (Sotelo et al., 1999).

There is also evidence for local protein synthesis in vertebrate axons. In the large myelinated Mauthner (M-) axon of goldfish, there was found evidence for local protein synthesis in vitro (Edstrom and Sjostrand, 1969) and in vivo (Alvarez and Benech, 1983). Later, many proteins exhibiting cycloheximide-sensitive labeling were shown to be apparent constituents of the slow transport rate

Contract grant sponsor: European Union; Contract grant number: CT1-CT93-0037UY; Contract grant sponsor: Japanese International Cooperation Agency (JICA); Contract grant sponsor: BID-CONICYT; Contract grant sponsor: MEYC; Contract grant sponsor: CSIC; Contract grant sponsor: CIDEC (Fac Veterinaria); Contract grant sponsor: PEDECIBA; Contract grant sponsor: OAS.

\*Correspondence to: Dr. José R. Sotelo, Department of Biophysics, Instituto de Investigaciones Biológicas Clemente Estable (IIBCE). Av. Italia 3318, C.P. 11600, Montevideo, Uruguay. E-mail: sotelo@iibce.edu.uy

Received 16 February 2000; Revised 9 June 2000; Accepted 12 June 2000

groups (Koenig, 1991). Local protein synthesizing activity has also been shown in the cat spinal accessory nerve root axons (Koenig, 1967), the rabbit hypoglossal nerve (Tobias and Koenig, 1975), in regenerating axonal fields of goldfish cultured retinal ganglion-cells (Koenig and Adams, 1982; Koenig, 1989), and in dorsal and ventral roots of rats (Koenig, 1991). In these studies, labeling of putative actin and tubulin was observed and was inhibited by cycloheximide. Local protein and RNA synthesizing activity (inhibited by cycloheximide and actinomycin-D, respectively) was also observed by autoradiography (Benech et al., 1982) and the synthesis of the 68 kDa neurofilament subunit was demonstrated (Sotelo et al., 1992) in the severed rat sciatic nerve. Vasopressin and oxytocin, messenger RNAs as well as neurofilament-L mRNA, were localized in axons of the hypothalamo-neurohypophyseal tract of the rat (Mohr and Richter, 1992), as well as mRNA coding for NF-M in the M-axon (Weiner et al., 1996).  $\beta$ -Actin mRNA was identified in growing axons of chick sympathetic ganglion cells (Olink-Coux and Hollenbeck, 1996) and in cortical neurons in culture (Bassell et al., 1998). Koenig (1979) has microextracted RNA from isolated axoplasm of Mauthner cells and shown that rRNA is present. Recently, Koenig and Martin (1996) showed that RNA containing domains were localized in cortical plaque-like formations of the M-axon. These periaxoplasmic plaques (PAP) were specifically stained with YOYO-1, a high-affinity nucleic acid-binding fluorescent dye. ESI of these PAP yielded ribosome-like phosphorus signals. The authors proposed that these structures could be protein synthesis centers localized in the cortical region of the M-axon.

This report focuses on endogenous expression of neurofilament mRNAs in the sciatic nerve of the rat, both in intact nerves and in response to sciatic nerve injury. In addition, experiments were performed to evaluate protein synthesis on sciatic nerve fibers in response to nerve injury. The results indicate that injury up-regulates expression of NF subunits mRNAs and protein synthesis in peripheral nerve.

## MATERIALS AND METHODS

### Surgical Procedures

Adult male rats were selected from the IIBCE colony (250–270 g body wt, 5 months old). Every surgery was performed under sodium pentobarbital anesthesia. Sciatic nerves were severed in the mid thigh, 4.5 cm distal to the fifth lumbar dorsal root ganglion (DRG). Normal nerves were obtained from animals of the same age.

**RNA purification.** For RNA extraction, 10 mm of proximal and distal stumps were excised 48 hr after cutting and accumulated frozen. In some animals RNA was extracted from uninjured sciatic nerves (normal).

**In situ hybridization (ISH).** For ISH studies, tissues were obtained after animal perfusion via cardiac puncture (0.1 M phosphate buffer, pH 7.4, followed by 4% paraformaldehyde in 0.1 M phosphate buffer, pH 7.4). Sciatic nerves samples were excised 48 hr after cutting.

**Analysis of local protein synthesis.** For the analysis of local protein synthesis, right and left sciatic nerves were treated as described in Surgical Procedures. Left proximal stumps served as controls (not radioactively labeled). In right proximal stumps, proteins were labeled using  $^{35}\text{S}$ -methionine (Sotelo et al., 1992).

**Liquid scintillation counting (LSC).** Both lumbar fifth DRG, and several 1-cm pieces of desheathed right and left nerves were excised above the proximal stumps and newly synthesized proteins were LSC counted after being trichloroacetic acid (TCA) extracted and solubilized in NCS Tissue Solubilizer from Amersham (Sotelo et al., 1992). These samples were used to evaluate radioactivity reaching dorsal root ganglia by blood flow, that would be incorporated into protein that could then be conveyed to the nerve by axonal transport.

**Autoradiography.** In another group of animals, sciatic nerves were crushed instead of cutting, and both proximal and distal stumps were labeled together 1 hr before excising by immersion in a pool of either tritiated amino acids (3H-AA experiments, 100  $\mu\text{Ci}$ ), or tritiated uridine (3H-Ur, 100  $\mu\text{Ci}$ ). Crushed nerves were excised 1, 2, 3, 4, or 8 days after injury in which a tight ligature at the crush marked the site for later identification. They were fixed with paraformaldehyde and washed and then fixed a second time with osmic acid, washed again and dehydrated, as previously described (Benech et al., 1982). Proximal and distal stumps were separated at this step and embedded in individual araldite blocks. Each stump was cut into 1-cm pieces, and microtome sections (1  $\mu\text{m}$ ) of proximal and distal stumps from the same animal were mounted on the same glass slide, covered with radioautographic emulsion, and exposed at 4°C. Those labeled with amino acids were developed after a month and the nerves labeled with 3H-Ur were developed 3 months later. Silver grains were counted and grain densities (grains/100  $\mu\text{m}^2$ ) over myelin and axoplasm of proximal and distal stumps were calculated, as described previously (Benech et al., 1982).

## Detection of Neurofilament NA Transcripts

### RT-PCR

**Oligonucleotide primers.** Oligonucleotide primers were synthesized according to sequences available at the GenBank for the three rat neurofilament proteins light (NF-L), medium (NF-M) and high (NF-H) subunits. The primers were specially designed to avoid overlap with sequences that would be amplified among the three different mRNAs, and also overlap with any other mRNAs coding for other intermediate filaments. Primers used were the following: for NF-L, 5'-GATCGAAGCCTGCCGGGTAT-3' and 5'-CGTAGCCTCAATGGTCTCCTC-3' (annealing temperature: 55°C; product length, 408 base pairs); for NF-M, 5'-GAAGGAAAAGAGGAGGAGGAG-3' and 5'-CAAGGACTGAGGAGGCACCC-3' (annealing temperature: 56°C; product length, 500 base pairs); for NF-H: 5'-GCACAGACCAAAAAGACAGCC-3' and 5'-GGGGCAGTTTTTAGTCACGC-3' (annealing temperature: 58°C; product length, 380 base pairs); for aldolase: 5'-GTGCTGAAGAATGGGGAACA-3' and 5'-

ACCGTTGCCATGGCAATCTCCTC-3' (annealing temperature: 52°C; product length, 310 base pairs).

**Amplification by the cDNA polymerase chain reaction: pre-treatment of total RNA.** A series of experiments were performed in which RNase, DNase, or both were added in excess before the reverse transcriptase reaction. In another series, the reverse transcriptase reaction was omitted. Total liver RNA (DNase digested) was used in the RT-PCR as a negative control. Total brain RNA (DNase digested) was used in the RT-PCR as a positive control.

**RT-PCR.** Ten  $\mu\text{g}$  of total RNA, treated as described above, were retro-transcribed using the Reverse Transcription System Kit (Promega). PCR was performed according to Saiki et al. (1988). One microliter of serial dilutions of cDNA was amplified with the primers described in "Oligonucleotide primers" section. The amplification cycle consisted of denaturation at 94°C for 1 min, annealing at the temperatures indicated in "Oligonucleotides primers" section, and extension at 72°C for 1 min. In the first cycle, the denaturation was prolonged for 5 min, and in the last cycle, the extension step was 5 min. A total of 30 cycles was performed. The resulting DNA fragments were electrophoresed on a 6% polyacrylamide gel and stained with silver nitrate according to Sanguinetti et al. (1994). To confirm the identity of the PCR products, the fragments were purified and cloned into vector T (Marchuk et al., 1991) and then sequenced (Sanger et al., 1977).

### Northern Blot Analysis

Total RNA was prepared from proximal and distal stumps of sciatic nerves 48 hr post-transection according to Chomczynski and Sacchi (1987). Twenty to 30  $\mu\text{g}$  of total RNA (isolated from 10–15 sciatic nerve stumps, 10 mm of length) were electrophoresed in a 1.2% agarose-formaldehyde gel. All these procedures were performed according to Sambrook et al. (1989).

RNA was transferred to nylon filters. DNA [ $^{32}\text{P}$ ]dATP labeled probes were hybridized and washed thereafter to a final stringency of  $0.2\times$  SSC and 0.1% SDS (60°C, 20 min). Filters were exposed 1 week ( $-80^\circ\text{C}$ ) to Kodak X-Omat AR films using an intensifying screen. Films were developed in the standard manner.

### In Situ Hybridization

Sciatic nerve proximal stumps (48 hr after sectioning), were excised and fixed, as described in the Surgical Procedures section. Eight to 10  $\mu\text{m}$  sections were obtained in a cryostat. Single-stranded digoxigenin-UTP labeled RNA probes were transcribed, using the Boehringer-Mannheim T3/T7 transcription kit according to manufacturer's instructions. The full length cDNA encoding mouse 68 kDa subunit of neurofilament, cloned into the multiple cloning site of pBluescribe ( $\pm$ ) (a gift from Dr. N. Cowan; Lewis and Cowan, 1985), was used to generate antisense or sense labeled transcripts.

The in situ hybridization technique is basically that of Jordan et al. (1989). Sections were then pre-hybridized

for 2 hr with a mixture containing 50% deionized formamide,  $4\times$  SSC, 500  $\mu\text{g}/\text{ml}$  sheared single-stranded salmon sperm DNA, 250  $\mu\text{g}/\text{ml}$  yeast t-RNA,  $1\times$  Denhardt's and 10% dextran sulfate. Sections were hybridized in humid chamber overnight (42°C), with 50  $\mu\text{l}$  of the same mixture containing 2  $\text{ng}/\mu\text{l}$  of previously denatured (95°C, 3 min) digoxigenin-UTP labeled transcripts. After that, sections were RNase A digested and washed to a final stringency of  $0.1\times$  SSC, 50°C (two 15 min changes). Probes were detected using an anti-digoxigenin-alkaline phosphatase conjugate (Boehringer-Mannheim) according to manufacturer's instructions.

### In Vivo Translation of Neurofilament Proteins

**Two dimensional electrophoresis, immunoblotting and fluorography.** Frozen incubated segments were thawed, desheathed and homogenized in an ice-cold Teflon-glass pestle homogenizer using 100  $\mu\text{l}$  of O'Farrell's lysis buffer, containing LKB ampholytes pH 4–6 and pH 3.5–10. Ten  $\mu\text{l}$  of the supernatant intermediate phase (after  $1,000\times g$  centrifugation) were taken for TCA precipitation, to estimate fluorography exposure time. Nerve proteins contained in this same fraction were separated by the O'Farrell 2-D electrophoresis method (O'Farrell, 1975). The second dimension was run in 8–15% acrylamide concentration gradient gels and transferred to nitrocellulose membranes (Dunbar, 1987). The three NF subunits were identified with commercial specific monoclonal antibodies (Amersham). The immunoreaction was carried out using an alkaline phosphatase conjugated anti-mouse IgG, (Promega). After the immunoreaction, the same membranes were pressed against two X-ray films and stored in a cassette at  $-70^\circ\text{C}$ .

### Immunohistochemistry

Immunohistochemical procedures were performed according to Sotelo et al. (1999), but for light microscopy. Five to 10  $\mu\text{m}$  cryostat sections were used for developing the immunoreaction and light microscopic examination. Osmium tetroxide (0.01%) was used to post-fix samples. A specific monoclonal antibody (1/100 dilution), against S1 ribosomal protein (kindly supply by Dr. B. Hügle) was used. The secondary antibody used was an anti-mouse IgG conjugated to peroxidase (1/200) and it was developed with 0.02% diaminobenzidine (Sigma), 0.06%  $\text{H}_2\text{O}_2$  (v/v) (10 min at 37°C).

## RESULTS

### Detection of Neurofilament RNA Transcripts in the Sciatic Nerve

**RT-PCR.** Using specific oligonucleotides complementary to the sequences of the three neurofilament subunits in RT-PCR on total RNA (digested with DNase-RNase free) from normal uninjured nerves yielded the expected size of amplified fragments for each subunit (see Fig. 1). Specific oligonucleotides complementary to a mRNA coding for aldolase (a housekeeping enzyme) were used as internal control to show the pres-



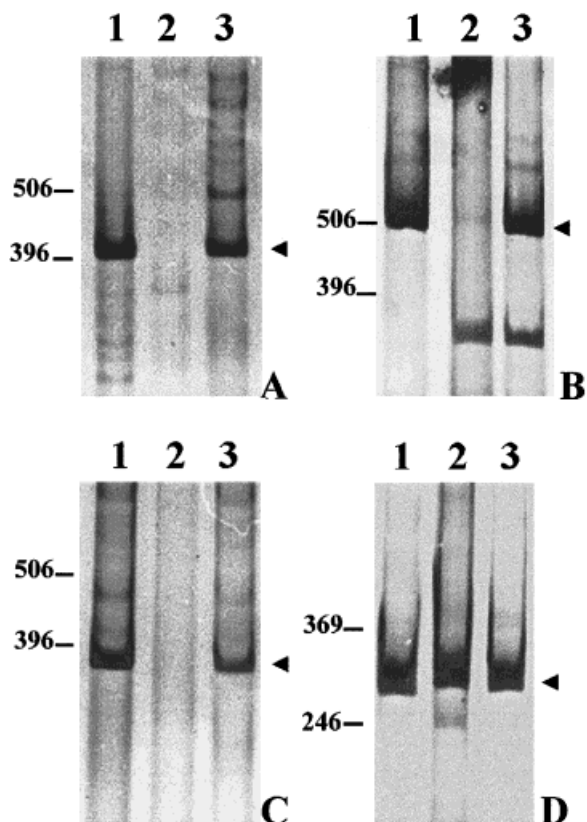


Fig. 1. Polyacrylamide gel electrophoresis of products of RT-PCR of the three neurofilament subunits in the normal (uninjured) sciatic nerve. The figure shows amplification products obtained by RT-PCR using specific oligonucleotide primers for NF-L (A), NF-M (B), NF-H (C), and for aldolase (D). In **lane 1**, cDNA was synthesized using total RNA (1  $\mu$ g) from rat brain cortex. In **lane 2**, cDNA was synthesized using total RNA (1  $\mu$ g) from rat liver. In **lane 3**, cDNA was synthesized using total RNA (1  $\mu$ g) from normal (uninjured) rat sciatic nerve. The cDNA used was always the same for the same lane number. The size in base pairs of the standard (1 kb ladder, Gibco) is shown at left of A, B and C. The standard of D is 123 bp ladder (Gibco). Arrowheads show the expected size of the amplification products for the three neurofilament subunits.

ence of cDNA in all samples. The identity of each amplified fragment was confirmed after cloning by DNA sequencing using the dideoxy chain terminator method.

Similarly, using oligonucleotides complementary to the specific sequences for the three neurofilament subunits in RT-PCR on total RNA (digested with DNase-RNase free) from proximal and distal stumps, amplified fragments of the expected size for each subunit from both stumps were obtained. For each pair of primers, serial dilutions of the cDNA were performed to confirm the specificity of the amplified product size (see relevant dilutions in Fig. 2). In each case the amplification was dependent on the presence of RNA in the sample before making the cDNA, as confirmed by RNase digestion (see relevant dilutions in Fig. 3).

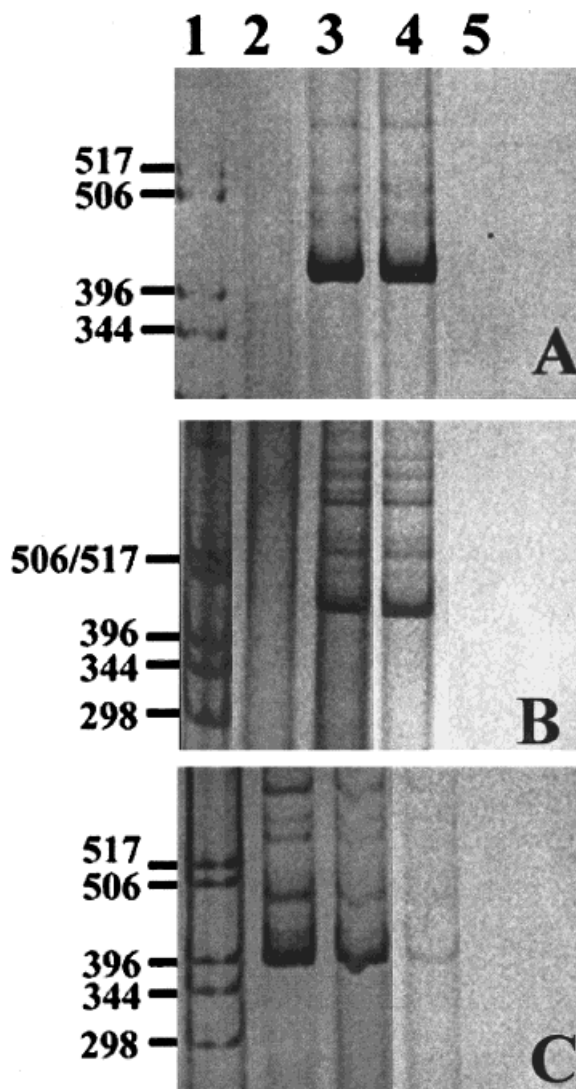


Fig. 2. (A–C). Polyacrylamide gel electrophoresis of the products of RT-PCR for the three neurofilament subunits, using total RNA extracted from the proximal and distal stumps of the severed sciatic nerves after 48 hr. RT-PCR amplification products were obtained using the NF-L (A), NF-M (B) or NF-H (C) specific oligonucleotides primers. Each **lane 1** contains the molecular weight standard 1 kb ladder (Gibco); the size (bp) is detailed at left. Each **lane 2** represents RT-PCR reactions obtained using rat genomic DNA as a template (0.015  $\mu$ g). In each **lane 3**, cDNA was derived from RNA extracted from the proximal stump (only dilution  $\frac{1}{4}$  is shown). In each **lane 4**, cDNA was from the distal stump (same dilutions as used in the proximal stump). In each **lane 5**, RT-PCR reactions were carried out without cDNA.

The treatment of the sample with DNase before reverse transcription did not affect the amplification of the three neurofilament mRNAs. Digestion of the sample with RNase together with DNase before reverse transcription, completely eliminated the amplification of the three neurofilament mRNAs as well. The DNase con-

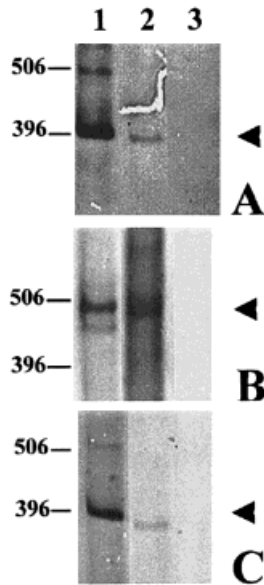


Fig. 3. (A–C). Polyacrylamide gel electrophoresis of RT-PCR products of the three neurofilament subunits from proximal stump of the severed sciatic nerve: RNA dependence of the specific amplification. RT-PCR amplification products were obtained using the NF-L (A), NF-M (B) or NF-H (C) specific oligonucleotides using total RNA of the sciatic nerve proximal stump (48 hr after injury). In each case only relevant dilutions are shown. DNase (RNase-free) digestion is shown in each **lane 1** (cDNA dilution: 1/10). RNase (DNase free) digestion is shown in each **lane 2** (cDNA dilution: 1/10). DNase plus RNase digestion is shown in each **lane 3** (cDNA dilution: 1/10). The size in base pairs of the standard (1 kb ladder, Gibco) is shown at left of each figure. Arrowheads show the expected size of the amplification products for the three neurofilament subunits.

centration necessary to eliminate the amplification was determined, and this concentration of DNase was added in excess to the corresponding purified total RNA before all reverse transcriptase reactions.

**Northern blot.** The use of the  $^{32}\text{P}$  labeled cDNA probe coding for the 68 kDa neurofilament (NF-L) protein, yielded a clear signal from the total RNA isolated from the proximal stump of the severed sciatic nerve. The apparent sizes of the transcripts recognized by the NF-L cDNA probes corresponded to the sizes of the NF-L mRNA (2.5 and 4.0 kb; see Fig. 4). A  $^{32}\text{P}$  labeled probe for NF-M was synthesized from the cloned PCR product (see RT-PCR results, below), using specific primers for the NF-M sequence. When hybridized on the same blotting membrane, it yielded a weaker signal with a molecular weight corresponding to 3.5 kb, (see Fig. 4). The same procedure carried on the same membrane for the NF-H did not yield a detectable signal.

#### In Vivo Incorporation of Tritiated Precursors to Protein and RNAs

**Autoradiography of proximal and distal stumps.** The autoradiographs of proximal and distal stumps showed incorporation of radioactive amino acids

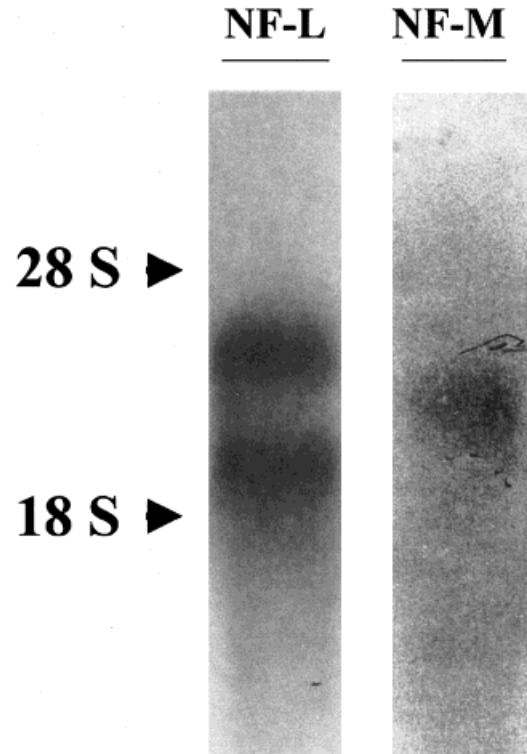


Fig. 4. Northern blot of NF-L and NF-M mRNAs. The two radioautographies (NF-L and NF-M) were obtained from the same nylon membrane in which 50  $\mu\text{g}$  of total RNA, extracted from proximal stumps of the sciatic nerves severed 48 hr before, was separated by electrophoresis. **Left lane** (NF-L) shows the signal obtained after hybridization with the complementary sequence probe to NF-L mRNA. This probe was dihybridized thereafter and hybridized again with a second probe, that was a complementary sequence to NF-M mRNA. **Right lane** shows the signal corresponding to the latter hybridization.

(3H-Aa) into proteins of myelin and axoplasm, as well as incorporation of tritiated uridine (3H-Ur) into RNA of the same structures. The density of grains over myelin and axoplasm in autoradiograms after amino acid incorporation was always greater than that after 3H-Ur incorporation in both stumps. For both the 3H-Aa and the 3H-Ur experiments, the density of grains was always higher over myelin than that over axoplasm for both stumps. On the other hand, the density of grains over myelin and axoplasm of the proximal stumps was always higher than the density of grains over myelin and axoplasm of the distal stumps (see Fig. 5). The difference in grain density between proximal and distal stumps, in both 3H-Aa and 3H-Ur experiments, was always statistically significant; however, the distal stumps grain density was always significantly higher than the grain density of unlabeled control ganglia.

**Radioactivity in unexposed control tissues.** TCA precipitable radioactivity associated with tissues not directly exposed to the radioactive precursor including

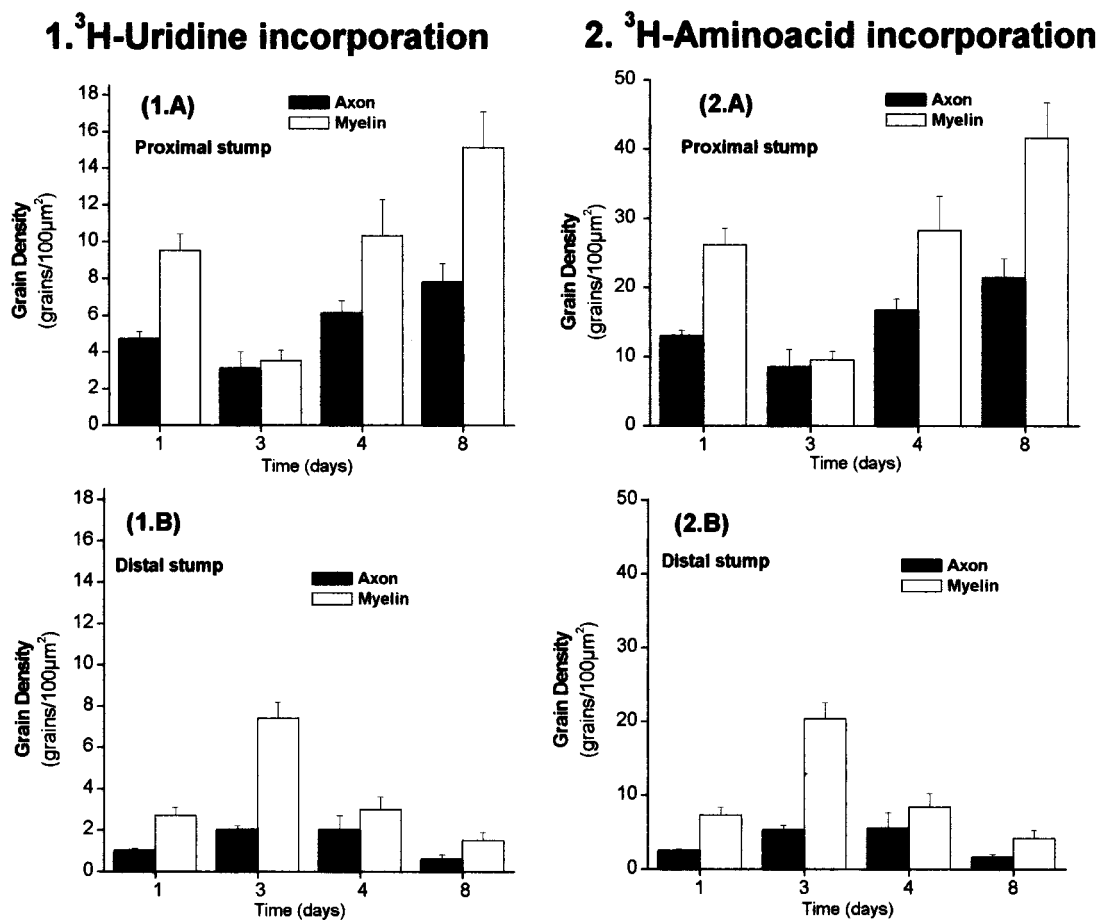


Fig. 5. In vivo incorporation of tritiated precursors to protein and RNAs after nerve injury. Data derived from autoradiography at the light microscopy level. **Panel 1** represents tritiated uridine incorporation and panel 2 represents tritiated aminoacids incorporation. In abscises is represented the time (days) after injury when the radio-tracer was supplied to the nerve. In ordinates is shown the autoradiographic grain density counted over myelin area (white bars, all graphs), or

axoplasmic area (black bars, all graphs), normalized to 100 square  $\mu\text{m}$ . In **1.A** and **2.A** data come from proximal stumps. In **1.B** and **2.B** data come from distal stumps. Note that myelin grain density counted for both radio-tracers was always significantly higher than axoplasmic grain density (in proximal and distal stumps). Also note that the grain density counted for both precursors (in myelin and axoplasm) of proximal stump was always significantly higher than distal stumps grain density.

pieces of sciatic nerve, the DRGs, and 4 cm of sciatic nerve between the DRG and the proximal stump, was not more than 5% of the radioactivity of the proximal stump.

**Translation of neurofilament RNA transcripts. Immunoblotting of newly synthesized neurofilament subunits.** TCA precipitable radioactivity of control samples taken from the fifth lumbar DRG, and right and left desheathed nerves, proximal to the nerve transection was only 1% of the precipitable radioactivity of the incubated proximal sciatic nerve stumps. Two dimensional fluorography of the membranes blotted with radioactive proteins yielded several spots, suggesting active protein synthesis (Fig. 6). The spots identified as NF proteins by immunoblotting can also be seen as clear spots in the X-ray film. The newly synthesized neurofilament proteins were identified by the molecular weight of the different subunits, calculated from their Rf compared to a regression plot of standard protein markers. They were also identified by the experimentally

determined pI, obtained for the three different proteins, that corresponded to 4.96, 5.0, and 5.13 for the 68, 160, and 200 kDa subunits, respectively. Finally, the three subunits were identified on nitrocellulose immunoblots with monoclonal antibodies against the three NF proteins. The fluorographs yielded three spots with molecular weights and isoelectric points of neurofilament protein subunits that corresponded to the spots obtained in the immunoblot (see framed area in Fig. 6).

Although NF-L was relatively easy to label in 1 hour pulse experiments, NF-M and NF-H showed very faint spots, if any, under these conditions. Newly synthesized NF-M and NF-H, however, were clearly seen after 4 hr of incubation with <sup>35</sup>S-methionine.

#### Localization of NF RNA Transcripts

**In situ hybridization for NF-L.** Sections of the sciatic nerve proximal stumps, 48 hr after injury, hybrid-

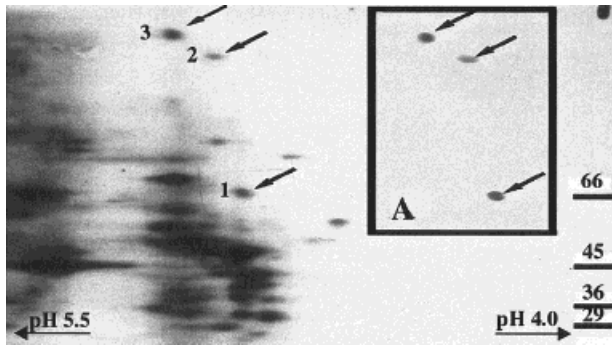


Fig. 6. Two-dimensional electrophoresis and fluorography of the nitrocellulose blot of newly synthesized proteins of the proximal stump of the rat sciatic nerve labeled with  $^{35}\text{S}$ -methionine. Spot number 1 corresponds to the NF-L protein; spot number 2 is NF-M and spot number 3 is the NF-H. The three proteins labeled in the fluorograms were detected by immunoblot with specific monoclonal antibodies. The spots identified by immunoblotting (see frame) corresponded to the fluorogram spots.

ized with the antisense riboprobe for the 68 kDa mRNA, showed labeling over myelin, and the interface boundary between myelin and axoplasm (Fig. 7). Few axons showed reaction over the axoplasm. Labeling with the antisense riboprobe was clearly different from that obtained by control hybridizations with the sense riboprobe, performed over similar proximal stump sections.

**Immunohistochemistry of S1 ribosomal protein.** The examination of nerve sections immunostained with the monoclonal antibody against S1 ribosomal protein, yielded an immunoreaction in the region bordering myelin and axoplasm (see Fig. 7D). Immunostaining of the Schwann cell bodies can be observed and sometimes the immunoreaction was observed extending over myelin.

## DISCUSSION

The three mRNAs coding for the neurofilament subunits were detected in the intact sciatic nerve, as well as in the proximal and distal stumps of the severed sciatic nerve of rats using RT-PCR and Northern blot. The validity of RT-PCR analysis was supported by the following: (a) the amplified DNA fragments had the predicted size (see Fig. 1 and 2) and the cloning and sequencing of the amplified segments showed a complete correspondence with the sequences of the three target mRNAs; (b) the amplification was independent of genomic DNA and DNase digestion of nerve RNA before RT-PCR did not interfere with amplification; (c) the reaction was RNA dependent because RNase digestion of nerve RNA, before RT-PCR resulted in no amplification (see Fig. 3), and the same occurred when the reverse transcriptase reaction step was omitted (data not shown); (d) RT-PCR analysis, using cDNA from total liver RNA (negative controls), did not yield any amplification products (see Fig. 1); and (e) RT-PCR of rat brain RNA, produced amplification of the three target mRNAs (positive controls, Fig. 1).

The Northern blot analysis partially confirmed the results obtained from RT-PCR. The molecular weights of the mRNAs detected for the two neurofilament proteins in the proximal stumps were consistent with the previously reported sizes of 2.5 kb and 4.0 kb for NF-L, and 3.2 kb for NF-M (Julien et al., 1985; Hoffman et al. 1987; Wong and Oblinger, 1990). Thus, these data indicate that the full size transcripts are present in the proximal stump. This is consistent with the results of Roberson et al. (1992) who detected by Northern blot the NF-L mRNA in the distal stump of the severed sciatic nerve of rats. The latter finding has been extended because we not only found two of the three mRNAs in the proximal stump of severed sciatic nerves of adult rats by Northern blot, but also found the three mRNAs in the intact nerve, and in both stumps of the severed sciatic nerve of adult rats by RT-PCR. NF-M expression was only reported in normal nerves up to postnatal day eleven by Kelly et al. (1992) and Fabrizi et al. (1997).

Although the RT-PCR was not quantitative under the experimental conditions performed, our results indicate that the transcription products are up-regulated by nerve injury. The latter result is also consistent with incorporation of tritiated uridine and amino acids, as evaluated by autoradiography, that extended findings from previous reports (Benech et al., 1982). Axoplasmic grain density of the proximal stump reached a plateau 8 days after injury. During this interval, it was always higher than that of decentralized distal stump. Furthermore, in the latter, grain density decayed near to background at the end of this interval, that may be due to the axon degeneration in the distal stump. The plateau reached by RNA and protein synthesis of the proximal stump at Day 8 may be related to the formation of an amputation neuroma caused by blocking of re-growth into the distal stump. The presence of newly synthesized RNA as indicated by the radioautograms of distal stump axoplasm, as well as the detection by RT-PCR in this stump of mRNAs coding for the three neurofilament subunits, support the idea that these mRNAs must have been originated in Schwann cells, because the distal stump was separated from the neuronal perikaryon. Similarly, radioautograms of proximal stumps also indicated locally synthesized RNA, because the latter were separated at least 4 cm from neurons of origin, and the duration of radiolabeling was 60 min or less (i.e., the fastest axonal transport would have required more than 150 min to be transported 4 cm).

As indicated by the results of RT-PCR and Northern blot analysis, it can be inferred that there is a lower level of expression of NF-H compared to that of NF-L or NF-M. The relative differences could be related to the reported proportion, 5:2:1 (NF-L: NF-M: NF-H), of the three NF subunits in neurons (Shekhet and Lasek, 1982; Lee and Cleveland, 1996).

In situ hybridization of NF-L mRNA using the NF-L riboprobe in the proximal stump showed signals largely restricted to Schwann cells, myelin, and a zone between the myelin sheath and axoplasm, with scarcely



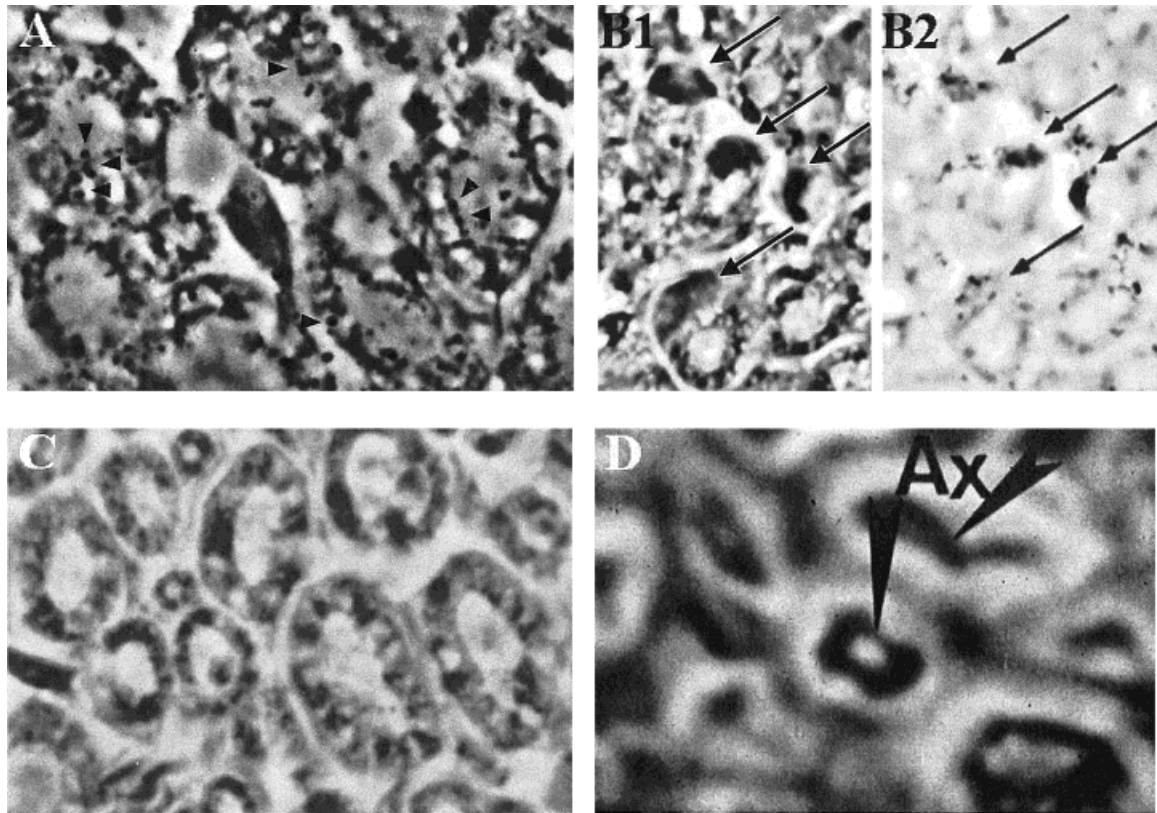


Fig. 7. In situ hybridization in the proximal stump of the severed sciatic nerve 48 hr after lesion. The riboprobe used was the RNA coding for the NF-L neurofilament subunit. Sections were stained only with alkaline phosphatase and reaction was observed as precipitates (arrowheads in **A**, arrows in **B2**; phase contrast microscopy). (**A**, **B1** and **B2**) Hybridization of the antisense riboprobe. (**B1**) Schwann cell perinuclear area (arrows), (**B2**) the same area in a different focal plane showing

the accumulation of the precipitate over the perinuclear area of Schwann cell. (**C**) Hybridization of the sense riboprobe (control). (**D**) Immunocytochemistry (bright-field microscopy) of the sciatic nerve using a monoclonal antibody against protein S-1 of ribosomes, arrowheads shows HRP immunostaining over a region between axon (Ax) and myelin.

any in the axoplasm. Whereas spatial resolution was insufficient to determine whether the hybridization signals at the myelin-axon boundary was localized in myelin, or at the periphery of axoplasm, it is important to note that there is evidence of specialized RNA-containing domains in the cortical zone of the axoplasm of goldfish Mauthner cell fibers. These are so-called periaxoplasmic plaque formations, that have been visualized at the light microscope (LM) level after YOYO-1 fluorescent staining. The presence of polyribosomes there, have been also documented by ESI at an EM level (Koenig and Martin, 1996). Correspondence between YOYO-1 fluorescence and specific immunostaining with an rRNA antibody (Y10B) in the same preparation, provides additional confirmation at LM level (Sotelo-Silveira and Koenig, unpublished observations). Similar periaxoplasmic plaque formations are present in axoplasmic whole mounts isolated from spinal root fibers of rabbits (Koenig and Martin, 1997) and rats (personal communication). The latter findings are also consistent with immunostaining of S1 ribosomal protein by a monoclonal antibody that localized in the same zone in the present study (see Fig. 7D).

One-dimensional ultramicroelectrophoresis in the goldfish M-axon in vitro, indicated that actin and tubulin are locally synthesized (Koenig, 1991). Radiolabeled NF proteins could also be identified in the latter study. Local de novo synthesis of NF-L in the sciatic nerve of the rat was identified by use of a monoclonal antibody and bi-dimensional electrophoresis (Sotelo et al., 1992). The present work further indicates that the three NF proteins are synthesized locally using endogenous cognate mRNAs, because NF proteins in the proximal stump were just labeled for 1 hr, and they are considered components of the slowest axonal transport rate group (Hoffman and Lasek, 1975), that precluded transport from neuronal body. Thus, the axon is a potential site of synthesis of NF polypeptides, that is supported by findings in the Mauthner axon (see above), where NF-M mRNA has also been identified (Weiner et al., 1996). The question of whether NF proteins are synthesized within the axon compartment is clearly an important issue that merits further study.

The detection of NF-L mRNA in Schwann cells and myelin of proximal stumps by in situ hybridization, also suggests that it is expressed there. All of these features

suggest that neurofilament mRNAs are transcribed, and translated locally in a manner related to nerve regeneration. The transcription of these mRNAs could be a normal occurrence in Schwann cells, that is down-regulated in intact nerve and up-regulated after injury.

Among issues to be addressed in the future are the exact location of synthesis of these RNAs and proteins, whether the latter are assembled into the 10 nm filament, and what role they play in normal nerve and during regeneration. Local translation of NF mRNAs could support the maintenance of the axonal cytoskeleton (Koenig, 1991). The finding of protein synthesis in axonal nerve endings of synaptosome preparations (Crispino et al., 1993a,b, 1997), provides additional evidence of the first possibility. Recent observations indicate that protein synthesis in synaptosomes can be modulated by calcium (Benecch et al., 1997) similar to that in the sciatic nerve (Sotelo et al., 1997). In general, these studies pose the question of significance of local protein synthesis in the context of the regulation of axonal growth and regeneration, as well as synaptic changes related to long term plasticity in the presynaptic terminals (Martin et al., 1997). Finally, local protein synthesis in the axonal compartment may also play a role in diseases states related to axonopathies, including diabetic neuropathy.

#### ACKNOWLEDGMENTS

This work was supported by the European Union Grant CT1-CT93-0037UY, Japanese International Cooperation Agency (JICA), BID-CONICYT, MEYC, CSIC, CIDEA (Fac Veterinaria), PEDECIBA and OAS. We thank Dr. Edward Koenig and Dr. Antonio Giuditta for the careful reading of the manuscript, Dr. Ricardo Ehrlich and all the people of the Biochemistry Section for their kind help. We also thank Miss Susana Pais for the technical assistance.

#### REFERENCES

- Alvarez J, Benecch CR. 1983. Axoplasmic incorporation of amino acids in a myelinated fiber exceeds that of its soma: a radioautographic study. *Exp Neurol* 82:25–42.
- Alvarez J, Giuditta A, Koenig E. 2000. Protein synthesis in axons and terminals: significance for maintenance, plasticity and regulation of phenotype—with a critique of slow transport theory. *Prog Neurobiol* 62:1–62.
- Bassell GJ, Zhang H, Byrd AL, Femino AM, Singer RH, Taneja KL, Lifshitz LM, Herman IM, Kosik KS. 1998. Sorting of beta-actin mRNA and protein to neurites and growth cones in culture. *J Neurosci* 18:251–265.
- Benecch C, Sotelo JR, Menendez J, Correa-Luna R. 1982. Autoradiographic study of RNA and protein synthesis in sectioned peripheral nerves. *Exp Neurol* 76:72–82.
- Benecch JC, Crispino M, Kaplan BB, Giuditta A. 1997. Protein synthesis in presynaptic endings of squid brain: regulation by  $Ca^{2+}$  ions. In: Sotelo JR, Benecch JC, editors. Calcium and cellular metabolism: transport and regulation. New York: Plenum Press. p 155–163.
- Chomczynski P, Sacchi N. 1987. Single-step method of RNA isolation by acid guanidinium thiocyanate-phenol-chloroform extraction. *Anal Biochem* 162:156–159.
- Chun JT, Gioio AE, Crispino M, Giuditta A, Kaplan BB. 1995. Characterization of the squid enolase mRNA: sequence analysis, tissue distribution, and axonal localization. *Neurochem Res* 20:923–930.
- Crispino M, Castigli E, Perrone-Capano C, Martin R, Menichini E, Kaplan BB, Giuditta A. 1993a. Protein synthesis in a synaptosomal fraction from squid brain. *Mol Cell Neurosci* 4:366–374.
- Crispino M, Kaplan BB, Martin R, Alvarez J, Chun JT, Benecch JB, Giuditta A. 1997. Active polysomes are present in the large presynaptic endings of the synaptosomal fraction from squid brain. *J Neurosci* 17:7694–7702.
- Crispino M, Perrone-Capano C, Kaplan BB, Giuditta A. 1993b. Neurofilaments proteins are synthesized in nerve endings from squid brain. *J Neurochem* 61:1144–1146.
- Edstrom A, Sjostrand J. 1969. Protein synthesis in the isolated Mauthner nerve fibre of goldfish. *J Neurochem* 16:67–81.
- Fabrizi C, Kelly BM, Gillespie CS, Schlaepfer WW, Scherer SS, Brophy PJ. 1997. Transient expression of the neurofilament proteins NF-L and NF-M by Schwann cells is regulated by axonal contact. *J Neurosci Res* 50:291–299.
- Gainer H, Tasaki I, Lasek RJ. 1977. Evidence for the glia-neuron protein transfer hypothesis from intracellular perfusion studies of squid giant axons. *J Cell Biol* 74:524–530.
- Gioio AE, Chun JT, Crispino M, Perrone-Capano C, Giuditta A, Kaplan BB. 1994. Kinesin mRNA is present in the squid giant axon. *J Neurochem* 63:13–18.
- Giuditta A, Cupello A, Lazzarini G. 1980. Ribosomal RNA in the axoplasm of the squid giant axon. *J Neurochem* 34:1757–1760.
- Giuditta A, Hunt T, Santella L. 1986. Messenger RNA in the squid axoplasm. *Neurochem Intern* 8:435–442.
- Giuditta A, Menichini E, Perrone-Capano C, Langella M, Martin R, Castigli E, Kaplan BB. 1991. Active polysomes in the axoplasm of the squid giant axon. *J Neurosci Res* 26:18–28.
- Giuditta A, Metafora S, Felsani A, Del Rio A. 1977. Factors for protein synthesis in the squid giant axon. *J Neurochem* 28:1393–1395.
- Hoffman PN, Cleveland DW, Griffin JW, Landes PW, Cowan NJ, Price DL. 1987. Neurofilament gene expression: a major determinant of axonal caliber. *Proc Natl Acad Sci USA* 84:3472–3475.
- Hoffman PN, Lasek RJ. 1975. The slow component of axonal transport. Identification of major structural polypeptides of the axon and their generality among mammalian neurons. *J Cell Biol* 66:351–366.
- Hügler B, Hazan R, Scheer U, Franke W. 1985. Localization of ribosomal protein S1 in the granular component of the interphase nucleolus and its distribution during mitosis. *J Cell Biol* 100:873–886.
- Jordan C, Friedrich V, Dubois-Dalcq M. 1989. In situ hybridization analysis of myelin gene transcripts in developing mouse spinal cord. *J Neurosci* 9:248–257.
- Julien JP, Ramachandran K, Grosveld F. 1985. Cloning of a cDNA encoding the smallest neurofilament protein from the rat. *Biochim Biophys Acta* 398–404.
- Kaplan BB, Gioio AE, Perrone-Capano C, Crispino M, Giuditta A. 1992.  $\beta$ -Actin and  $\beta$ -tubulin are components of a heterogeneous mRNA population present in the squid giant axon. *Mol Cell Neurosci* 3:133–144.
- Kelly BM, Gillespie CS, Sherman DL, Brophy PJ. 1992. Schwann cells of the myelin forming phenotype express neurofilament protein NF-M. *J Cell Biol* 118:397–410.
- Koenig E. 1967. Synthetic mechanisms on the axon. IV. In vitro incorporation of [ $^3$ H]precursors into axonal protein and RNA. *J Neurochem* 14:437–446.
- Koenig E. 1979. Ribosomal RNA in Mauthner axon: implications for a protein synthesizing machinery in the myelinated axon. *Brain Res* 175:95–107.
- Koenig E. 1989. Cycloheximide-sensitive  $^{35}$ S-methionine labeling of proteins in goldfish retinal ganglion cell axons in vitro. *Brain Res* 481:119–123.

- Koenig E. 1991. Evaluation of local synthesis of axonal proteins in the goldfish Mauthner cell axon and ventral roots of the rat in vitro. *Mol Cell Neurosci* 2:384–397.
- Koenig E, Adams P. 1982. Local protein synthesizing activity in axonal fields regenerating in vitro. *J Neurochem* 39:386–400.
- Koenig E, Giuditta A. 1999. Protein-synthesizing machinery in the axon compartment. *Neuroscience* 88:5–15.
- Koenig E, Martin R. 1996. Cortical plaque-like structures identify ribosome containing domains in the Mauthner axon. *J Neurosci* 16:1400–1411.
- Koenig E, Martin R. 1997. RNA containing periaxoplasmic plaques domains in rabbit axons. *Mol Biol Cell* 7(Suppl):652a.
- Lasek RJ, Gainer H, Barker JL. 1977. Cell-to-cell transfer of glial proteins to the squid giant axon. The glia-neuron protein transfer hypothesis. *J Cell Biol* 74:501–523.
- Lee MK, Cleveland DW. 1996. Neuronal intermediate filaments. *Annu Rev Neurosci* 19:187–217.
- Lewis S, Cowan NJ. 1985. Genetics, evolution, and expression of the 68,000-mol-wt neurofilament protein: isolation of a cloned cDNA probe. *J Cell Biol* 100:843–850.
- Marchuk D, Drumm M, Saulino A, Collins FS. 1991. Construction of T-vectors, a rapid and general system for direct cloning of unmodified PCR products. *Nucleic Acids Res* 19:11–54.
- Martin KC, Casadio A, Zhu H, Yaping E, Rose JC, Chen M, Bailey CH, Kandel ER. 1997. Synapse-specific, long term facilitation of Aplysia sensory to motor synapses: a function for local protein synthesis in memory storage. *Cell* 91:927–938.
- Martin R, Fritz W, Giuditta A. 1989. Visualization of polyribosomes in the post-synaptic area of the squid giant synapse by electron spectroscopic imaging. *J Neurocytol* 18:11–18.
- Mohr E, Richter D. 1992. Diversity of mRNAs in the axonal compartment of peptidergic neurons in the rat. *Reg Peptides* 45:21–24.
- Nixon RA, Shea TB. 1992. Dynamics of neuronal intermediate filaments: a developmental perspective. *Cell Motil Cytoskeleton* 22:81–91.
- O'Farrell PH. 1975. High resolution two-dimensional electrophoresis of proteins. *J Biol Chem* 250:4007–4021.
- Olink-Coux M, Hollenbeck PJ. 1996. Localization and active transport of mRNA in axons of sympathetic neurons in culture. *J Neurosci* 16:1346–1358.
- Rapallino MV, Cupello A, Giuditta A. 1988. Axoplasmic RNA species synthesized in the isolated giant axon. *Neurochem Res* 13:625–631.
- Roberson MD, Toews AD, Goodrum JF, Morell P. 1992. Neurofilament and tubulin mRNA expression in Schwann cells. *J Neurosci Res* 33:156–162.
- Saiki RK, Gelfand DH, Stoffel S, Scharf SJ, Higuchi R, Horn GT, Mullin KB, Ehrlich HA. 1988. Primer-directed enzymatic amplification of DNA with a thermostable DNA polymerase. *Science* 239:487–491.
- Sambrook J, Fritsch EF, Maniatis T. 1989. *Molecular cloning: a laboratory manual*. Cold Spring Harbor Laboratory Press, 2nd Ed.
- Sanger F, Nicklen S, Coulson AR. 1977. DNA sequencing with chain terminator inhibitors. *Proc Natl Acad Sci USA* 74:5463–5467.
- Sanguinetti CJ, Dias Neto E, Simpson AJG. 1994. Rapid silver staining and recovery of PCR products separated on polyacrylamide gels. *BioTechniques* 17:915–918.
- Shecket G, Lasek RJ. 1982. Preparation of neurofilament protein from guinea pig peripheral nerve and spinal cord. *J Neurochem* 298:277–279.
- Sotelo JR, Benech C, Kun A. 1992. Local radiolabeling of the 68 kDa neurofilament protein in rat sciatic nerves. *Neurosci Lett* 144:174–176.
- Sotelo JR, Verdes JM, Kun A, Benech JC, Sotelo Silveira JR, Calliari A. 1997. Regulation of neuronal protein synthesis by calcium. In: Sotelo JR, Benech JC, editors. *Calcium and cellular metabolism: transport and regulation*. New York: Plenum Press. p 125–143.
- Sotelo JR, Kun A, Benech JC, Giuditta A, Morillas J, Benech CR. 1999. Ribosomes and polyribosomes are present in the squid giant axon: an immunocytochemical study. *Neuroscience* 90:705–715.
- Tobias GS, Koenig E. 1975. Axonal protein synthesizing activity during the early outgrowth period following neurotomy. *Exp Neurol* 49:221–234.
- Van Minnen J, Bergman JJ, Van Kesteren ER, Smit AB, Geraerts WP, Lukowiak K, Hasan SU, Syed NI. 1997. De novo protein synthesis in isolated axons of identified neurons. *Neuroscience* 80:1–7.
- Weiner O, Zorn D, Krieg A, Bittner GD. 1996. Medium-weight neurofilament RNA in goldfish Mauthner axoplasm. *Neurosci Lett* 213:83–86.
- Wong J, Oblinger MM. 1990. Differential regulation of peripherin and neurofilament gene expression in regenerating rat DRG neurons. *J Neurosci Res* 27:332–341.

**Trabajo III:** Sotelo Silveira, J.R., Koenig E.  $\beta$ -actin is localized in ribosomal domains of myelinated axons. Manuscrito.

## **Actin mRNA is localized in periaxoplasmic ribosomal domains of myelinated axons.**

**José R. Sotelo Silveira\*<sup>o</sup> & Edward Koenig<sup>a</sup>.**

\* Department of Cell & Molecular Biology, Facultad de Ciencias, Universidad de la Republica, Montevideo, Uruguay.

<sup>o</sup> Laboratory of Proteins & Nucleic Acids, Instituto de Investigaciones Biológicas Clemente Estable, Montevideo, Uruguay.

<sup>a</sup> Physiology & Biophysics, State University of New York at Buffalo, New York, 14214, USA.

### **Abstract.**

Recent structural studies have shown that myelinated axons contain cryptic discrete ribosomal domains located around the periphery of axoplasm at intermittent intervals. They appeared evident if axoplasm is removed from its myelin sheath (wholemout) showing a structural correlate that overlies and marks the domain, which is the basis for calling them “periaxoplasmic ribosomal plaques” (PARP). Thus, the systematic localization of translational machinery in the PARP domain of Mauthner and mammalian axons can account for autochthonous protein synthesis included actin. The latter assumption suggest that PARP domain should contain the mRNA coding for actin. This question was evaluated in axoplasmic wholemounts isolated from the goldfish Mauthner fiber and myelinated fibers of rat and rabbit spinal nerve roots. Periaxoplasmic plaques domains were identified by epifluorescence microscopy with YOYO-1, with ribosome-specific monoclonal antibody Y10B, and by phase contrast microscopy revealing the plaque structural correlates. Occurrence and localization of beta actin mRNA was assessed by

fluorescence *in situ* hybridization and RT-PCR. The present paper shows that beta actin mRNA is enriched in periaxoplasmic plaques, which may indicate that plaque domains are very likely local sites of translational activity within the axon compartment.

Keywords: translation, mRNA transport, axon.

## **Introduction.**

Targeting and specific localization of mRNA, as well as its local translation, in different neuronal territories is recognized nowadays as an important mechanism underlying plasticity and pattern formation in the nervous system. Although RNA localization in axons has been well documented in recent years, evidence for RNAs in the axonal compartment has been a subject of controversial debate (Koenig and Giuditta 1999, Tiedge et al 1999, Alvarez et al 2000). In invertebrates (eg, squid) molecules like rRNA, tRNA and mRNA encoding cytoskeletal, motor and soluble protein has been found (for review Giuditta et al 2002). In the case of vertebrates the reports have been restricted mainly to *in vitro* approaches like developing neurons in culture where  $\beta$  actin mRNA was shown to be transported, localized and translated in the axonal growth cones (Bassell et al, 1998, Zheng et al, 2001). The mRNA encoding Tau axonal protein was shown to be targeted and translated in differentiated axons of P19 cells in culture (Aronov et al., 2001, Aronov et al., 2002). Furthermore, a series of reports identified mRNAs coding for neuropeptide precursors in mature mammalian axons of magnocellular hypothalamic neurons (Mohr, 1999). In vertebrates, the translation of axonal mRNAs was demonstrated mainly for

developing neurons in culture too. It has been documented for retinal axons (Koenig, 1984), for immature axons (Eng et al., 1999), in axonal growth cones (Campbell and Holtz 2001), in regenerating axons (Zheng et al., 2001) and axons growing in the developing spinal cord (Brittis et al., 2002). In the latter, transfected mRNAs coding for EphA2 receptor was translated and expressed on the axonal surface. In the case of mature axons, a pattern of newly synthesized protein was obtained from rat ventral root axons and the giant Mauthner axon, showing labeling of putative actin, tubulin and neurofilaments. In rat adult sciatic nerves, the three neurofilament subunits were shown to be locally synthesized in the proximal and distal stumps of the sectioned sciatic nerves (Sotelo et al, 1992; Sotelo-Silveira et al, 2000)

Although cellular and biochemical evidences supporting protein synthesis in axons has been accumulated over the years, localization of the translation machinery was elusive for a long period. Besides the reports of Zelena (1972) identification of ribosomes in axons was not clear. Using a high affinity nucleic acid binding dye YOYO-1 and Electron Spectroscopic Imaging Electron Microscopy (ESI-EM) and immunohistochemistry, Koenig and colleagues described that ribosomes were localized in restricted subaxolemal cortical domains in close relationship with cortical actin axonal network. These structures were called periaxoplasmic ribosomal plaques (PARPs) (Koenig & Martin 1996, Koenig et al., 2000). Whether these ribosomal domains are actively translating proteins, mRNA coding for those specific proteins should be preferentially localized inside these domains. According to Alvarez et al. (2000) the proteins transported by the slow axonal transport (cytoskeletal proteins like actin, tubulin and neurofilaments) are good candidates to be synthesized in the PARPs.

Since putative  $\beta$ -actin was shown to be locally synthesized in Mauthner axon and ventral root axons of rats (Koenig, 1991) and its mRNA was selectively transported to axonal territory (Bassell et al, 1998), our main goal in the present paper was to investigate the presence and localization of this mRNA in the axon and its relationship to the periaxoplasmic plaque domains. Results reported here indicate that  $\beta$  actin mRNA is localized in periaxoplasmic plaques of goldfish Mauthner axons and ventral roots axons of rabbit and rat. Since this is the first report, to our knowledge, of the localization of an mRNA in mammalian mature myelinated axons localized in PARPs, its role and function are discussed.

### **Material and Methods.**

#### **Isolation of axoplasmic wholemounts of myelinated spinal root fibers.**

Lumbar spinal nerve roots that were used in the present study were dissected from rats according to international rules of animal care. Several nerve root/rootlets were suspended in a modified gluconate-substituted calcium-free Cortland salt solution containing (in mM) 132 Na-gluconate, 5 KCl, 20 HEPES, 10 glucose, 3.5 MgSO<sub>4</sub>, and 2 EGTA, pH 7.2, stored at 4°C (Koenig and Martin, 1996, Koenig et al 2000). A piece of nerve root/rootlet (3-5 mm), was immersed in a solution of 30 mM zinc acetate, 0.1 M *N*-tris[hydroxymethyl]methylglycine (Tricine; Sigma, St. Louis, MO), pH 4.8, for 10 min and then it was placed in a 35 mm plastic culture dish containing 2 ml of a "pulling" solution, of aspartate neutralized by Tris at pH 5.5. A "critical permissive concentration" (CPC) of the "pulling" media was determined for each animal. The CPC usually was sharply defined for a given animal in a



range of concentrations of 35-45 mM of aspartate. The pulling media was made from a stock solution containing 0.2 M aspartic acid (Sigma), 0.192 M Tris, 5mM Na<sub>2</sub>S<sub>2</sub>O<sub>8</sub>, and 0.1% Tween 20 (to reduce surface tension), pH 5.5. For each test, plaque occurrence was evaluated after staining with YOYO-1 (see below). Isolated axoplasms were attached with the aid of eyebrow hair tools to a N<sup>o</sup> 1 coverslips coated with 1% 3-aminopropyltriethoxysilane (Polysciences, Warrington, PA) in ethanol.

### **Isolation of axoplasmic whole mounts and myelin sheath from the Mauthner cell.**

Common goldfish (4-5 inches, Grassy Forks Fisheries, Martinsville, IN) were used. The goldfish was anesthetized by cooling in ice water and all procedures with native tissues were performed in an ice bath. The isolated spinal cord and lower brain stem (Koenig and Martin 1996) were suspended in Cortland solution (see above). Axoplasms were translated out using N<sup>o</sup>5 forceps from 5 to 8 mm tissue segments in a pulling solution at a CPC containing a combination of Aspartate neutralized with Tris, pH 5.5, 10 mM Zinc Acetate and 1 mM MgSO<sub>4</sub>, 0.1% Tween 20. The CPC usually was between 35 to 55 mM Aspartate. Isolated axoplasms were attached as described above. Myelin sheaths were isolated using the same CPC conditions; after axons were pulled out the myelin sheath is left behind but protrudes out from spinal cord. Then, using N<sup>o</sup>5 forceps short segments of the sheath that surrounded the Mauthner axon were collected to isolate their RNA. Histochemical observation of the latter is not possible since the structure is not well preserved after axoplasm isolation.

YOYO-1 staining of axoplasmic whole mounts.

The presence of periaxoplasmic plaques in axoplasmic whole mounts was assessed by staining of the whole mounts with YOYO-1 iodide (491/509; Molecular Probes, Eugene, OR). One  $\mu$ l of stock YOYO-1 (1 mM in DMSO) was added to the pulling medium (final concentration, 1:5000) for 15 min. The YOYO-1 was washed out by brief immersion of the coverslip containing axons in acidified 0.15 M ammonium acetate (i.e., NH<sub>4</sub>OAc; pH-adjusted to 4.5 with acetic acid) and 0.1% Tween 20. For fluorescence microscopy the coverslip with axoplasmic sprays was mounted on a flow-thru chamber. The chamber was constructed by inverting the cover slip over spacers (0.5-1 mm thick) made of Silastic elastomer (Dow Corning, Midland, MI) attached to a large glass coverslip (35 x 50 mm) taped to a thin "U"-shaped metal plate, and the well was filled with acidified NH<sub>4</sub>OAc solution.

### **Microscopy.**

For routine fluorescence microscopy, axoplasms were observed in an Olympus BHS microscope equipped with an air cooled CCD camera (DAGE-MTI) or a Nikon Diaphot inverted microscope. The confocal microscope was a Bio-Rad MRC-1000 (Hercules, Ca.) with a krypton-argon laser in combination with an upright Nikon Optiphot microscope.

### **Probes.**

Digoxigenin-UTP (Boehringer-Manheim) labeled probes were synthesized by in vitro transcription with either T7 or SP6 RNA polymerase (Promega). The coding region of beta actin cDNA from goldfish (a gift from Dr.

R Peter, University of Alberta, Canada) was used as template of transcription reactions. The high degree of conservation between beta actin sequences among goldfish and rat or rabbit (approximately 87%) allowed us to use the probe in the other two different specimens (rat and rabbit).

### ***In situ* hybridization.**

Axonal wholemounts were fixed in 3.75% paraformaldehyde in 0.1 M sodium diethylmalonate [0.1 M diethylmalonic acid (Aldrich, Milwaukee, WI), pH-adjusted to 7.2 with NaOH] and 0.1% Tween 20, pH 7.2, for 3 h at room temperature. They were washed two times in 0.15 M ammonium acetate pH 7.0 and then dehydrated in alcohol (70%, 95% and 100% for 5 min each). After air-drying they were incubated in hybridization solution containing (4x SSC, 500.g/l salmon sperm DNA, 250µg/µl yeast tRNA, 1x Denhardt and 10% (w/v) dextran sulfate) for 15 min at 42°C in a humid chamber. Previously denatured sense or antisense beta actin RNA probe was mix with hybridization solution at a final concentration of 2ng/µl) and then axonal wholemounts were incubated for 3 hours at 42°C in humid chamber. Coverslips were washed under agitation in 4X SSC for 20 min., at room temperature. Two final high stringency washes (0.2x SSC, 0.2% BSA) were performed at 50°C under agitation. Detection of bound digoxigenin probe was performed using the Tyramide signal amplification protocol (Perkin Elmer Inc) according to manufacturer instructions. Digoxigenin was detected using an anti digoxigenin antibody conjugated with peroxidase (1/500) and tyramide reagent was labeled with Cy3 fluorochrome. Developing was carried out in the presence of 10% dextran sulfate to improve localization of tyramide deposition (Van Gijlswijk R et al., 1996).

### **Immunofluorescence staining.**

Axoplasmic whole mounts attached to a coverslip were fixed by immersion in 3.75% paraformaldehyde in 0.1 M sodium diethylmalonate [0.1 M diethylmalonic acid (Aldrich, Milwaukee, WI), pH-adjusted to 7.2 with NaOH] and 0.1% Tween 20, pH 7.2, for 15 min. They were washed in 0.15 M ammonium acetate and 0.1% Tween 20, pH 6.7, three times for 5 min each and then immersed in an immunoblocking solution, composed of 25 mM Tris HCl, 0.9% NaCl, 3.75% glycine, 1% of normal goat and/or donkey serum, 0.05% Tween 20, and 5 mM NaN<sub>3</sub> for 15 min. Incubation with primary antibody was for 1 hr on an orbital shaker. Coverslips were washed three times with a working buffer (i.e., blocking buffer with 0.1% serum) and incubated for 45 min with a secondary antibody conjugated to one of two Alexa fluorophores (Molecular Probes) having an excitation maximum at either 488 or 546 nm. The immunostained specimens were washed further three times for 5 min each before being mounted over spacers of the flow-thru chamber for microscopic examination (see above).

### **RNA isolation.**

Axons and myelin (see above) were isolated in the critical permissive concentration previously determined for each animal. Two RNA isolation methods were tested on those preparations. One is the Tri Reagent (MRC), the classical guanidine acid phenol extraction (Chomzinski and Sacchi, 1987) with the addition of a polyacrylic carrier recommended by the manufacturer. The other method was a single-phase phenol RNA isolation developed originally for ultramicroextraction of axonal samples (Koenig et al, 1979) with

minor modifications. The axons were immersed in 50-100ul of PEM (7.5M phenol, 50mM dithiothreitol, 0.7M propionic acid, 0.75M ethylenediamine, pH 8). The samples were centrifuged at 10.000xg at 4°C. The RNA precipitate was washed with 70% Ethanol, 1% SDS, then 70% Ethanol, then a wash of 95% Ethanol and air-dried. The precipitate was resuspended in 2 or 3 µl of RNase free water and stored at -80°C.

### **RT-PCR.**

RT-PCR analysis was performed using a one-tube system. This system uses a polymerase that can act as reverse transcriptase and DNA polymerase. The system was engineered to show very high affinity for RNA. Briefly, axonal or myelin RNA was added in different dilutions, to a mixture containing all the reagents to perform first strand synthesis and PCR amplifications (MasterAmp, Epicentre). Specific first strand primer (beta actin or GFAP) was used to synthesize the cDNA at 60° to 65°C. A total of 50 to 60 cycles were performed. The cycling temperatures were the following: 95°C for 1 min, 65 for 1 min. A final extension was performed for 5 min. at 65°C. RT-PCR amplification products were electrophoresed in non denaturing 6% acrylamide gels and detected using silver nitrate. PCR products of the expected size were purified from agarose gels and sequenced automatically by the BIGDYE chain terminator method (Applied Biosystem). Identity was confirmed using BLAST software.

## Results

### **Periaxoplasmic plaques of Mauthner axons have ribosomes that colocalize with structural correlates in phase contrast microscopy.**

Koenig & Martin (1996) showed that preserved PARP domains have structural correlates when observed using DIC or phase contrast microscopy. This correlates could be very useful to mark the presence of PARP domains when immunohistochemistry and *in situ* hybridization are difficult to be performed in sequence over the same preparation. Regarding the latter, the immunohistochemical characterization of Mauthner axon PARPs domains showed a very good colocalization between YOYO-1 and anti rRNA (Y10B) staining (figure 1, 1A-C). Colocalization is also seen between the YOYO-1 staining and the phase dense correlates seen in figure 1 (2A-B, and 3A-B), showing that goldfish plaques are not different to mammalian PARP (Koenig et al., 2000).

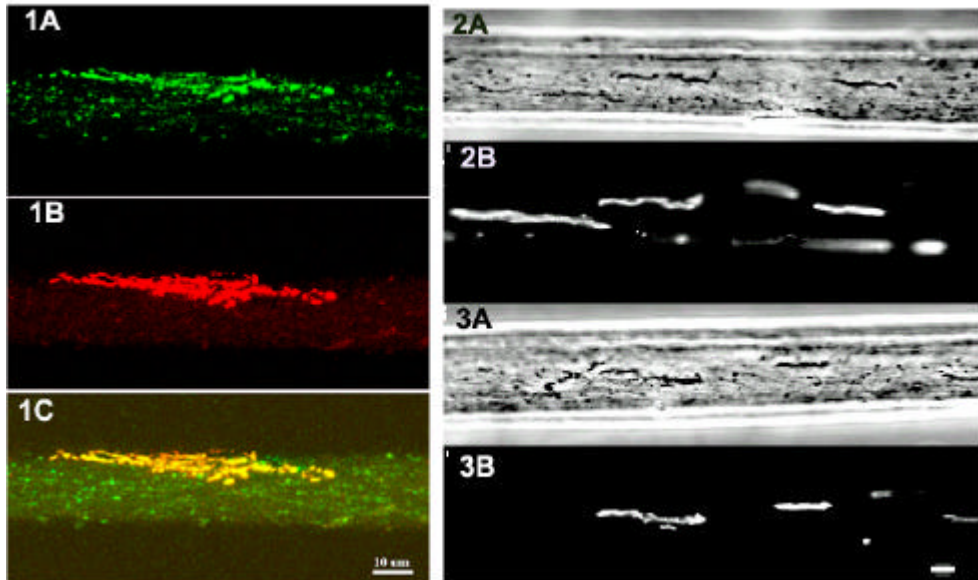


Figure 1. **Colocalization of YOYO-1, rRNA and phase dense correlates in periaxoplasmic plaques of Mauthner axons.** 1A-C, shows the labeling pattern of YOYO-1 (1A) and the anti rRNA monoclonal antibody (1B, Y10B) over a Mauthner axon. The merged image is shown in 1C, were a high degree of colocalization could be observed. 2 and 3 shows two examples of phase dense correlates (2A, 3A) that colocalize with high intensity YOYO-1 fluorescence (2B, 3B).

**$\beta$ -actin mRNA is enriched in periaxoplasmic ribosomal plaques of Mauthner axons.**

The *in situ* hybridization was performed on Mauthner axons that had phase contrast dense correlates identifying PARP domains using the anti sense and sense riboprobes from beta actin cDNA from goldfish. Anti-sense and sense probes were tested on spinal cord sections to standardize the signal to noise ratio (Figure 2, A and A'). Considering these results as starting conditions the ISH performed on Mauthner axons showed (figure 2) several examples of PARP domains with phase contrast dense correlates where beta actin signal was enriched. The pattern of the ISH signal was more intense in the periphery of PARP domain. Signal outside PARP domain was also observed to a minor level and could not be sharply distinguished of background fluorescence. Sense probes did not show particular enrichment in PARP domain areas (Figure 2F, F').



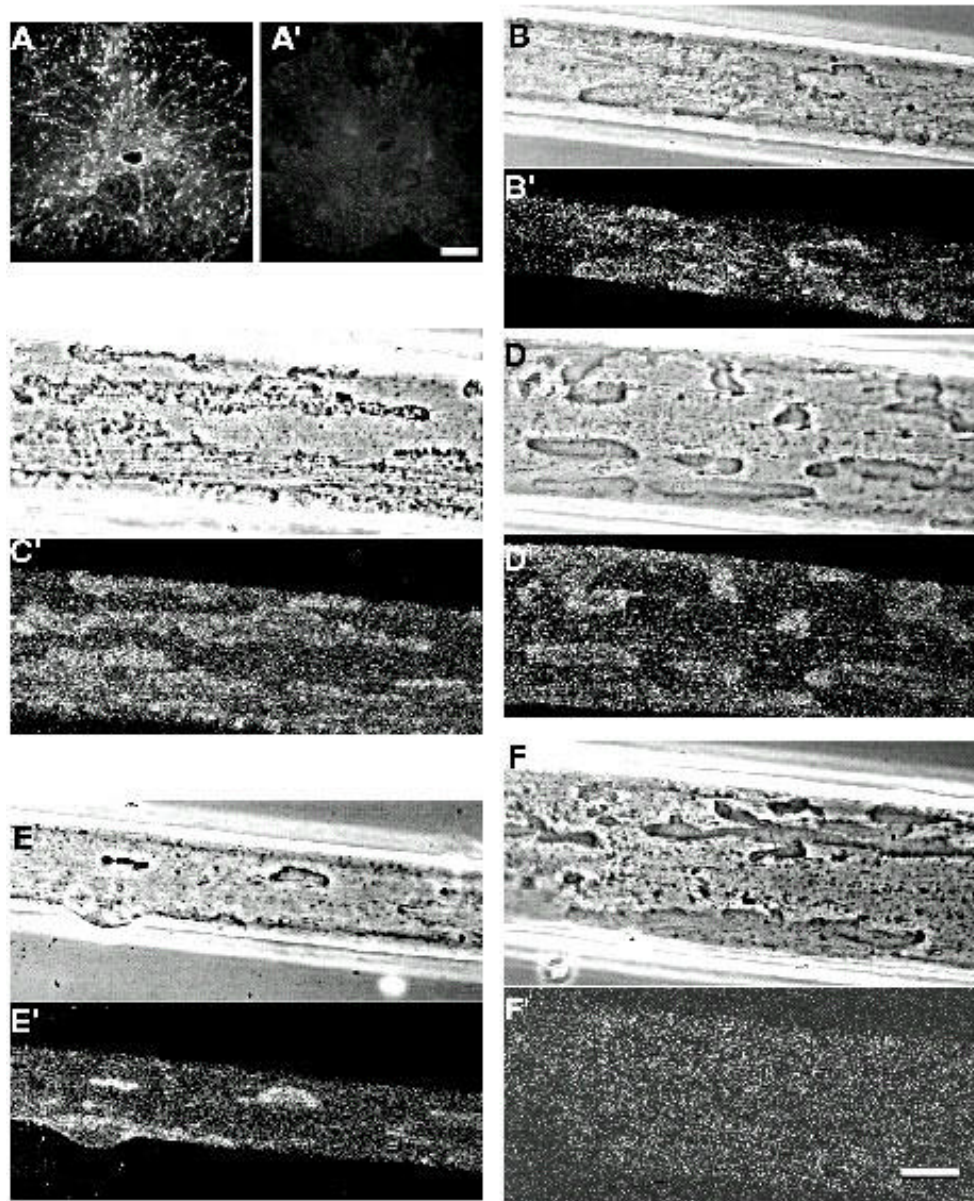


Figure 2. **beta Actin mRNA is enriched on PARP domains of Mauthner axons.** **A-A'**, ISH performed with actin antisense (A) and sense (A') riboprobes over a goldfish spinal cord cryostat section (positive control). From **B** to **D**, ISH performed with the anti sense riboprobe on several different axons. Images were obtained by confocal laser microscopy (approximately 0.5 $\mu$ m in thickness). Each pair of images is the phase contrast image (**B,C,D,E,F**) and its epifluorescence counterpart showing the Cy3-tyramide deposition (**B',C',D',E',F'**). **F,F'**, shows results obtained using the actin sense riboprobe.

$\beta$ -actin mRNA is detected by RT-PCR in RNA extracts from Mauthner axons.

The presence of beta actin mRNA was confirmed in Mauthner axons RNA extracts by RT-PCR using specific primers complementary to the 3' end untranslated region of this mRNA. As a control of glial cell RNA contamination GFAP mRNA specific primers were used. Results obtained are shown in figure 3. After 55-60 cycles of amplification, PCR products of the expected size for actin or GFAP were observed. Figure 3A shows the results of the analysis of an axonal RNA sample with both primers in comparison with 1ng of total goldfish brain RNA. This is an example of an axon that contains beta actin but not GFAP mRNA. Figure 3B is showing the analysis of RNA extracts from axons and its myelin in parallel. It can be observed that axonal RNA lacks GFAP mRNA but myelin has both mRNAs. Amplification reactions that lack template or the RNA is diluted just to a half or to a fifth does not show any amplification products. It is important to note that it was very frequent to find axonal RNA extracts with GFAP mRNA (not shown). Usually, beta actin mRNA was detected in axonal extracts regardless the presence or absence of GFAP. Both products had the expected size and were shown to be the target sequence after being fully sequenced.

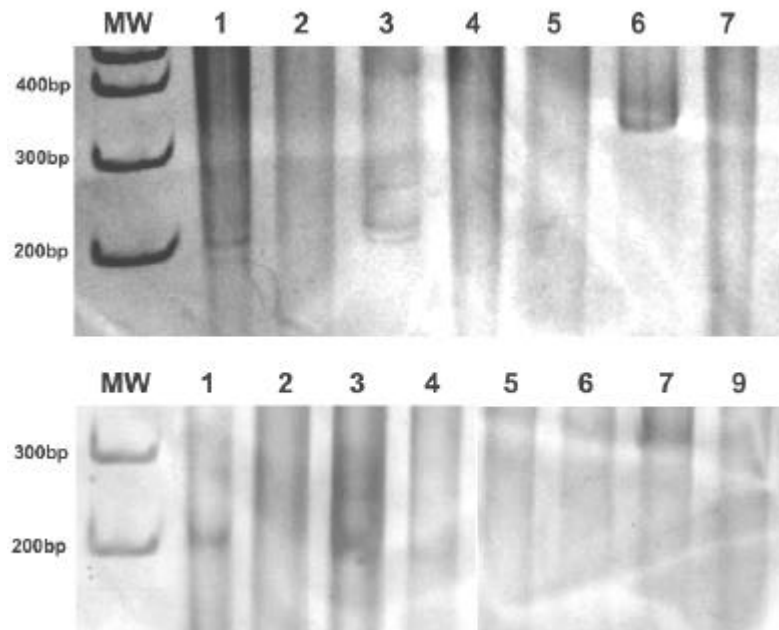


Figure 3. **Beta Actin mRNA is detected in RNA extracts of Mauthner axons by RT-PCR.** **A.** The same axonal RNA extract was reverse transcribed and PCR amplified using specific primers for the 3'UTR of beta actin mRNA (lanes 1 to 3) or for GFAP mRNA (4 to 6). Lanes 1 and 4 have pure RNA as template, lanes 2 and 5 the RNA used was diluted five times. In lanes 3 and 6 approximately 1ng of total brain RNA was used. Lane 7 is no cDNA control using GFAP primers. **B.** Axonal (lanes 1, 2, 5, 6) and myelin (lanes 3,4,7,9) RNA extracts were tested by RT-PCR with either beta actin primers (lanes 1,2,3,4) or GFAP primers (5,6,7,9). Pure RNA extracts were utilized on lanes 1,3,5 and 7. RNA extracts diluted to a half were used in lanes (2,4,6,9). Molecular weight markers are shown in the left lane (**MW**). The two gels are 6% acrylamide electrophoresis stained with silver nitrate.

**Actin mRNA is enriched in periaxoplasmic ribosomal plaques of rat and rabbit ventral root axons.**

*In situ* hybridization of rat and rabbit ventral root axons showed that actin riboprobe was localized in PARP domain. Fluorescence ISH signals for actin mRNA was also coincident with phase contrast dense correlates (Koenig et al., 2000). Figure 4 and 5 shows the results obtained in rat or rabbit ventral root axons wholemounts, respectively. Sense riboprobes do not show evident staining. Differences in size between PARP domains of rat and rabbit axons could be observed, but a careful analysis was not carried out. Fluorescent signals outside PARP domains were observed but this issue needs to be addressed with higher sensitive techniques.

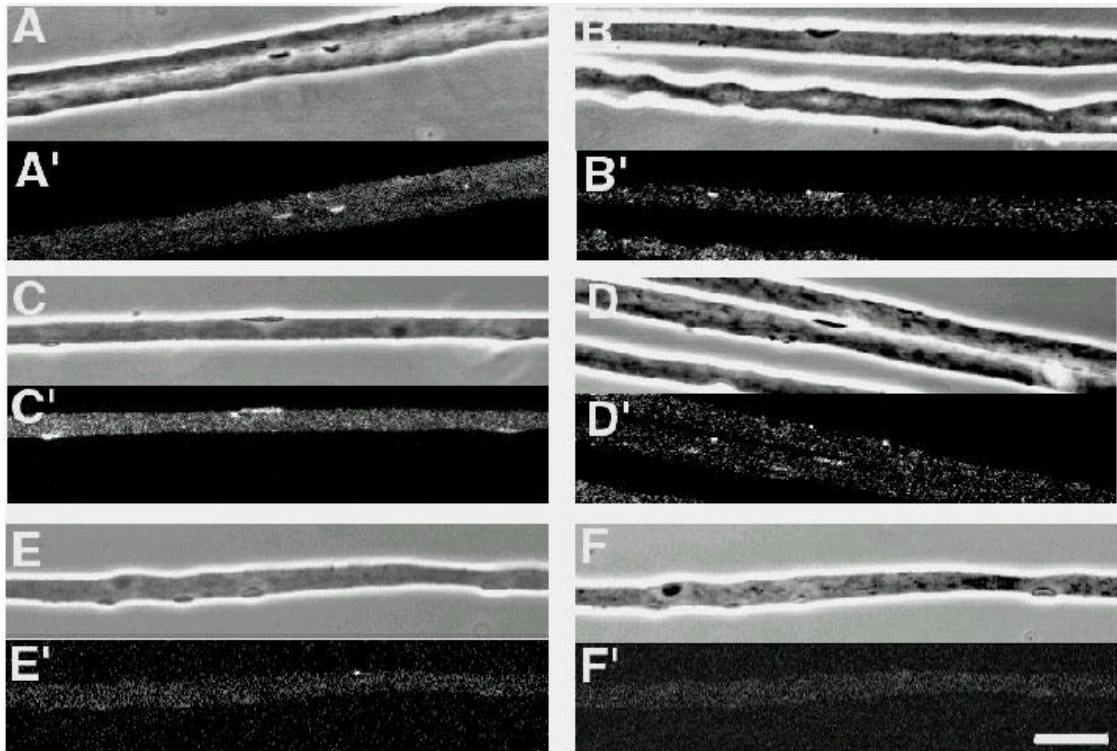


Figure 4. **Actin mRNA is detected by ISH in PARP domains of rat ventral root (VR) axons wholemount.** Paired micrographs of phase contrast (top, A, B, C, D, E, F), and ISH fluorescence (bottom, A', B', C', D', E', F') of the same axon area were obtained with a laser confocal microscope (0.5 $\mu$ m thick). ISH images (A' to D') were obtained using the anti sense riboprobe. ISH images (E' and F') were obtained using the sense riboprobe. Scale bar is 10  $\mu$ m.



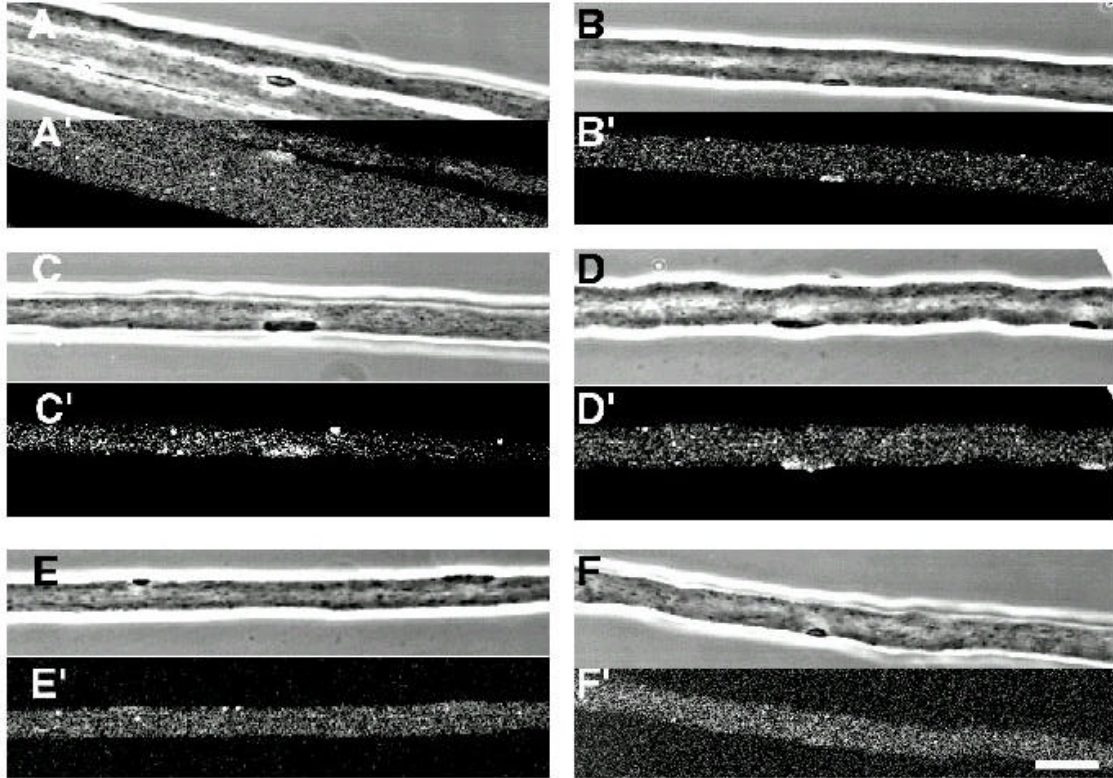


Figure 5. **Actin mRNA is detected by ISH in PARP domains of rabbit ventral root (VR) axons wholemounts.** Paired micrographs of phase contrast (top, A, B, C, D, E, F), and ISH fluorescence (bottom, A', B', C', D', E', F') of the same axon area were obtained with a laser confocal microscope (0.5 $\mu$ m thick). ISH images (A' to D') were obtained using the anti sense riboprobe. ISH images (E' and F') were obtained using the sense riboprobe. Scale bar is 10  $\mu$ m.

## Discussion.

Axonal localization of beta actin mRNA was visualized by *in situ* hybridization in axonal wholemounts of different species. The distribution found was mainly cortical, enriched in areas that were identified as periaxoplasmic ribosomal domains. As reported previously these domains are rich in RNA and ribosomes, and could be identified by structural correlates when observed using phase contrast or DIC microscopy (Koenig & Martin, 1996; Koenig et al., 2000). The latter criterion was used to identify these structures and study co localization with *in situ* signals. The results obtained indicate that in the species studied, there is a high degree of colocalization between the distributions of ribosomal domains and the actin RNA regardless the different plaque shape observed.

The probe used in the present study was specific to detect beta actin from goldfish, since it was prepared from a goldfish beta actin cDNA. The same was used to detect actin message in mammalian axons. The specificity of the probe in mammals ISH is based on the percentage of conservation between the sequences coding for actin in these species (approximately 87%). Based on the results obtained in the Mauthner axon beta actin mRNA is localized in ribosomal domains. In the case of mammalian axons we can only say that actin mRNA is localized in these domains, since the probe used could probably detect other isoforms of this protein.

The presence of beta actin mRNA was confirmed in the Mauthner axon using RT-PCR analysis of gene expression. This preparation was used since it was estimated that Mauthner axon RNA content would be sufficient to be detectable due to the large size of axons as well as the size of ribosomal

domains determined by YOYO-1 specific fluorescence. PARPs found in mammalian axons are very small and axons wholemounts too. Furthermore, these axon wholemount are attached to a tiny mass of tissue after their isolation that could compromise purity of the sample with myelin debris. On the other hand, Mauthner axon wholemount preparation is cleaner and easier to manipulate. To check a possible contamination of axon preparation of myelin, GFAP mRNA was monitored in each RNA preparation isolated from axons. The latter was made following a previous study that analyzed GFAP mRNA in the same way, along with RT-PCR to detect neurofilament mRNA expression in Mauthner axon (Weiner et al., 1996). Reflecting the likelihood of axonal contamination with glial mRNAs, GFAP presence was detected in the majority of RNAs isolated from axons (using several dissection methodologies), nevertheless several examples were free of GFAP mRNA. These experiments suggest that beta actin mRNA could be detected by RT-PCR in the Mauthner axons, supporting signals resulting ISH, but minimal glial contamination should not be disregarded.

The presence of beta actin mRNA in the periaxoplasmic ribosomal domains could mean at least two interesting possibilities. On one hand, the machinery found in these locations could translate this mRNA, being the source of the newly synthesized putative actin seen by Koenig (1991) when analyzed the pattern of radiolabeled proteins synthesized by the Mauthner axon. In agreement of our findings, are the reports of translation of beta actin in growth cones and axons in cultured neurons (Bassell et al., 1998, Eng et al., 1999, Olink-Coux and Hollenbeck, 1996). On the other hand and supporting the later our findings indicate that mature neurons target specific mRNAs to particular locations in distant areas of axons. This is also in



agreement with reports that show that beta actin mRNA is selectively targeted to neuronal projections in vitro. This transport is dependent on the presence of a “zipcode” sequence on its 3' end untranslated region where an RNA binding protein was shown to be bound (Ross et al, 1997).

The evidence shown here is the first, to our knowledge, that demonstrates that an mRNA is located in mature myelinated axons. Although, there is no direct evidence showing that this mRNA is translated in the ribosomal domains, it is hypothesized here that this mRNA is synthesized in the soma, transported to the periaxoplasmic ribosomal domains in association with RNA binding proteins. The mRNAs located in PARP domain could be either translated on arrival or stored there to be translated when needed.

## **References.**

Aronov S, Aranda G, Behar L, Ginzburg I. (2001) Axonal tau mRNA localization coincides with tau protein in living neuronal cells and depends on axonal targeting signal. *J Neurosci.*21: 6577-87.

Aronov S, Aranda G, Behar L, Ginzburg I. (2002). Visualization of translated tau protein in the axons of neuronal P19 cells and characterization of tau RNP granules. *J Cell Sci.* 115: 3817-27.

Bassell GJ, Zhang H, Byrd AL, Femino AM, Singer RH, Taneja KL, Lifshitz LM, Herman IM, Kosik KS. (1998). Sorting of beta-actin mRNA and protein to neurites and growth cones in culture. *J Neurosci.* 18: 251-65.

Brittis PA, Lu Q, Flanagan JG (2001). Axonal protein synthesis provides a mechanism for localized regulation at an intermediate target. *Cell* 110: 223-35.

Campbell DS, Holt CE. (2001) Chemotropic responses of retinal growth cones mediated by rapid local protein synthesis and degradation. *Neuron* 32:1013-26.

Chomczynski P, Sacchi N. (1987) Single-step method of RNA isolation by acid guanidinium thiocyanate-phenol-chloroform extraction. *Anal Biochem.* 1987 Apr;162(1):156-9.

Eng H, Lund K, Campenot RB. (1999). Synthesis of beta-tubulin, actin, and other proteins in axons of sympathetic neurons in compartmented cultures. *J Neurosci.* 19:1-9.

Giuditta A, Kaplan BB, van Minnen J, Alvarez J, Koenig E. (2002) Axonal and presynaptic protein synthesis: new insights into the biology of the neuron. *Trends Neurosci.* 25: 400-4.

Koenig E. (1979) Ribosomal RNA in Mauthner axon: implications for a protein synthesizing machinery in the myelinated axon. *Brain Res.* 174: 95-107.

Koenig E. (1989). Cycloheximide-sensitive [<sup>35</sup>S]methionine labeling of proteins in goldfish retinal ganglion cell axons in vitro. *Brain Res.* 481: 119-23.

Koenig E (1991) Evaluation of local synthesis of axonal proteins in the goldfish Mauthner cell axon and axons of dorsal and ventral roots of the rat in vitro. *Mol Cell Neurosci* 2:384–394.

Koenig E, Martin R. (1996). Cortical plaque-like structures identify ribosome-containing domains in the Mauthner cell axon. *J. Neurosci.* 16:1400-11.

Koenig E, Martin R, Titmus M, Sotelo-Silveira JR. (2000) Cryptic peripheral ribosomal domains distributed intermittently along mammalian myelinated axons. *J Neurosci.* 20: 8390-400.

Koenig, E. and Giuditta, A. (1999) Protein synthesizing machinery in the axon compartment. *Neuroscience* 89, 5–15.

Mohr E. (1999) Subcellular RNA compartmentalization. *Prog Neurobiol.* 57:507-25.

Olink-Coux M, Hollenbeck PJ. (1996). Localization and active transport of mRNA in axons of sympathetic neurons in culture. *J Neurosci.* 16(4):1346-58

Ross AF, Oleynikov Y, Kislauskis EH, Taneja KL, Singer RH. (1997) Characterization of a beta-actin mRNA zipcode-binding protein. *Mol Cell Biol.* 17: 2158-65.

Sotelo JR, Benech CR, Kun A. (1992) Local radiolabeling of the 68 kDa neurofilament protein in rat sciatic nerves. *Neurosci Lett.* 144: 174-6.

Sotelo-Silveira JR, Calliari A, Kun A, Benech JC, Sanguinetti C, Chalar C, Sotelo JR. (2000). Neurofilament mRNAs are present and translated in the normal and severed sciatic nerve. *J Neurosci Res.* 62: 65-74.

Tiedge H, Bloom FE, Richter D. (1999) RNA, whither goest thou?. *Science.* 1999 283: 186-7.

van Gijlswijk RP, Wiegant J, Raap AK, Tanke HJ. (1996) Improved localization of fluorescent tyramides for fluorescence in situ hybridization using dextran sulfate and polyvinyl alcohol. *J Histochem Cytochem.* 44: 389-92.

Weiner OD, Zorn AM, Krieg PA, Bittner GD. (1996). Medium weight neurofilament mRNA in goldfish Mauthner axoplasm. *Neurosci Lett.* 213: 83-6.

Zelena J. (1972) Ribosomes in myelinated axons of dorsal root ganglia. *Z Zellforsch Mikrosk Anat.* 124: 217-29.

Zheng JQ, Kelly TK, Chang B, Ryazantsev S, Rajasekaran AK, Martin KC, Twiss JL. (1999) A functional role for intra-axonal protein synthesis during axonal regeneration from adult sensory neurons. *J Neurosci.* 21:9291-303.

### **Generación de ESTs a partir de ARN total de axón de Mauthner.**

Una de las estrategias para comenzar a caracterizar los ARNm presentes en el territorio axonal fue clonar y secuenciar fragmentos de ADNc generados al azar mediante PCR, utilizando una variación de la técnica amplificación de extremos terminales 3' (Dixon y cols., 1998). La preparación utilizada para extraer ARN total fue el axón de Mauthner dado su tamaño y presencia abundante de dominios PARP. De esta forma se generaron más de 100 clonas diferentes, comenzando con la caracterización a nivel de su secuencia, de un conjunto de las mismas. Aún no se ha comenzado con la caracterización de la distribución subcelular, mediante hibridización *in situ*, de los ARNm encontrados.

Las EST generadas a partir de ARN total extraído de axón de Mauthner fueron secuenciadas y comparadas con las secuencias del GeneBank del NCBI-NIH utilizando el programa BLAST. Los resultados pueden observarse en la siguiente tabla.

Tabla. Identidad de las EST de ARN total de axón de Mauthner.

Tipo de ARN	Identidad de la EST.	Largo aprox. (pb)	Identidad ADN pb/pb (%)	Identidad PTN (%)
ARNm	Miosina V (Pollo)	269		I = 17/52 (32%), P = 30/52 (57%)
	GADPH (pez)	236	182/203 (89%),	I: 24; P:56
	Similar a NOD3 (pez)	236		I = 140/488 (28%) P = 241/488 (49%),
	ORF FLJ23316	325	38/41 (92%)	
	14-3-3 ( <i>H.sapiens</i> )	165	56/62 (90%)	
	Ribosomal S19	265	188/212 (88%)	I = 21/26 (80%), P = 23/26 (87%)
	Ribosomal L5b	240	66/76 (86%)	
	Ribosomal L36a	419	300/336 (89%)	Identities = 15/28
	E-MAP 115-95	128		(53%), Positives = 20/28 (70%)
	Similar a matrin cyclophilin (pez)	77	65/77 (84%)	
ARN mitocondrial	NADH reductasa (pez)	230	48/149 (99%)	
	Citocromo C Sub III (pez)	429	292/316 (92%)	I = 59/65 (90%), P = 63/65 (96%)
	Citocromo C Sub III (pez)	186	186/186 (100%)	
	NADH reductase	195	162/163 (99%)	
	ADN Mitocondrial	268	155/158 (98%)	
	23S rRNA	158	132/134 (98%)	
	23S rRNA	131	69/77 (89%)	I = 88/104 (84%), P = 91/104 (86%)
	23S rRNA	300	239/239 (100%)	

## **Comentario sobre los trabajos II y III.**

En el presente capítulo se ha analizado desde distintas perspectivas la distribución subcelular de ARNm en axones de diferentes vertebrados.

En lo que respecta al análisis de la expresión de los ARNm que codifican para los neurofilamentos hemos comunicado su estudio detallado en mi tesis de maestría (Sotelo Silveira, 1998). Este trabajo fue completado para su publicación (trabajo II). Del mismo es interesante destacar que se demostró claramente que dichos ARNm se expresaban en el nervio ciático y en las células de Schwann. A su vez, el ARNm codificante para los neurofilamentos livianos se localizaba en las regiones limítrofes entre el axón y la vaina mas interna de la mielina. En la misma región se encontró también a la proteína ribosomal S1. Aunque la hibridización *in situ* e inmunohistoquímica a nivel óptico, no tienen la resolución suficiente para determinar la localización subcelular intra-axonal exacta de estas moléculas, esto coincidía con la presencia de dominios ribosomales del tipo de las placas periaxoplásmicas (trabajo I). La posibilidad de que la célula de Schwann fuera el sitio de origen de este ARNm axonal fue propuesta y discutida detalladamente en mi tesis de maestría, pero aún no se poseen pruebas que apoyen esa hipótesis.

Para resolver el problema de la localización intra-axonal de ARNm las preparaciones de axones *in toto*, representaban una excelente oportunidad. Como se conocía que proteínas con pesos moleculares similares a los neurofilamentos, tubulina y actina se sintetizaban en axones de animales adultos (Koenig, 1991), se comenzó la búsqueda del ARNm de la subunidad menor de los neurofilamentos (Sotelo Silveira 1998) y del ARNm codificante



para la beta actina (trabajo III). El manuscrito III se centra en este último aspecto, ya que es en el que se ha avanzado más.

Por la importancia y las dificultades del desarrollo de métodos implicados en los trabajos presentados, se considera de interés enfatizar ciertos aspectos de los mismos en la presente sección.

La ausencia de membrana axoplásmica y la ubicación cortical de las placas periaxoplásmicas en los axones *in toto*, determinaron dos modificaciones esenciales en la técnica de HIS. En primer lugar, las PARPs resultaron ser lábiles frente a la exposición prolongada a concentraciones de 50% de formamida (12-14 hs). Frente a varios fracasos en la detección de señales, se comenzó a observar el grado de preservación de la estructura durante el protocolo de hibridización. Se observó que la tinción con YOYO-1 era negativa luego de 3 horas de incubación en soluciones de hibridización conteniendo dicha concentración de formamida. Para aumentar la preservación, se incrementó el tiempo de fijación en paraformaldehído al 4%, hasta llegar a 3 horas a temperatura ambiente y se disminuyó la incubación en solución de hibridización a 3 horas a 42°C. Estas observaciones se combinaron con el uso de métodos de detección de la ribosonda marcada con digoxigenina, recientemente desarrollados, con la sensibilidad suficiente como para detectar copias únicas de genes en cromosomas metafásicos. Estos se basan en la deposición de un fluorocromo (rodamina) mediante la acción de la peroxidasa ligada al anticuerpo anti-digoxigenina. El ajuste de este protocolo refleja, desde el punto de vista técnico, las diferencias que existen entre un corte histológico (preparado por congelación o inclusión en parafina) y la preparación de axones *in toto*. Resalta, a su vez, la importancia

del ajuste previo de los protocolos, para maximizar la detección y localización subcelular de un ARNm en particular.

Asimismo, se tuvo que ajustar los protocolos para realizar RT-PCR a partir de muestras que poseen apenas unos pocos nanogramos de ARN total. De acuerdo con resultados de Edstrom y cols (1969) y Koenig (1979), se podía extraer aproximadamente 1ng de ARN total por centímetro de axón de Mauthner. En este rango de cantidades, la RT-PCR sería la técnica a aplicar, pero el desafío era lograr recuperar el ARN total a partir del axón, luego sintetizar el ADNc en forma eficiente y por último optimizar la reacción de PCR. Para el primer paso se comenzó por utilizar el método clásico de extracción de ARN (Chomzinski y Sachi, 1987) con la ayuda de diferentes "carriers". La partición hacia la fase acuosa demostró ser variable, motivando el cambio hacia una a una precipitación en presencia de etylendiamina-ácido propiónico y una extracción de proteínas en fenol en fase única (Koenig 1979). Este protocolo maximizaba la recuperación del ARN sin pérdidas debido a fraccionamientos en diferentes fases. Luego de lavado el precipitado podía utilizarse directamente para la transcripción reversa. Para la PCR se intentaron metodologías como la PCR "nested", hasta que comenzaron a estar disponibles en el mercado diferentes tipos de transcriptasas reversas recombinantes que poseían una mayor afinidad por el ARN que las del tipo AMV o MMLV. De esta forma y luego de aproximadamente 50 a 60 ciclos de amplificación se lograba obtener señales, ARN dependientes, a partir de ARN extraído de axones.

Utilizando esta experiencia se aplicaron métodos similares de amplificación pero con base aleatoria, para generar pequeños fragmentos de ADNc o ESTs que nos brindaran información sobre la población total de

ARNm presentes en los axones de Mauthner. La principal conclusión de estos resultados, que se discutirán con profundidad en el capítulo 5, nos permite afirmar que se puede aplicar esta metodología con este objetivo en muestras de ARN provenientes de axones, pero que hay que prestar especiales cuidados a la introducción accidental de ARNm exógenos al axón.

Los datos obtenidos nos permiten concluir que el ARNm codificante para la actina se encuentra enriquecido en las placas periaxoplásmicas, posiblemente para ser traducido localmente para la posterior incorporación de dicha proteína a las redes de citoesqueleto circundantes. A su vez, la localización cortical de este ARNm coincidía con la localización cortical del ARNm codificante para la subunidad menor de los neurofilamentos en los axones de nervio ciático, aseverando la importancia de la zona cortical del axón en el tráfico de ARN mensajeros y su posible traducción.

Estos resultados abren caminos de investigación que se dirigen hacia direcciones diversas. Por ejemplo, un ARNm localizado específicamente sobre las placas periaxoplásmicas requiere, necesariamente, de mecanismos de transporte que lo localicen en forma activa en dichas locaciones. En el próximo capítulo se presentarán resultados que indican que en la corteza axónica y en las placas periaxoplásmicas, se encuentran localizados preferencialmente, proteínas pertenecientes a la maquinaria de transporte axoplásmico rápido. La localización de proteínas motoras como la Miosina V y la kinesina en estos dominios podrían ser la base de la localización específica del ARNm codificante para la actina, así como de otros diferentes.

## **Capítulo 3.**

### **Sistemas de transporte subcelular asociados a las placas periaxoplásmicas.**

En la última década se han producido avances en el campo del tráfico intracelular en las células neuronales, específicamente en la caracterización de los motores moleculares responsables del mismo. Uno de los avances conceptuales más importantes concierne a la gran variedad de proteínas involucradas en los diversos modos de transporte intra-axonal. En una primera instancia se pensaba que una proteína como la kinesina era responsable de todas las formas de transporte anterógrado rápido encontradas en el axón, pero análisis posteriores demostraron que la primer kinesina caracterizada formaba parte de una numerosa familia de kinesinas (Hirokawa, 1998). Actualmente se está comenzando a caracterizar las funciones específicas de dichas isoformas. Esto sucedió también con proteínas como la miosina, que originalmente se pensaban que tenían funciones restringidas, y hoy en día se encuentran dentro de una súper-familia que esta compuesta de aproximadamente 17 clases diferentes. Sumado a esto, estas proteínas llevan a cabo su función utilizando proteínas adaptadoras que diversifican la especificidad y funciones de los complejos formados (Karcher y cols, 2002).

Los trabajos presentados en el presente capítulo se centran en el estudio de la localización subcelular de los transportadores Miosina V y Kinesinas ya que podrían estar, de acuerdo con observaciones previas, involucrados en transporte de ARN y ribosomas hacia el territorio axonal (Ohashi y cols 2002, Aronov y cols., 2002). El trabajo IV se centra en el estudio de la expresión de la Miosina V en axones y glía del nervio ciático de la rata en condiciones normales y durante la regeneración. Esto constituyó una primera caracterización de los patrones de expresión de dicha proteína en el sistema nervioso periférico y su regulación frente a la injuria. La

distribución axonal de la misma fue estudiada in situ mediante inmunohistoquímica mostrando una localización axonal cortical.

Esta distribución, junto con las comunicaciones que vinculan a diferentes proteínas transportadoras con el transporte de ARN (Ohashi y cols 2002, Aronov y cols., 2002), motivaron que estudiásemos la distribución subcelular de la Miosina V y diferentes kinesinas en relación con las placas periaxoplásmicas en axones de Mauthner y axones de raíces ventrales de rata. Los resultados obtenidos se presentan a continuación (manuscrito IV y V).

**Trabajo IV:** Calliari A., Sotelo Silveira J.R., Costa MC, Nogueira J, Cameron LC, Kun A, Benech J, Sotelo JR. (2002). Myosin Va is locally synthesized following nerve injury. *Cell Motyl Cytoskeleton* 51: 169-176.

# Myosin Va Is Locally Synthesized Following Nerve Injury

A. Calliari,<sup>1,2</sup> J. Sotelo-Silveira,<sup>2,5</sup> M.C. Costa,<sup>3</sup> J. Nogueira,<sup>2</sup> L.C. Cameron,<sup>4</sup>  
A. Kun,<sup>2</sup> J. Benech,<sup>1,2</sup> and J.R. Sotelo<sup>2\*</sup>

<sup>1</sup>*Departament of Molecular and Cell Biology, Facultad de Veterinaria, Universidad de la República, Montevideo, Uruguay*

<sup>2</sup>*Laboratory of Proteins & Nucleic Acids, Instituto de Investigaciones Biológicas Clemente Estable, Montevideo, Uruguay*

<sup>3</sup>*Departament of Biochemistry, Faculdade de Medicina de Ribeirão Preto, Universidade de São Paulo, São Paulo, Brazil*

<sup>4</sup>*Laboratory of Protein Biochemistry, Universidade do Rio de Janeiro, Rio de Janeiro, Brazil*

<sup>5</sup>*Laboratory of Biochemistry, Facultad de Ciencias, Universidad de la República, Montevideo, Uruguay*

The presence of Myosin Va (an actin-based molecular motor) in the peripheral nervous system was examined and its subcellular distribution within the axons of the sciatic nerve was demonstrated via immunocytochemistry. Myosin Va (M-Va) in the nerve was detected by using SDS-PAGE and Western blot techniques with a polyclonal antibody specifically raised against the M-Va globular tail domain. In addition, purification of M-Va from the rat sciatic nerve prior to immunoblotting yielded a M-Va standard band. Likewise, optical immunocytochemical procedures revealed the presence of M-Va, particularly in the cortical axoplasmic territory, but also in the Schwann cell soma. The above experiments were carried out both on intact as well as on severed sciatic nerves with similar results. The proximal stumps of severed sciatic nerves (from 0 to 72 h after injury) were labelled in vivo with <sup>35</sup>S-methionine. SDS-PAGE autoradiography of the immunoabsorbed M-Va from the radiolabelled homogenized nerve tissue showed a significant increment of the radioactive intensity of M-Va heavy chain band through time. Moreover, a significant increment of transcripts coding for M-Va heavy chain was detected through time using RT-PCR after nerve injury and compared to intact nerves. This data suggest that M-Va is up-regulated in a time-dependent manner. The latter suggests a possible involvement of M-Va in nerve regeneration processes. *Cell Motil. Cytoskeleton* 51:169–176, 2002. © 2002 Wiley-Liss, Inc.

**Key words:** local protein synthesis; calmodulin; sciatic nerve; cellular transport; nerve regeneration

## INTRODUCTION

Myosins are proteins capable of catalyzing the splitting of ATP and then either moving cargo along actin filaments, or moving actin filaments themselves [Sellers and Goodson, 1995]. To date, 17 myosin classes have been found in the myosin super-family [Hodge and Cope, 2000]. Of these, Myosin-V (M-V) is particularly interesting because it was found to be abundantly expressed in the brain. Myosin V is a multimeric protein composed of two heavy chains (HC), each with three functional domains: the head (N terminal) containing both the actin-binding site and the catalytic site; the neck, which has 6 IQ sites (consensus domains for the binding of calmodulin and other regulatory light chains); and the tail, the most variable of its domains, where the cargo is

attached [Espreafico et al., 1992; Cheney et al., 1993; Reck-Peterson et al., 2000].

Contract grant sponsor: PEDECIBA; Contract grant sponsor: MEyC; Contract grant sponsor: OAS; Contract grant sponsor: JICA; Contract grant sponsor: Universidad de la República (CSIC and CIDEc).

Abbreviations used: CaM = calmodulin; DTT = dithiothreitol; EDTA = ethylenediamine-tetraacetic acid; EGTA = ethylene glycol-bis(β-aminoethyl ether)N,N,N',N'-tetraacetic acid; PMSF = phenylmethylsulfonyl fluoride.

\*Correspondence to: J. R. Sotelo, Laboratory of Proteins and Nucleic Acids, Instituto de Investigaciones Biológicas Clemente Estable, Av. Italia 3318, Montevideo, Uruguay. E-mail: sotelo@iibce.edu.uy

Received 27 June 2001; Accepted 14 November 2001

Published online in Wiley InterScience (www.interscience.wiley.com). DOI: 10.1002/cm.10017



This protein (p190, brain myosin V, BM-V), was initially characterized as a  $\text{Ca}^{2+}$  and  $\text{Mg}^{2+}$ -dependent molecule whose ATPase activity was induced by calmodulin (CaM) and actin [Larson et al., 1988]. M-V is also phosphorylated by calmodulin kinase II (CaM K II) in the tail segment [Coelho and Larson, 1993]. The symbiotic behavior of M-V and CaM K II suggests that M-V might be responsible for the activation of the kinase through the donation of CaM molecules [Costa et al., 1999]. In the presence of actin,  $\text{Ca}^{2+}$  leads CaM to bind to the M-V heavy chain, but it also leads CaM to dissociate from BM-V if actin is absent [Cameron et al., 1998].

Endoplasmic reticulum vesicles were shown to be transported on actin filaments by Myosin-V in isolated squid axoplasm [Tabb et al., 1998]. Earlier results provided by electron microscopy analysis have revealed that the extensions of smooth endoplasmic reticulum into the dendritic spines of Purkinje cells were absent in *dilute* mice [Takagishi et al., 1996]. On the other hand, as there is a close association between the location of Myosin-V and the tubulin cytoskeleton [Evans et al., 1998; Wu et al., 1998; Espreafico et al., 1998]; it has been proposed that Myosin-V might be moved within cells in a passenger-like form via microtubule-based motors (kinesin), switching thereafter to the actin network, where it will act as a motor [Evans et al., 1997; Wu et al., 1998]. Moreover, a dynein-like light chain has been found to bind to Myosin V tail [Espindola et al., 1996].

Myo4p, a yeast member of Myosin V family, has the ability of transporting mRNA molecules [Long et al., 1997]. Although not yet proven in vertebrates, the study of this model of RNA transport might make it possible to understand the movement and location of rRNA and mRNA within the distinct regions of the neuron, including the axonal territory [Bassell et al., 1998; Koenig and Martin, 1996; Olink-Coux and Hollenbeck, 1996; Sotelo-Silveira et al., 2000].

Cargo transport and plastic changes in cells (including axons) seem to be closely related functions [Igarashi et al., 1996]. In this study, new data in support of the hypothesis that Myosin-V is present in the peripheral nervous system are discussed in conjunction with the possible implications of the protein in peripheral axonal distribution. It is also demonstrated that both the messengers coding for myosin V and the radiolabeled protein are increased in injured nerves compared to intact ones. This result might mean that myosin V is one of the several proteins that are synthesized after local injury [Benech et al., 1982; Sotelo et al., 1992; Sotelo-Silveira et al., 2000]. In any case, at the same time, there are indications that Myosin Va might also take part in the resulting plastic changes within the nerve. Considering these data as a whole, the results so far suggest that M-Va

may play a key role in neuroplasticity during the regenerative process.

## MATERIALS AND METHODS

### Reagents

ATP, EDTA, EGTA, PMSF, buffers, electrophoresis reagents, molecular weight markers, protease inhibitors, anti-rabbit IgG HRP conjugate, and di-amino benzidine were purchased from Sigma Chemical Co. Anti-rabbit IgG AP conjugate as well as the substrates for the detection method were purchased from the Promega Chemical Co. Chromatography resins and Protein A-Sepharose were obtained from Pharmacia Biotech Inc. Radioactive methionine was supplied by Amersham International. All solutions were prepared with Milli-Q (Millipore Corp.) deionized water.

### Antibody

An affinity purified polyclonal antibody against the C-terminal domain (931 amino acid residues) of chicken brain Myosin Va [Espreafico et al., 1992] was kindly donated by Dr. Roy Larson. This antibody was used for Western blots as well as immunohistochemical and immunoprecipitation assays.

### Animals and Nerve Radiolabeling

Young Wistar rats (150–200 g) were ether anesthetized and both sciatic nerves severed at the mid thigh, 4.0 cm distal to the dorsal root ganglion (DRG). After the surgery, in a set of assays considered as time "0 hour" ( $n = 2$ ), the tip of the proximal stump (0.5 cm) was placed in vivo and in situ in a 10-mm-long polyethylene tube cut in half longitudinally to form a trough (inner diameter 2 mm; length 5 mm). Both ends of the trough were sealed with silicone grease, after which the chamber thus formed was filled with 100  $\mu\text{l}$  of a Ringer solution (pH 7.4) containing 0.1  $\mu\text{Ci}/\mu\text{l}$  of  $\text{L}^{-35}\text{-S}$  methionine ( $>1,000 \text{ Ci}/\text{mmol}$ ). After a 1-h incubation period, free radioactive methionine was eliminated by washing each nerve five times with Ringer solution. Then, each proximal stump was excised, desheathed, and stored ( $-20^\circ\text{C}$ ) or immediately processed. In another set of animals, the wound was sutured and the animals remained alive for varying hours: 24 ( $n = 5$ ), or 72 h ( $n = 4$ ). Finally, the proximal stumps were subsequently re-exposed under pentobarbital anesthesia and labelled as described above.

### Proteins

Radiolabelled right and left proximal stump nerves (0.5 cm long) were homogenated in a Teflon glass homogenizer (Wheaton, Millville, NJ) in 5 ml of freshly prepared ice cold buffer (100 mM Tris-HCl, pH 7.7, 10 mM ATP, 10 mM EDTA, 2 mM 2-mercaptoethanol, 0.3

mM PMSF). The homogenate was centrifuged ( $40,000g_{max}$ , 45 min) and the supernatant obtained was collected and concentrated approximately  $7\times$  prior to performing the immunoprecipitation assay.

To study the presence of myosin-V in normal (non-injured) sciatic nerves, 3-cm-long pieces were used. The connective sheath (epineurium) was mechanically removed and the nerve tissue homogenized and centrifuged as previously described. The pellet and supernatant fractions were then analysed by electrophoresis and Western blot.

The fifth supernatant (S5) of chick brain myosin V purification (25 mM Tris-HCl, pH 8.2, 600 mM NaCl, 1 mM EGTA, 10 mM ATP, 20 mM  $MgCl_2$ , and 2 mM DTT) was obtained as previously described [Cameron et al., 1998] and used as an enriched preparation of the protein as well as a control in electrophoresis and Western blot.

### Total RNA Isolation, RT-PCR Amplification, and Semiquantification

Proximal stumps of sciatic nerves (0.5 cm long) were excised at 24 and 72 h after injury, and normal nerves (0.5 cm long) were dissected as time 0 h. RNA was extracted following the guanidinium-acid-phenol extraction protocol [Chomczynski and Sacchi, 1987]. Purified RNA was resuspended in 20  $\mu$ l of water (nuclease free) and 5  $\mu$ g of RNA was taken for DNase I (Promega) treatment (5 U, 30 min, 37°C). After this, 1  $\mu$ g of RNA was retro-transcribed according to the Reverse Transcription System Kit protocol (Promega) using poly(dT)<sub>15</sub> as a primer. Semiquantitative PCR analysis of Myosin Va mRNA levels was performed according to Jaegle et al. [1996]. Amplification of cDNA corresponding to different conditions was carried out in separate tubes (using 1  $\mu$ l of cDNA per tube). Tubes were taken at different cycles as follows: condition 0 h, cycles 28, 30, and 36; conditions 24 and 72 h, cycles 26, 28, and 30. Oligonucleotide primers were designed to amplify specifically rat Myosin Va isoform according to the sequences available at the GenBank (5'-primer TGTCAG-CATGGCATGGACCCAG and 3'-primer ATGGCTT-CCGCGTCATCGTCAG). The amplification cycle consisted of initial denaturation at 95°C for 30 sec, annealing at 55°C for 30 sec, and extension at 72°C for 30 sec using Taq DNA polymerase from Promega. In the first cycle, the denaturation was prolonged for 5 min at 95°C. The resulting DNA fragments were electrophoresed on a 6% polyacrylamide gel, stained with ethidium bromide and photographed using a digital photographic camera (EDAS 120, Kodak Digital Sciences). To confirm the identity of PCR products, the fragments were sequenced directly using BIGDYE terminator (Applied Biosystem) and an ABI 377 sequencer (Applied Biosystem).

### Immunoprecipitation Assays

The supernatant of enriched nerve proteins underwent reaction via incubation with 2% protein A-Sepharose beads for 4 consecutive hours under gentle agitation in an immunoprecipitation media composed of 50 mM Tris-HCl (pH 7.4), 150 mM NaCl, 5 mM EDTA, 5 mM  $NaN_3$ , 100  $\mu$ M PMSF, and Triton X-100, 0.25% (high stringency buffer) or 10 mM Tris-HCl (pH 7.4), 30 mM NaCl, 1 mM EDTA, 1 mM  $NaN_3$ , 100  $\mu$ M PMSF, and Triton X-100, 0.25% (low stringency buffer) in order to eliminate contaminants from the sample (pre-clearing step).

Protein A Sepharose-anti-myosin antibody complexes were simultaneously prepared by incubating an appropriate dilution of anti-myosin antibody (2 or 5  $\mu$ g/ml anti-myosin antibody) in 400  $\mu$ l of 2% protein A-Sepharose bead suspension prepared in either a low or a high stringency buffer for 2 consecutive hours by way of gentle agitation. The unbound antibody was then eliminated by washing the protein A-Sepharose five times in reaction media.

Finally, the immunoprecipitation assay was carried out by incubating the pre-cleared sample with the protein A-Sepharose-antibody complex (obtained under the same buffer conditions) overnight via gentle agitation at 4°C. Control samples were incubated in the absence of the primary antibody. Immunocomplexes were pelleted by centrifugation (10,000 rpm, 15 sec) and washed with reaction media five times to eliminate unbound proteins. The pellet was then recovered for further experiments.

### Electrophoresis and Western Blot Assays

SDS-PAGE was performed on 10% acrylamide minigels that had been stained with Coomassie blue. The apparent molecular weight was calculated by way of a Sigma molecular weight marker (SDS-7B, 190, 125, 88, 65, 56, 38, and 33.5 kDa). Immunoblotting on nitrocellulose membranes (0.22  $\mu$ m, BioRad) was performed, as previously described by using the alkaline phosphatase detection method [Towbin et al., 1979]. The transference of proteins was performed for 1 h, 250 mA, 4°C, and 10% methanol.

### Autoradiography and M-Va Quantification

Immunoprecipitated Myosin-V was recovered by adding 50  $\mu$ l of Laemmli's sample buffer to the protein A-Sepharose immunocomplex pellet and then boiled for 1 min.

In order to visualize the radiolabelled immunoprecipitated nerve proteins, the sample was electrophoresed and subsequently transferred to nitrocellulose membranes (as detailed above). Transferred proteins were autoradiographed by exposing the nitrocellulose membrane against an X-ray Kodak film in the dark at  $-80^\circ C$ .

The films were developed at different exposure times (for 1-, 2-, or 3-week periods) to assure the best images, after which they were fixed, dried, and photographed.

The developed X-ray films were scanned for transparent material with an AGFA Arcus II scanner and the proteins bands analyzed by way of Scion Image software. The amount of radiolabelled M-Va was calculated as the ratio between M-Va integrated optical density and total integrated optical density present in the same lane. The results were normalized against the ratio obtained at 0 h (basal radiolabeling).

### Immunocytochemistry

Young animals (150–200 g) were anaesthetized and perfused with 4% paraformaldehyde in 0.1 M phosphate saline buffer pH 7.2 (PBS). Intact normal sciatic nerves and dorsal root ganglia from the lumbar region were removed and post-fixed for 1 h in 4% paraformaldehyde in PBS. Afterwards, the samples were equilibrated overnight at 4°C in PBS containing 30% of sucrose and then included in Tissue Tek OCT compound. Frozen sections (5 to 10  $\mu$ m) were mounted on gelatine-coated cover slips. Endogenous peroxidase activity was blocked by incubating the sections in PBS containing 0.01% hydrogen peroxide for 30 min. The specimen was subsequently washed three times with PBS, incubated for 2 h with normal goat serum (1:30 in PBS) for 30 min in order to block non-specific epitopes, and then incubated overnight with anti-chicken Myosin-Va antibody raised in rabbit at a dilution of 10  $\mu$ g/ml in PBS. Immunostaining was carried out with an anti-rabbit IgG peroxidase conjugate (2-h incubation period), di-amino benzidine (0.2 mg/ml in PBS), and hydrogen peroxide (0.01%, final concentration) as substrate. Control sections were processed in the same way as above except that, instead of using anti-Myosin antibody, either pre-immune sera or no primary antibody was used. Sections were mounted on Entellan (Merck), examined under a light microscope, and photographed with commercial Kodak 400-ASA film.

## RESULTS

### Myosin Va Is Present in the Peripheral Nervous System

**Western blot of sciatic nerves.** The Western blot of the supernatant fraction of nerve homogenate incubated with anti-Myosin Va antibody showed a clear 200-kDa band, coincident with the expected myosin Va molecular weight and the chick myosin Va standard (see Materials and Methods and Fig. 1). Myosin Va is mostly in the supernatant fraction and, hence, clearly recognized by the antibodies. On the other hand, the pellet tends to contain very low concentrations of the protein (data not shown). This observation

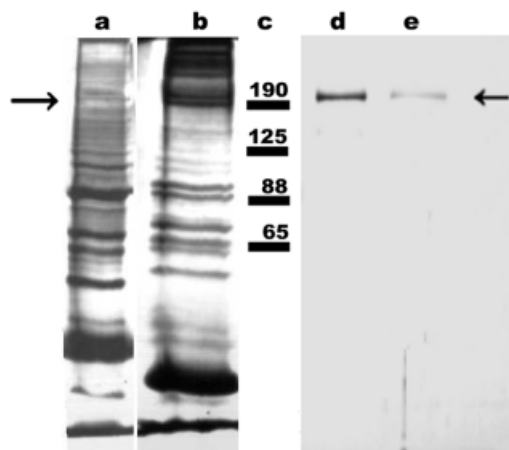


Fig. 1. SDS-PAGE nerve profiles (a, b) and Western blot (d, e) showing M-Va in not-injured normal nerves. Sciatic nerves were homogenized using a 7-ml Teflon on glass homogenizer with 5 ml of a buffer composed of 25 mM Tris-HCl pH 7.7, 10 mM EDTA, 10 mM ATP, 2 mM 2-mercaptoethanol, 300  $\mu$ M phenylmethylsulfonyl fluoride, and centrifuged at 40,000 $g_{max}$  (45 min). The supernatant and pellet fractions obtained were mixed with Laemmli's sample buffer and aliquots were applied to the gel. This fraction was transferred to nitrocellulose membrane after SDS-PAGE, incubated with the anti Myosin-Va antibody thereafter, and finally immunostained using a secondary antibody conjugated to alkaline phosphatase. **a:** Supernatant fraction enriched in M-Va by addition of ATP. **b:** Pellet fraction. The *left arrow* shows the position where the heavy chain of M-Va should be (200 kDa). **c:** Molecular weight standards (kDa). **d:** Standard chick brain (S5). **e:** Sciatic rat nerve (supernatant fraction). The *right arrow* shows the heavy chain of M-Va.

indicates, as it has been already reported, that the protein is soluble in the presence of ATP without any need for detergents [Espindola et al., 1992].

**Immunocytochemical analysis.** Dorsal root ganglion neurons were used as a positive control of the antibody specificity. The cells are widely and quite homogeneously labelled (Fig. 2b). In some images, the peroxidase precipitates were concentrated in the perinuclear region (Fig. 2b,c and arrows). No reaction was observed in control sections (Fig. 2a).

The morphological study of the nerves reveals the presence and sub cellular localization of the protein in the peripheral nervous system. Di-amino benzidine precipitates in nerve sections appear mainly in the area of the cortical axoplasm and the internal edge of the myelin (Fig. 2e, arrow), although the rest of the myelin sheath appears to be clear of reaction (Fig. 2e, asterisk). Abundant precipitates occupying the axoplasmic area can be appreciated in some fibers. Among the smaller fibers, a clear reaction filling the axoplasmic space is more frequently observed (Fig. 2g); Schwann cells were also heavily labelled in the soma (Fig. 2e, arrowhead).

### Myosin-Va Is Locally Synthesized After Injury

The autoradiography of the immunoprecipitate fraction previously electrophoresed and transferred to



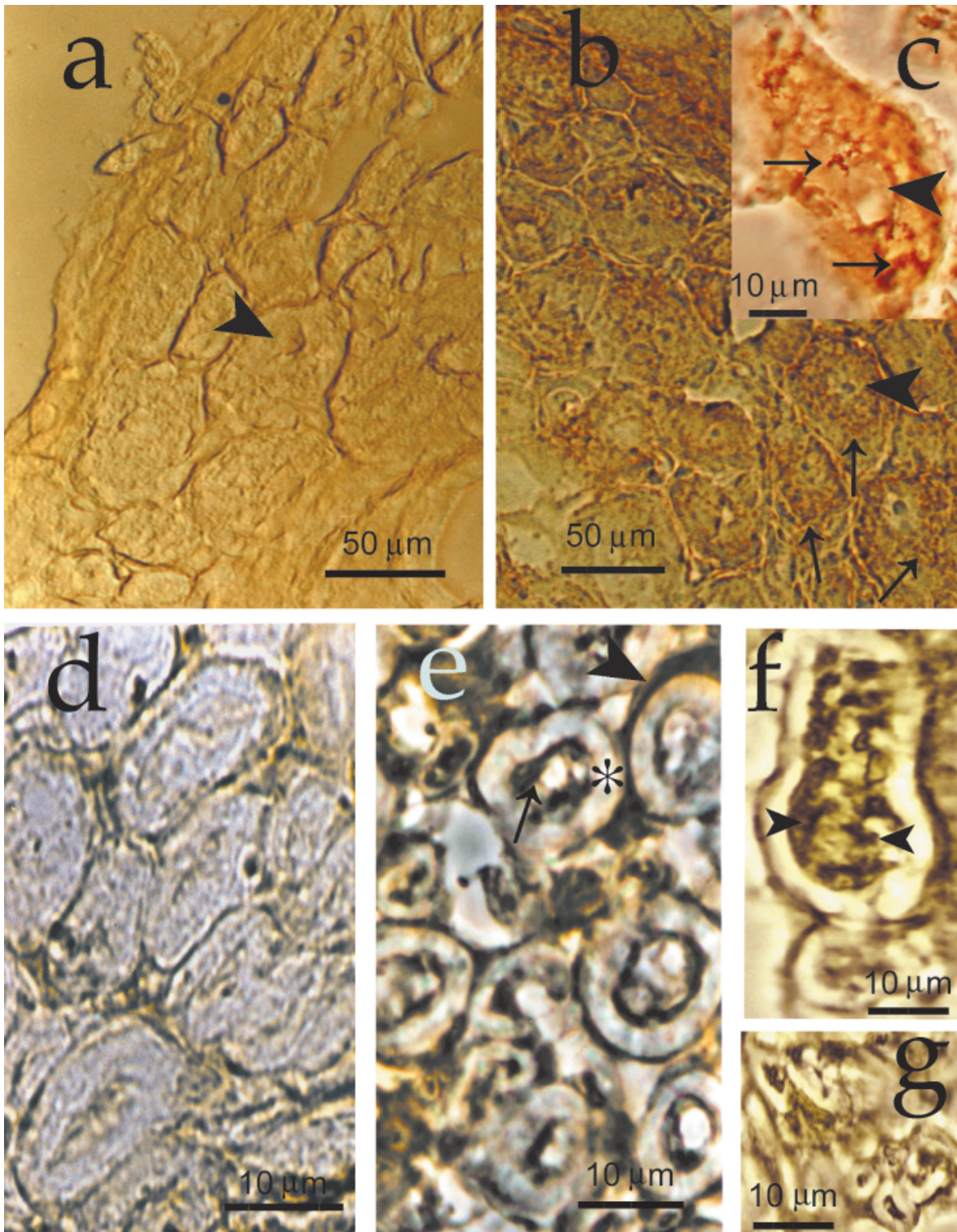


Fig. 2. Immunocytochemistry of M-Va at dorsal root ganglion and intact normal sciatic nerves (5–10  $\mu\text{m}$  frozen sections) using a primary antibody against M-Va. The secondary antibody was conjugated to Peroxidase. **a:** Dorsal root ganglion (DRG) sections without primary antibody (negative control, *arrowheads* indicate the nuclear region). **b:** Low magnification of DRG neurons stained with primary antibody. **c:** High magnification. The distribution of M-Va granules can be appreciated widely spread at the cytoplasm (*arrows*). Note that the

nuclear region appears to be free of reaction (*arrowheads* in b and c). **d–g:** Sciatic nerve cross sections. **d:** Negative control without primary antibody. **e:** Another cross section incubated with the primary antibody. In some cases, the Diamino Benzidine (DAB) precipitates can be observed at the external edge (Schwann cells) of the myelin sheath (*arrowhead*) and the myelin-axon boundary (*arrow*). Asterisk (\*) indicates the myelin free of precipitate. **f,g:** Intraganglionic fibers showing immunoreaction filling all the axoplasm (*arrowheads* in f).

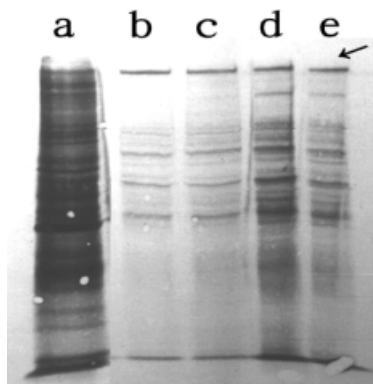


Fig. 3. M-Va was locally radiolabelled 24 h after nerve injury. Sciatic nerves were severed 4 cm distal to the ganglion and incubated in a medium containing  $0.1 \mu\text{Ci}/\mu\text{l}$  of  $^{35}\text{S}$ -methionine for 1 h. After this, the nerves were homogenized, centrifuged, and the supernatant was used for immunoprecipitation assays with different antibody concentrations and different stringency washing conditions. After immunoprecipitation, the samples were electrophoresed and transferred to a nitrocellulose membrane. The membrane was autoradiographed. **a**: Total locally synthesized protein profile; **b,c**: immunoprecipitated M-Va using 150 mM NaCl-buffer (high stringency buffer), with either (b) 2  $\mu\text{g}/\text{ml}$  or (c) 5  $\mu\text{g}/\text{ml}$  antibody against M-Va. **d,e**: Immunoprecipitated M-Va using 30 mM NaCl-buffer (low stringency buffer), with either (d) 2  $\mu\text{g}/\text{ml}$  or (e) 5  $\mu\text{g}/\text{ml}$  of antibody against M-Va.

nitrocellulose membranes yielded a clear and sharp 200-kDa band on the X-ray film. This band was always similar in intensity despite the immunoprecipitation conditions (Fig. 3, arrow). Interesting, the amount of radioactivity incorporated to M-Va after the injury was increased with time (100% at 0 hour, 260% after 24 h and 559% after 72 h; Fig. 4). The cell of origin of newly synthesized myosin Va cannot be determined from this experiment.

Other radioactive proteins were co-purified during the immunoprecipitation assay, some of which were eliminated upon the increase in the stringency conditions during the antigen-antibody recognition, leaving at least three faint bands (Fig. 3b and c). Control experiments were carried out in the absence of the antibody. The background levels of radioactivity were not high enough to produce any band or background reaction on the X-ray film (data not shown).

#### Amount of Myosin Va Transcripts Is Incremented After Nerve Injury

The content of myosin Va mRNA present in the proximal stump increases through time after injury. The lowest level of messenger were found at time "0 hour," while a higher level was present at time "24 hours," and increased at "72 hours" (see Fig. 5).

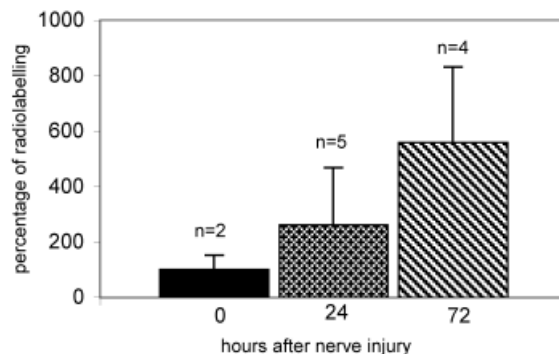


Fig. 4. Myosin V radiolabeling is time dependent.  $^{35}\text{S}$ -methionine incorporation 72 h after the nerve lesion is more than five times higher than the radioactive incorporation of normal (0 h) not injured nerves ( $P < 0.05$ ). It is almost three times higher than the incorporation 24 h after injury ( $P < 0.05$ ). Data are means  $\pm$  SEM.

#### DISCUSSION

Intracellular compartment communication and transport are crucial functions in the nervous system. This fact is most evident in the peripheral nervous system, where axons are normally very long. In the present study, we show that a molecular motor (Myosin Va) dealing with transport functions is present in the peripheral nervous system. Previously, there have been several suggestions about Myosin V possible function, including participation in filopodia extension of growth cones and movement of synaptic vesicles in nerve terminals [Wang et al., 1996, Prekeris and Terrian, 1997]. However, these putative roles do not account for the apparent widespread distribution of Myosin-V into the peripheral axons and Schwann cells shown in the present study.

The *dual filament model of transport* hypothesis has been used to explain the movement of vesicles from a functional compartment to a closely adjacent microtubule domain or from this domain to an actin-rich cortical territory of cells [Langford, 1995]. Myosin V biological properties and sub cellular localization into axons fit very well with this model. Furthermore, in the case of peripheral axons, such vesicles could be ER components as suggested by Tabb et al. [1998] for squid axons but, probably different from the kind of vesicles conveyed by the fast anterograde transport system. The presence of Myosin-V in actin-rich domains was already reported in mammalian neurons [Evans et al., 1997], associated with some small organelles (50–100 nm) and plasma membrane, but not associated with larger organelles such as mitochondria or clathrin-coated vesicles. It is also remarkable that the same type of organelles to which the Myosin seems to be associated was visualized both on tubulin and actin structures, suggesting that a given organelle could be transported from one network system to the other. In concordance with this idea, a co-localization of kinesin and Myosin-V has been found by Evans et al.



[1997], as well as the association of Myosin-V with the tubulin cytoskeleton in a variety of cell types including neurons [Wu et al., 1998].

The immunochemical labeling of the cortical region of the axoplasm can be appreciated in several images. This region is normally occupied by the actin cytoskeleton. It could be considered as indirect evidence of an actin-myosin-Va functional association also in the axonal territory. The functional significance of an actin-myosin-Va association within axons has not been established, but it suggests the possibility of a role in any mechanism of transport. In some fibers, mainly in those with a small diameter, the reaction was shown to fill all the axoplasmic space, showing that at least in some cases Myosin V is not restricted to the cortical actin-rich zone. Indeed it may be associated with other structures, such as the microtubule network, probably while they are transported through it.

An intriguing hypothesis to explain the peripheral distribution within axons could be some functional association of M-Va with the novel structures known as Peri-Axoplasmic Plaques (PAP). These structures were described in Mauthner axons as well as in rabbit and rat dorsal or ventral root fibers, as discrete peri-axoplasmic cortical zones containing rRNA and mRNA. Furthermore, the higher density of F-actin subjacent to the plaque suggested to the authors that the actin cytoskeleton may govern the plaque morphology, distribution, and components [Koenig and Martin, 1996; Koenig et al., 2000]. This possibility was not explored in the present work (no isolation of axons from myelin was made to visualize the so-called PAP), but the peripheral distribution of M-Va immunoreaction in axons should not be disregarded.

The movement of the ER membranes is very important during growth and the regeneration process. Regarding M-Va putative roles in axoplasmic territory, this protein could be implicated in such functions. Moreover, its intense local radiolabeling a few hours after experimental injury suggests that the enhanced vesicles transport found during regeneration processes may need an active participation of newborn Myosin V molecules. Our experimental design excludes the soma as the origin of this newly synthesized proteins. On the other hand, it is not possible to discriminate either the axoplasmic (local translation of pre-existing mRNA), or glial source. Although controversial, both possibilities have been reported earlier [Sotelo et al., 1992]. The Schwann cell origin (despite not excluding the axoplasmic source), seems to be most likely because this cell is also able to express the protein.

Coincidentally, the amplification by RT-PCR of mRNAs from normal nerves as well as from the proximal stump of sciatic severed nerves, showed that they contain the M-Va heavy chain coding mRNA. The latter is in

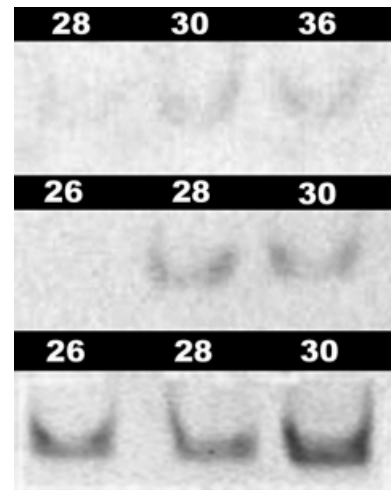


Fig. 5. Semiquantitative PCR analysis of expression level of Myosin Va mRNA in sciatic nerve of the rat. For each condition (normal, **top**; 24 h after injury, **middle**; 72 h, **bottom**) samples were taken at different cycles (as indicated by the numbers). Note that in injured condition, PCR products are observed at earlier amplification cycles, suggesting that the amount of mRNA coding for Myosin Va increases after lesion.

agreement with the findings of Sotelo-Silveira et al. [2000], which showed the presence of the three neurofilament subunits coding mRNAs in normal and severed rat sciatic nerves. Furthermore, the content of M-Va transcript increased with time after injury in the same way as its translation product content (M-Va protein).

However, even in the latter case the significance of a local response to nerve injury by Schwann cells must be emphasized because it could mean that the M-Va of glia is involved in the degeneration-regeneration process of nerves. The existence of a local response by the injured nerve characterized by an increase in the amino acid incorporation into TCA precipitable fraction has been reported [Benech et al., 1982]. This phenomenon that is maximal about 24 h after injury and occurring mainly in the proximal stump region (Fig. 3, lane a) is a local response. Myosin-Va seems to be one of these proteins.

The identification of the Myosin-Va as the main radiolabeled protein among those immunoprecipitated with the anti-myosin antibody was clearly established. However, the meaning of the other weakly labelled proteins co-purified with Myosin appearing in the autoradiography was difficult to establish. On the one hand, the presence of those weakly labelled proteins could be due to a normal specific interaction with Myosin Va, occurring during cell life. On the other hand, a non-specific cross-reaction with the antibody, or the interaction with Protein-A Sepharose, could be ruled out regarding the specificity showed by the same antibody on Western blot experiments (see Fig. 1), as well as in control experiments in which the homogenate was incubated alone

with Protein A Sepharose without the primary antibody (data not shown).

To establish the identity of such newly synthesized co-purified proteins should be the next step in our attempt to determine the role of Myosin-V in the peripheral nervous system.

## ACKNOWLEDGMENTS

We thank Dr. R. Larson for the gift of the anti-Myosin V antibody and Dr. E. Brown for the critical reading of the manuscript.

## REFERENCES

- Bassell GJ, Honglai Z, Byrd AL, Femino AM, Singer RH, Taneja KL, Lifshitz LM, Herman IM and Kosik KS. 1998. Sorting of  $\beta$ -actin mRNA and protein to neurites and growth cones in culture. *J Neurosci* 18:251–265.
- Benech C, Sotelo JR, Menendez J and Correa-Luna R. 1982. Autoradiographic study of RNA and protein synthesis in sectioned peripheral nerves. *Exp Neurol* 76:72–82.
- Cameron LC, Carvalho RN, de Araújo JRV, Martins-Teixeira F, Santos AC, Tauhata S, Larson RE, Sorenson M. 1998. Calcium-induced quenching of intrinsic fluorescence in Brain Myosin V is linked to dissociation of Calmodulin light chains. *Arch Biochem Biophys*. 355:35–42.
- Cheney RE, O'Shea MK, Heuser JE, Coelho MV, Wolenski JS, Espreafico EM, Forscher P, Larson RE, Mooseker MS. 1993. Brain Myosin-V is a two headed unconventional myosin with motor activity. *Cell* 75:13–23.
- Chomczynski P, Sacchi N. 1987. Single-step method of RNA isolation by guanidinium thiocyanate-phenol-chloroform extraction. *Anal Biochem* 162:156–159.
- Coelho MV, Larson RE. 1993.  $Ca^{2+}$ -dependent phosphorylation of the tail domain of Myosin-V, a Calmodulin-binding myosin in vertebrate brain. *Braz J Med Biol Res* 26:465–472.
- Costa MC, Mani F, Santoro W Jr, Espreafico EM, Larson RE. 1999. Brain Myosin-V, a Calmodulin-carrying myosin, binds to Calmodulin-dependent Protein Kinase II and activates its kinase activity. *J Biol Chem* 274:15811–15819.
- Espindola FS, Cheney RE, King SM, Sutter DM, Mooseker MS. 1996. Myosin-V and dynein share a similar light chain. *Mol Biol Cell* 7:372a.
- Espreafico EM, Cheney RE, Matteoli M, Nascimento AA, De Camilli PV, Larson RE, Mooseker MS. 1992. Primary structure and cellular localization of chicken brain Myosin V (p190), an unconventional myosin with calmodulin light chains. *J Cell Biol* 119:1541–1557.
- Espreafico EM, Coling DE, Tsakraklides V, Krogh K, Wolenski JS, Kalinec G, Kachar B. 1998. Localization of Myosin-V in the centrosome. *Proc Natl Acad Sci USA* 95:8636–8641.
- Evans LL, Hammer J, Bridgman PC. 1997. Subcellular localization of Myosin-V in nerve growth cones and outgrowth from *dilute-lethal* neurons. *J Cell Sci* 110:439–449.
- Evans LL, Lee AJ, Bridgman PC, Mooseker MS. 1998. Vesicle-associated Brain Myosin-V can be activated to catalyze actin-based transport. *J Cell Sci* 111:2055–2066.
- Hodge T, Cope J. 2000. A myosin family tree. *J Cell Sci* 113:3353–3354.
- Igarashi M, Kosaki S, Terakawa S, Kawano S, Ide C, Komiya Y. 1996. Growth cones collapse and inhibition of neurite growth by botulinum neurotoxin C1: A t-SNARE is involved in axonal growth. *J Cell Biol* 134:205–215.
- Jaegle M, Mandemakers W, Broos L, Zwart R, Karis A, Visser P, Grosveld F, Meijer D. 1996. The POU factor Oct-6 and Schwann Cell differentiation. *Science* 273:507–510.
- Koenig E, Martin R. 1996. Cortical plaque-like structures identify ribosome-containing domains in the Mauthner cell axon. *J Neurosci* 16:1400–1411.
- Koenig E, Martin R, Titmus M, Sotelo-Silveira JR. 2000. Cryptic peripheral ribosomal domains distributed intermittently along mammalian myelinated axons. *J Neurosci* 20:8390–8400.
- Langford GM. 1995. Actin and microtubule-dependent organelle motors: interrelationships between the two motility systems. *Curr Opin Cell Biol* 7:82–88.
- Larson RE, Pitta DE, Ferro JA. 1988. A novel 190 kDa Calmodulin-binding protein associated with brain actomyosin. *Braz J Med Biol Res* 21:213–217.
- Long RM, Singer RH, Meng X, Gonzalez I, Nasmyth K, Jansen RP. 1997. Mating type switching in yeast controlled by asymmetric localization of ASH-1 mRNA. *Science* 277:383–387.
- Olink-Coux M, Hollenbeck PJ. 1996. Localization and active transport of mRNA in axons of sympathetic neurons in culture. *J Neurosci* 16:1346–1358.
- Prekeris R, Terrian D. 1997. Brain Myosin-V is a synaptic vesicle-associated motor protein: evidence for a  $Ca^{2+}$ -dependent interaction with the Synaptobrevin-Synaptophysin complex. *J Cell Biol* 137:1589–1601.
- Reck-Peterson SL, Provance DW Jr., Mooseker MS, Mercer JA. 2000. Class V myosins. *Biochim Biophys Acta* 1496:36–51.
- Sellers JR, Goodson HV. 1995. Motor proteins II: myosins. *Protein Profile* 2:1323–1423.
- Sotelo JR, Benech CR, Kun A. 1992. Local radiolabelling of the 68 kDa neurofilament protein in rat sciatic nerves. *Neurosci Lett* 144:174–176.
- Sotelo-Silveira JR, Calliari A, Benech JC, Kun A, Sanguinetti C, Chalar C, Sotelo JR. 2000. Neurofilament mRNAs are present and translated in the normal and severed sciatic nerve. *J Neurosci Res* 62:65–74.
- Tabb JS, Molyneaux BJ, Cohen DL, Kuznetsov SA, Langford GM. 1998. Transport of ER vesicles on actin filaments in neurons by myosin V. *J Cell Sci* 111:3221–3234.
- Takagishi Y, Oda S, Hayasaka S, Dekker-Ohno K, Shikata T, Inouye M, Yamamura H. 1996. The *dilute lethal (dl)* gene attacks a  $Ca^{2+}$  store in dendrite spine of Purkinje cells in mice. *Neurosci Lett* 215:169–172.
- Towbin H, Staehelin T, Gordon J. 1979. Electrophoretic transfer of proteins from polyacrylamide gels to nitrocellulose sheets: procedure and some applications. *Proc Natl Acad Sci USA* 76:4350–4354.
- Wang FS, Wolensky JJ, Cheney RE, Mooseker MS, Jay DG. 1996. Function of Myosin-V in filopodial extension in neuronal growth cones. *Nature* 273:660–663.
- Wu X, Kocher B, Wei Q and Hammer JA III . 1998. Myosin-V associates with microtubule-rich domains in both interphase and dividing cells. *Cell Motil Cytoskeleton* 40:286–303.

**Trabajo V:** Sotelo Silveira J.R., Calliari A., Cardenas M., Koenig E., Sotelo J.R. Myosin Va and kinesin motor proteins are enriched in ribosomal domains (periaxoplasmic plaques) of myelinated axons. Manuscrito.



**Myosin Va and Kinesin II motor proteins are concentrated in ribosomal domains (periaxoplasmic ribosomal plaques) of myelinated axons.**

**José R. Sotelo-Silveira<sup>1,2</sup>, Aldo Calliari<sup>2,3</sup>, Magdalena Cárdenas<sup>2</sup>, Edward Koenig<sup>4</sup> and José R. Sotelo<sup>2</sup>.**

<sup>1</sup> Department of Cell & Molecular Biology, Facultad de Ciencias, Universidad de la Republica, Montevideo, Uruguay.

<sup>2</sup> Laboratory of Proteins & Nucleic Acids, Instituto de Investigaciones Biológicas Clemente Estable, Montevideo, Uruguay.

<sup>3</sup> Department of Molecular & Cell Biology, Facultad de Veterinaria, Montevideo, Universidad de la República, Uruguay.

<sup>4</sup> Physiology & Biophysics, State University of New York at Buffalo, New York, 14214, USA.

## **ABSTRACT**

Periaxoplasmic ribosomal plaques (PARPs) are discrete ribosome-containing domains distributed intermittently along the periphery of axoplasm in myelinated fibers. Thus, they are structural formations in which translational machinery is spatially organized to serve as centers of protein synthesis for local metabolic requirements and perhaps repair as well. Because of evidence that RNA is transported to putative PARP domains, involving both

microtubule- and actin-based mechanisms, it was of interest to investigate whether cytoskeletal motor proteins exhibit a nonrandom localization within PARP domains. Axoplasm, from large Mauthner fibers and rat or rabbit spinal ventral nerve root fibers, removed from the myelin sheath in the form of an 'axoplasmic wholemount' was used for this analysis.

PARP domains were identified either by specific immunofluorescence of rRNA, ribosomal P antigen, or by nonspecific RNA fluorescence using RNA binding dyes YOYO-1 or POPO-1. A polyclonal antibody (pAb) against the motor domain of myosin Va showed prominent non-random immunofluorescence labelling in PARP domains. Similarly, monoclonal antibodies (mAb) against kinesin KIF 3A and a pan-specific anti-kinesin (mAb IBII) also showed a preponderant immunofluorescence in PARP domains. On the other hand, H2, a mAb anti-kinesin KIF 5A, exhibited only random immunofluorescence labelling in axoplasm, as was also the case with pAb anti-dynein heavy chain immunofluorescence. Several possible explanations for these findings are considered, primary among which is targeted trafficking of translational machinery that results in local accumulation of motor proteins. Additional possibilities are trafficking functions intrinsic to the domain, and/or functions that govern dynamic organizational properties of PARPs.

**Keywords.** myosin V, kinesin, RNA localization, axons, local protein synthesis.

## INTRODUCTION

A systematic periodic occurrence of restricted periaxoplasmic ribosomal plaques (PARPs) was documented in axoplasmic wholemounts isolated from myelinated fibers (Koenig & Martin, 1996; Koenig, et al. 2000). PARPs contain a ribosome-associated ultrastructural matrix, localized the actin-rich cortical zone, and can be seen as protruding plaque-like structural correlates. Thus, PARPs can account for earlier metabolic studies documenting protein synthesis in myelinated vertebrate axons (Tobias & Koenig, 1975; Benech et al, 1982, Koenig, 1991; Sotelo et al, 1992, see Alvarez et al. (2000) for review). As discrete loci of potential protein synthesis, there is likely to be bi-directional macromolecular trafficking associated with these domains. Indeed, transport of BC1 RNA depends on microtubules for long-range axial transport and actin filaments for local radial transport to putative PARPs in the periphery of the Mauthner axon (Muslimov et al, 2002).

We showed previously that myosin Va has a cortical localization in axons of rat sciatic nerves (Calliari et al 2002). Because PARPs are localized in the actin-rich cortex (Koenig & Martin 1996 and Koenig et al 2000), transport within this zone may depend on a molecular motor that interacts with the actin cytoskeleton. Thus, it is possible that myosin Va plays a role in trafficking and/or in organizational dynamics of PARPs, because it has been shown to transport cargo on actin filaments (Tabb et al 1998), and to participate in transport to axons and dendrites (Langford, 2002). Interestingly, Myo4p, a member of the myosin V class in yeast, has been shown to mediate specific mRNA transport to the bud tip (Long et al, 1997, Kruse et al, 2002).

Cargoes targeted to PARPs from remote sites would probably utilize a kinesin dependent microtubule pathway. New additional cargoes and functions of kinesins are now emerging (Hirokawa, 1998, Goldstein and Yang, 2000). Also, as shown by Aronov et al (2002) in axons of P19 neurons, and Ohashi et al (2002) in CNS, kinesins may be involved in RNA transport. In the former study, KIF3A kinesin is a component of tau ribonucleoprotein (RNP) transport granules, while in the latter study, mRNA coding for FMRP protein is bound to RNP particles together with KIF5A/C kinesin and myosin Va. Furthermore, these motor proteins interact with each other, forming an “heteromotor complex” (Huang et al 1999, Stafford et al 2000).

The main goal of this study was to investigate the distribution of motor proteins in relation to PARPs in vertebrate myelinated axons. We used immunofluorescence to examine axoplasmic wholemounds isolated from myelinated fibers from rat and rabbit spinal ventral nerve roots, and goldfish Mauthner neuron. Western blots were used to evaluate immuno-specificity. Our results indicate that while neither conventional kinesin I, nor dynein are localized in PARPs, myosin Va and the KIF 3 kinesin are concentrated in PARP domains. These findings suggest that these molecular motors may play important roles associated with trafficking of key components, including mRNA in these domains. As such, they may also govern the dynamic spatial organization of PARP domains.

## MATERIALS AND METHODS.

### Isolation of axoplasmic wholemounts from myelinated spinal root fibers.

Lumbar spinal nerve roots that were used in the present study were dissected from dead rats. The tissues (several nerve root/rootlet) were suspended in a modified gluconate-substituted calcium-free Cortland salt solution (Koenig and Martin, 1996, Koenig et al 2000) containing 132 mM Na-gluconate, 5 mM KCl, 20 mM HEPES, 10 mM glucose, 3.5 mM MgSO<sub>4</sub>, and 2 mM EGTA, pH 7.2, stored at 4°C. A nerve root/rootlet, 3-5 mm, was immersed in a solution of 30 mM zinc acetate, 0.1 M *N*-tris[hydroxymethyl]methylglycine (Tricine; Sigma, St. Louis, MO), pH 4.8, for 10 min and then was placed in a 35 mm plastic culture dish containing 2 ml of a "pulling" solution (i.e., a solution in which axoplasm was translated out from its myelin sheath), of aspartic acid neutralized by Tris at pH 5.5. A "critical permissive concentration" (CPC) of the "pulling" media was determined for each animal. The CPC usually was sharply defined for a given animal in a range of concentrations of 35-45 mM with respect to aspartate. The pulling media were made from a stock solution containing 0.2 M aspartic acid (Sigma), 0.192 M Tris, 5 mM NaN<sub>3</sub>, and 0.1% Tween 20 (Bio-Rad, Hercules, CA) to reduce surface tension, pH 5.5. For each test, plaque occurrence was evaluated after staining with YOYO-1 (see below). Isolated axoplasmic whole mounts were attached with the aid of eyebrow hair tools to a N<sup>o</sup> 1 coverslips coated with 1% 3-aminopropyltriethoxysilane (Polysciences, Warrington, PA) in ethanol.

### **Isolation of axoplasmic whole mounts from the Mauthner cell.**

Common goldfish (4-5 inches, Grassy Forks Fisheries, Martinsville, IN) were used. The goldfish was anaesthetized by cooling in ice water and all procedures with native tissues were performed in an ice bath. The dissected spinal cord and lower brain stem (Koenig and Martin 1996) were suspended in Cortland solution (see above). After Zn denaturation (see above), Mauthner cell axoplasm in 5 to 8 mm tissue segments was isolated as described for spinal nerve roots above.

### **YOYO-1 and POPO-1 staining of axoplasmic wholemounts.**

Recovery of periaxoplasmic ribosomal plaques was assessed by staining of the wholemounts with YOYO-1 iodide (491/509) or POPO-1 iodide (434/456) (Molecular Probes, Eugene, OR). One  $\mu$ l of a 1:10 stock of YOYO-1 or POPO-1 in DMSO was added to the pulling medium (final concentration, 1:5000) for 15 min. The dye was washed out by brief immersion in acidified 0.15 M ammonium acetate (i.e.,  $\text{NH}_4\text{OAc}$ ; pH-adjusted to 4.5 with acetic acid) and 0.1% Tween 20. For fluorescence microscopy the coverslip with axoplasmic sprays was mounted on a flow-thru chamber. The chamber was constructed by inverting the coverslip over spacers (0.5-1 mm thick) made of Silastic elastomer (Dow Corning, Midland, MI) attached to a large glass coverslip (35 x 50 mm) taped to a thin "U-shaped" metal plate, and the well was filled with acidified  $\text{NH}_4\text{OAc}$  solution.

### **Immunofluorescence staining.**

Axoplasmic wholemounts attached to a coverslip were fixed by immersion in 3.75% paraformaldehyde in 0.1 M sodium diethylmalonate [0.1 M diethylmalonic acid (Aldrich, Milwaukee, WI), adjusted to pH 7.2 with NaOH] and 0.1% Tween 20 for 15 min. They were washed in 0.15 M ammonium acetate and 0.1% Tween 20, pH 6.7, three times for 5 min each and then immersed in an immunoblocking solution, composed of 25 mM Tris HCl, 0.9% NaCl, 3.75% glycine, 1% of normal goat and/or donkey serum, 0.05% Tween 20, and 5 mM NaN<sub>3</sub> for 15 min. Incubation with primary antibody was for 1 hr on a rocker. Coverslips were washed three times with a working buffer (i.e., blocking buffer with 0.1% serum) and incubated for 45 min with a secondary antibody conjugated to one of three Alexa fluorophores (Molecular Probes) having an excitation maximum at either 488 nm, 546 nm, or 555 nm. The immunostained specimens were washed further three times for 5 min each before being mounted over spacers of the flow-thru chamber for microscopic examination (see above).

### **Antibodies.**

The immunoreagents that were used were as follows: (1) monoclonal antibody Y-10B, against the large ribosomal subunit RNA (a generous gift of Dr. Joan A. Steitz, Yale University, New Haven, CT; see Lerner et al., 1981), (2) polyclonal antibody against human ribosomal P antigen (US Biological; Swampscott, MA), (3) rabbit affinity purified polyclonal against a recombinant protein containing the Myosin Va head domain (amino acids 5 to 752) and a

rabbit affinity purified polyclonal against the Myosin Va C terminal domain (931 amino acids; a generous gift of Dr. Roy Larson, Universidade Sao Pablo, Riberao Preto, Brazil, Espreafico et al 1992), (4) monoclonal IBII against Kinesin heavy chain (Sigma-Aldrich), (5) monoclonal H2 against Kinesin KIF5A/C (Chemicon), (6) monoclonal anti-kinesin KIF3A (clone 28, Transduction Laboratories, BD Biosciences Pharmingen), and (7) rabbit polyclonal R-325 against Dynein (Santa Cruz Biothechology). Primary antibodies were used at 1:200. Alexa conjugated secondary antibodies were obtained from Molecular Probes and used according to manufacturer's instructions in dilutions ranging from 1/1000 to 1/2000.

### **Microscopy.**

For routine fluorescence microscopy axoplasmic wholemounds were observed in an Olympus BHS microscopy equipped with an air-cooled CCD camera (DAGE-MTI) or a Nikon Diaphot inverted microscope. The confocal microscope was a Bio-Rad MRC-1000 (Hercules, Ca.) with a krypton-argon laser in combination with an upright Nikon Optiphot microscope.

### **Electrophoresis and Western blot assays.**

SDS-PAGE was performed in extracts from ventral roots and central nervous system on 10% acrylamide minigels and stained with Coomassie blue. The apparent molecular weight was calculated using a Sigma molecular weight marker (SDS-7B. 190, 112, 88, 65, 56, 38, and 33.5 kDa). Immunoblotting on nitrocellulose membranes (0.22  $\mu$ m, BioRad) was performed, as previously described by using the alkaline phosphatase



detection method (Towbin et al., 1979). The transfer of proteins was performed for 1 hour, 250 mA, 4°C, and 10% methanol.

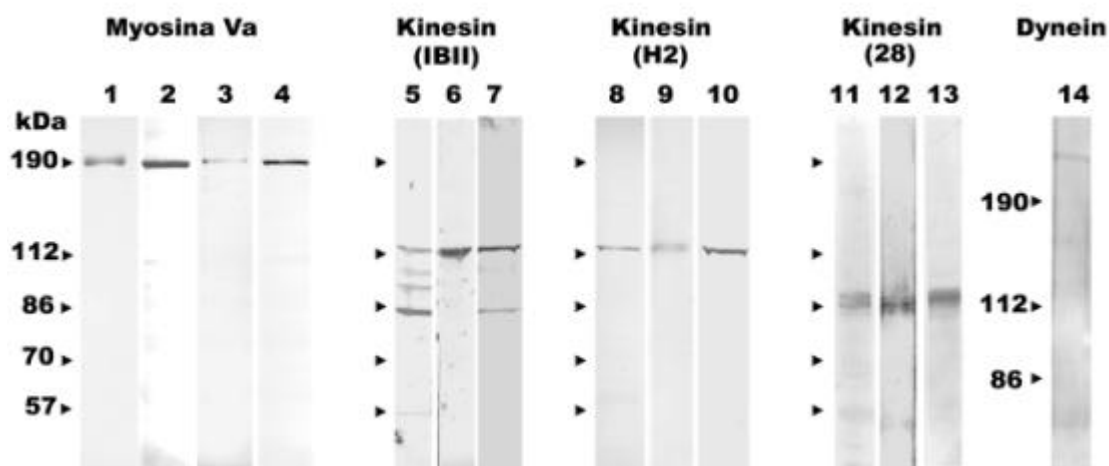
## **RESULTS.**

### **Specificity of the antibodies used in protein extracts from rat ventral roots and goldfish brain.**

The cross-reactivity of the antibodies to myosin Va and kinesin proteins used for immunofluorescence cytochemistry was evaluated by western blot analysis of rat and goldfish CNS protein extracts. The antibody against the head domain of Myosin Va, previously characterized by Espreafico et al (1992), showed the expected 190 kDa band in rat and goldfish extracts (figure 1 A).

The monoclonal IBII, against kinesin, recognized two bands of approximately 125 and 80 kDa in rat brain extracts (figure 1 B, lane 1). When the same lane, containing the rat protein extract, was probed with a monoclonal antibody which recognized KIF5A and C (clone H2, Chemicon), it labeled the same 125 kDa band that was recognized by the IBII clone (figure 1 B, lane 1'). A monoclonal antibody against KIF3A (clone 28) subsequently revealed that the 80 kDa band was the KIF3A kinesin isoform (figure 1 B, lane 4 and 5). Thus, the KIF5A/C and KIF3A isoforms were both recognized by the IBII antibody. When IBII, H2 and KIF3A anti-kinesins were tested on protein extracts from goldfish CNS, the pattern observed was similar to that obtained with rat protein extracts (figure 1 B, lanes 3, 3' and 6). Dynein western blots of

rat ventral roots showed the expected high molecular band of the heavy chain of cytoplasmic dynein (figure 1 C).



**Figure 1: Myosin Va and Kinesin are present in protein extracts from ventral roots and goldfish spinal cord.** Western blots from different protein extracts showing the specificity of the antibodies used. The protein extracts used are the following: **lane 1**, purified Myosin Va from chick brain; **lanes 2, 5, 8, 11 and 14** total protein from rat brain; **lanes 3, 6, 9 and 12**, total protein from rat ventral roots; **lanes 4, 7, 10, 13**, total protein from goldfish brain. Each extract was probed with the following antibodies: **lanes 1 to 4** were probed with a polyclonal antibody against Myosin Va; **lanes 5 to 7** were probed with the monoclonal antibody IBII which has a pan specific recognition of kinesins; **lanes 8 to 10** are showing the pattern obtained when a monoclonal antibody anti KIF5A/C (H2) was used (note that IBII antibody detects a single band of 125 kDa in common with H2 antibody); **lanes 11 to 13** were probed with a monoclonal antibody anti KIF3 (note that the KIF 3A antibody recognizes a band of about 85kDa, which has the same molecular weight as the one detected by the IBII antibody in rat and goldfish CNS); **lane 14** was probed with a polyclonal antibody against dynein heavy chain.

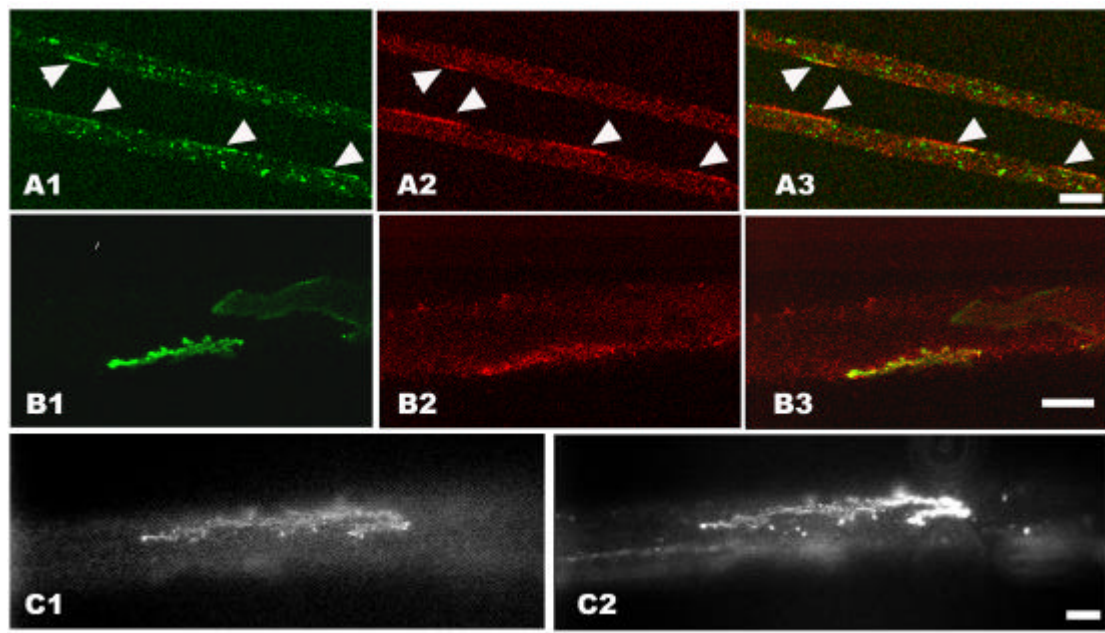
Molecular weights standards showed at the left of the figure are the same for all lanes except for lane 14 where they are specified. Asterisks shows the specific immunoreaction for each antibody used.

### **Myosin Va localization in mammalian and Mauthner axoplasmic wholemounds.**

To analyse the distribution of myosin Va in the axonal compartment, advantage was taken of the isolated axoplasmic wholemound preparation, which consists of axoplasm that is translated out from its myelin sheath with a pair of micro forceps (Koenig, 1965). We performed immunofluorescence cyochemistry using a specific antibody against the head domain of myosin Va. Representative confocal laser microscope images are shown in figure 2. Double labelling with YOYO-1 and myosin Va antibody on rat ventral root axons (figure 2 A1-3), showed co-localization in PARP domains, which can be seen in the merged image (figure 2, A3). An enrichment of the myosin V signal over the PARP area was observed but discrete signals in other areas of the axons could also be observed. Similar results were obtained using the antibody that recognized the C terminal tail domain of Myosin Va (data not shown).

The PARP domains reported for the unusually large diameter myelinated axon of the Mauthner cell (Koenig & Martin, 1996) provided an opportunity to study the distribution of Myosin Va with improved resolution. In this series of experiments, either the monoclonal antibody Y10B against the large rRNA subunit or YOYO-1 fluorescence staining was used to identify

PARP domains. As shown in figure 2, either myosin Va with Y10B immunofluorescence signals (figure 2 B1-3), or myosin Va immunofluorescence with dye binding YOYO-1 fluorescence signals (figure 2 C1-2) co-localize in PARP domains. The confocal laser image (figure 2 B) revealed that the immunolabelling in PARPs was particulate in character.



**Figure 2: Myosin Va localization in mammalian and Mauthner axoplasmic wholemounds.** **A** and **B**, confocal laser microscopy of doubly labelled whole mounts. **A**, a rat ventral root axon doubly stained with YOYO-1 (**A1**) and myosin Va antibodies (**A2**), the merged image is shown in **A3**; (optical section thickness 0.5  $\mu\text{m}$ ; scale bar, 10 $\mu\text{m}$ ). Arrowheads indicate PARP domains. **B**, Mauthner axon stained with rRNA (Y10B) monoclonal (**B1**) and myosin Va polyclonal antibodies (**B2**); the merged image is shown in **B3** (optical section thickness 0.5  $\mu\text{m}$ , scale bar, 50  $\mu\text{m}$ ). **C**, additional example of a Mauthner axon PARP stained with YOYO-1 (**C1**) and anti myosin Va (**C2**), using epifluorescence microscopy, (scale bar, 20  $\mu\text{m}$ ). Note that in each

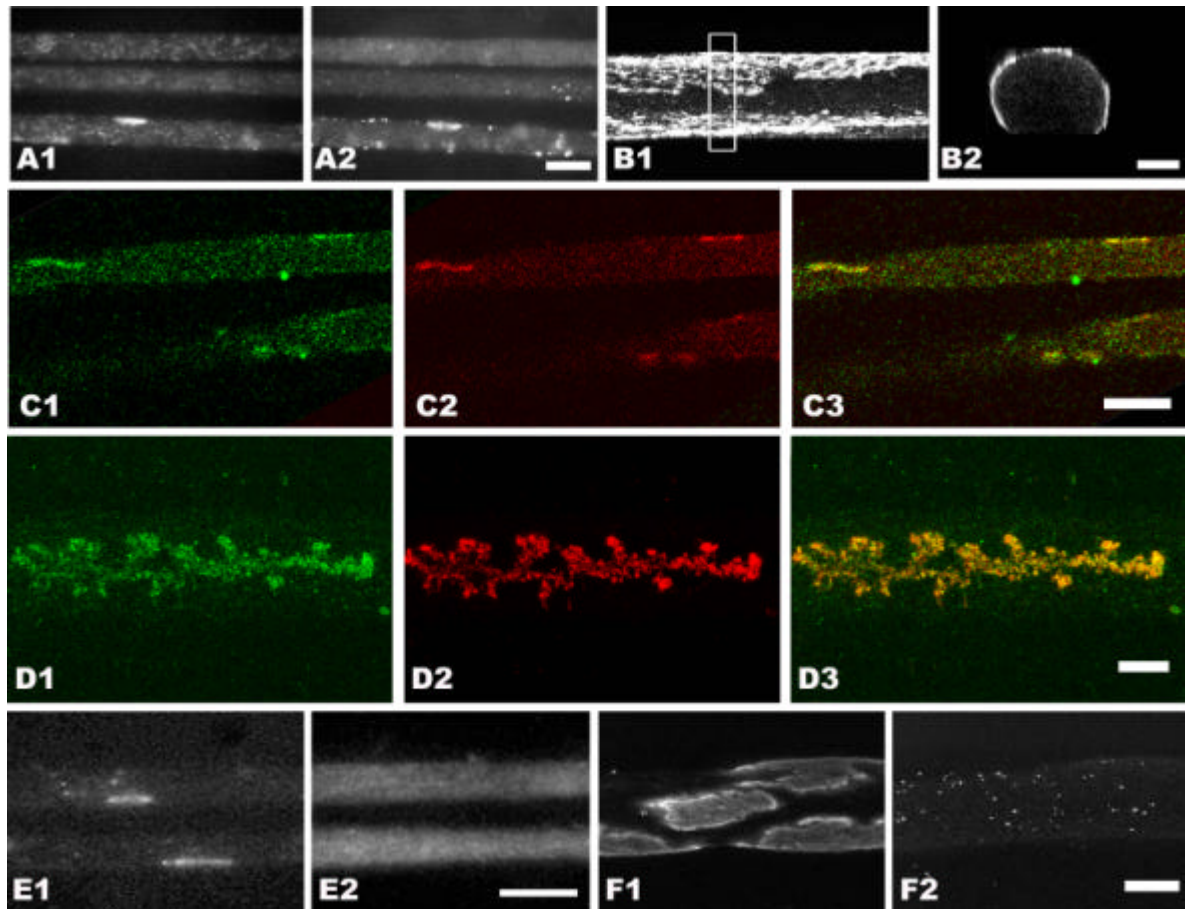
example shown, there is a high correlation of kinesin localization with PARP domains.

### **Kinesin localization in mammalian and Mauthner axoplasmic wholemounds.**

To study the distribution and localization of kinesin immunoreactivity we used the same approach as was used for myosin Va experiments. Rat or rabbit axoplasmic wholemounds were doubly labeled with the nucleic acid binding dyes, YOYO-1 or POPO-1, and one of the three different monoclonal antibodies against Kinesin characterized in western blot experiments; namely, clone IBII, anti-KIF3A (clone 28) or anti-KIF5A/C (clone H2; figure 3). Monoclonal antibodies IBII and anti-KIF3A each showed a prominent nonrandom labelling of PARP domains in rat (figure 3 A) and rabbit axons (figure 3 C), although some diffuse or punctate fluorescence was also apparent extrinsic to the PARP domains. In contrast, the H2 antibody labeled axoplasm in a rather homogeneous fashion without nonrandom localization (figure 3 E).

The same pattern of labelling was obtained when large axoplasmic wholemounds from Mauthner fibers were studied. Both the IBII (figure 3 B) and the anti-KIF3A monoclonal antibodies (figure 3 D) labeled the cortical zone in a discrete pattern that co-localized with labeled ribosomes, suggesting a preferential localization of the protein in PARP domains. On the other hand, the H2 antibody showed a punctuate immunofluorescence pattern that

typically failed to co-localize with YOYO fluorescence staining of PARPs (figure 3 F).

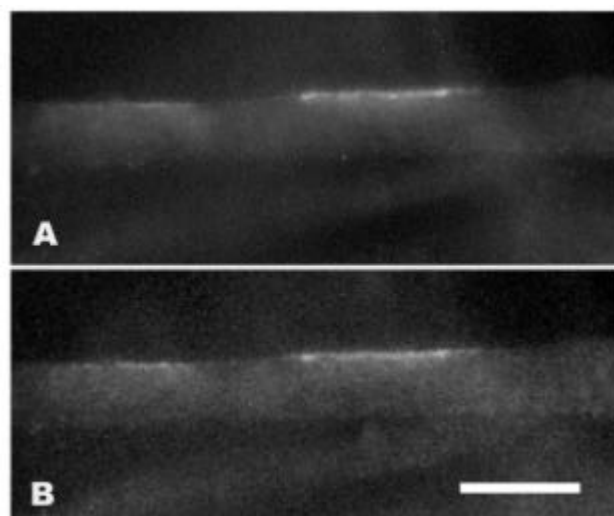


**Figure 3: Kinesin localization in mammalian and Mauthner cell axoplasmic wholemounts.** Kinesin localization in rat axons as evidenced with monoclonal antibody IBII using epifluorescence microscopy. **A1**, Rat ventral root axons stained with YOYO-1; **A2**, the same area stained with monoclonal IBII. Scale bar, 10 $\mu$ m. **B**, kinesin localization in the large Mauthner axon. **B1**, A Z-projection of 45 confocal optical sections (0.5 $\mu$ m) of kinesin mAb IBII immunofluorescence, rotated 90° on the X-axis. **B2**, the area framed in B1 rotated 90° on the Y-axis to show that the immunofluorescence is restricted to the axonal cortex. **C**, Confocal microscopy showing KIF 3A distribution in PARP domains in rabbit axons. **C1**, KIF3A detected by specific monoclonal antibodies. **C2**, PARP domains detected by POPO-1 fluorescence. **C3**, the merged image. Scale bar 10 $\mu$ m. **D**, A confocal z-projection of 15 0.5- $\mu$ m optical sections showing KIF 3A localization in a large PARP domain of a

Mauthner axon. **D1**, mAb KIF 3A was by specific monoclonal antibodies. **D2**, A PARP domain, identified by human ribosomal P antigen immunofluorescence; **D3**, the merged image. Scale bar 20  $\mu\text{m}$ . **E**, KIF5A/C kinesin in rat axons, detected by H2 antibody. **E1**, PARP domains shown by YOYO-1 fluorescence. **E2**, H2 immunofluorescence showing no co-localization with YOYO-1 signals. Note that the immunofluorescence distribution pattern obtained with this antibody is very different from that of IBII, in that it does not localize in PARP domains. Scale bar is 10  $\mu\text{m}$ . **F**, the same experiment as that in E, but carried out in Mauthner axons. **F1** represents the YOYO-1 fluorescence of PARPs, and **F2** shows the absence of corresponding H2 immunofluorescence labelling. Scale bars, 20  $\mu\text{m}$ .

### **Myosin Va and kinesin co-localize in periaxoplasmic ribosomal plaques.**

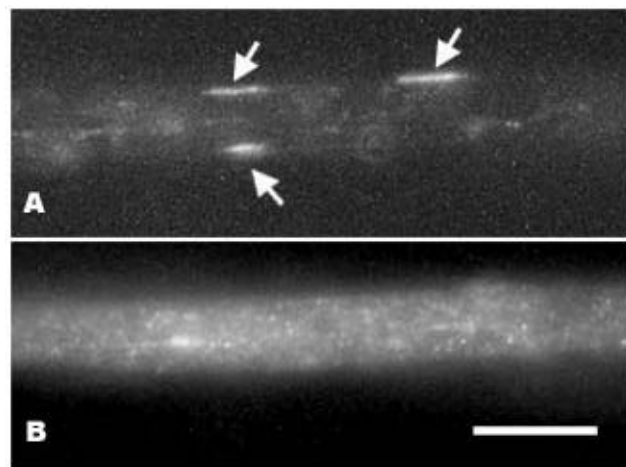
When the experimental conditions were adjusted for each antibody, both antibodies were tested on the same axoplasmic wholemounts from rat ventral roots. As shown in figure 4, pAb myosin Va and mAb kinesin IBII co-localized in periaxoplasmic ribosomal plaques.



**Figure 4: Cortical co-localization of myosin Va and kinesin in putative rat PARPs.** Myosin Va and kinesin co-localize in discrete cortical domains resembling periaxoplasmic plaques. Corresponding region of a rat axon labeled (A) with myosin Va pAb, and (B) with IBII mAb for kinesin demonstrate that both proteins are present in the same domain, and that they share a very similar pattern of distribution. Scale bars, 10  $\mu\text{m}$ .

**Dynein localization in mammalian axoplasmic wholemounds.**

Dynein immunofluorescence was distributed throughout the axoplasmic wholemound and showed no preferential localization in ribosomal domains identified by YOYO-1 fluorescence labelling (figure 5).



**Figure 5: Dynein localization in mammalian axoplasmic wholemounds.** A, PARPs labeled with YOYO-1. B, dynein immunofluorescence shows a typical pattern of fine and diffuse punctate signals in axoplasm without preferential localization in PARPs shown in A (arrows). Scale bar, 10  $\mu\text{m}$ .



## DISCUSSION

Interest in RNA trafficking and localization in dendrites and axons has grown considerably in recent years. The 'axoplasmic wholemount' preparation has provided an unconventional approach to studying localization of translational machinery and RNA trafficking in mature myelinated axons (Koenig & Martin, 1996; Koenig et al., 2000; Muslimov et al., 2002). Thus, the existence of a systematic distribution of ribosomal machinery in myelinated axons was unknown until axoplasmic wholemounts were removed from the myelin sheath after denaturation and under conditions that were permissive for recovery of PARPs (Koenig & Martin, 1996; Koenig et al., 2000).

PARPs are restricted domains, spaced at periodic random intervals around the periphery of axoplasm in the actin-rich cortex, and are marked in least disrupted preparations by a structural correlate protruding at the surface of the axoplasmic wholemount. Although the structural organization PARP domains have not been analysed in detail, they contain an amorphous matrix to which ribosomes appear to be bound, and F-actin co-distributes with putative polysomes that may extend below the cortical layer (Koenig & Martin 1996, Koenig et al 2000). In the latter studies Electron Spectroscopic Imaging (ESI) and immunofluorescence were used to document ribosomal phosphorus signals, rRNA, and ribosomal P antigen. Actin mRNA in Mauthner PARPs was also identified by ISH (Sotelo-Silveira and Koenig, 2000). Cycloheximide-sensitive metabolic radiolabelling of axonal proteins were earlier assayed in vertebrate myelinated axons (Tobias and Koenig, 1975; Benech et al, 1982, Koenig, 1991). The findings from these studies are consistent with the hypothesis that periaxoplasmic ribosomal plaques are discrete centers of local

protein synthesis in myelinated axons. As such, they are likely to be dynamic structural formations, wherein components of translational machinery are localized and turnover. In a preliminary report (Sotelo-Silveira et al., 2002), and here, we show for the first time that specific myosin and kinesin motor protein isoforms are concentrated in these domains.

#### Molecular motors are enriched in PARP domains.

As it is shown in figure 2, the polyclonal antibody against the motor domain of myosin Va yielded an immunolabelling pattern of axoplasmic wholemounds that was concentrated in PARPs (identified by YOYO-1 fluorescence of RNA), with some diffuse labelling within the axoplasmic core, According to previous reports (Calliari et al 2002, and Espreafico et al 1992), and shown by the western blot in this report, the antibody recognized only a 190 kDa band that corresponded to myosin Va (figure 1 A). Another antibody against a mid-segment of the tail region of this protein showed essentially the same pattern in axoplasmic wholemounds (data not shown). Dispersed punctate immunofluorescence within the axoplasmic core (figure 2) was consistent with previous reports of binding to vesicle cargo (Bridgman 1999), the association of myosin Va with the light neurofilament subunit (Rao et al 2002), and labelling of axoplasm in sciatic nerve fibers (Calliari et al, 2002).

Localization of kinesin in axoplasmic wholemounds was performed using monoclonal antibodies against KIF3A, KIF5A/C and IBII, a pan specific antibody. The latter antibody labels a band of approximately 125 kDa, and an additional 85 kDa band in brain and rat ventral roots protein extracts (figure. 1 B1, B2). These bands were recognized by KIF5A/C and KIF3A mAbs,

respectively. Comparable results were obtained when protein extracts from goldfish CNS tissue was probed with the same antibodies, except that the mobility of the heavier band in the latter case was slightly faster on western blots than that from rat (Figure. 1 B3). The different patterns of protein labelling in the Western blot experiments may explain the different immunofluorescence staining patterns in the axons. While both anti-KIF3A mAb and the pan-specific mAb yielded intense fluorescence labelling of PARPs and distributed punctate fluorescence in the Mauthner and rat axons, H2 mAb yielded only a diffuse fluorescence distribution in axons (figure. 3E and 3F). This indicates that the KIF3A kinesin isoform is present in PARP domains, and that IBII mAb is also recognizing the 85 kDa KIF3A heavy chain of heterotrimeric Kinesin II.

In contrast to myosin Va and kinesin immunoreactivities in PARP domains, a polyclonal antibody against the carboxy terminus of rat dynein heavy chain, which yielded a single band in western blots, appeared only as random punctate fluorescence signals in axoplasm (figure 5). It appears unlikely that there is a direct dynein function dedicated specifically to the biology of PARPs.

#### Putative roles of molecular motors in ribosomal domains of myelinated axons.

Evidence indicates that a variety of cargoes, including mRNAs, ribosomes and RNPs, can interact either directly with the heavy chain, with light chains, or indirectly through adaptor proteins, and then be transported by myosin Va and kinesin molecular motors (Rogers and Gelfand, 2000; Palacios and St Johnston, 2001; Karcher et al., 2002). Myosin Va can also interact

directly with the kinesin heavy chain (Huang et al., 1999), and there are reports of other cooperative interactions of actin- and microtubule-based transport systems (see Vale, 2003). Recently, radiolabelled rat neuronal BC1 RNA was shown to be rapidly transported *in vivo* in the Mauthner neuron after intracellular injection, and to localize in cortical “foci” along the Mauthner axon that were inferred to be PARP domains (Muslimov et al 2002). It was further shown that the localization of BC1 in the axon was a two-step process that required the sequential participation of microtubules for long-range axial transport and of actin filaments for local radial transfer and focal accumulation in cortical domains.

Inasmuch as PARPs are discrete domains in which RNA-containing translational machinery is likely to be translocated and/or docked, it is noteworthy that some potential motor proteins have been identified that could serve such functions. Myo4p, a yeast myosin V ortholog, was the first example of mRNA transport dependence on a class V myosin (Long et al 1997). She2p mediates RNA binding to Myo4p and apparently directs the complex to its final destination (Kruse et al, 2002), and, as shown by Ohashi, et al. (2002), this type of interaction is not just restricted to yeast. Both KIF5A or C (125 kDa) and KIF3A (~80 kDa) are found in neurons associated with ribosomes (Ohashi et al 2002) and mRNA (Aronov et al 2002). In the former report, RNP complexes containing mRNA, ribosomes, RNA binding proteins, myosin Va and kinesin were shown in mouse brain extracts and rat hippocampal neurons in culture. Furthermore, RNP granules that contained tau mRNA, kinesin KIF3A and HuD RNA binding protein were shown to be targeted to axons of differentiated P19 neurons (Aronov et al 2002), which is

consistent with a potential kinesin II-mediated microtubule dependent mechanism of RNA translocation to the immature axon.

What is the significance of the novel preferential localization of myosin Va and of kinesin in PARP domains? Clearly, RNA trafficking to these targeted domains would presumably represent a major activity of molecular motors. Thus, a concentration of molecular motors may reflect off-loading of cargoes from distant sources leading to a local accumulation. On the basis of available ultrastructural and immunocytochemical information (see above), PARPs appear to be highly organized domains. Thus, molecular motor proteins may also mediate trafficking intrinsic to the domain, along with their cognate cytoskeletal systems. In addition, or alternatively, molecular motors may govern the domain's dynamic organizational properties, as is exemplified in the case of the Golgi complex (De Matteis, and Morrow, 1998).

#### **ACKNOWLEDGMENTS.**

We thank Dr. Roy Larson and Dr. Luciana Cassaletti for the gift of the antisera against Myosin Va head domain and the antibody against the Myosin Va medial tail domain, respectively. We thank Dr. Wade Sigurdson for the assistant in confocal imaging. Research was supported in part by contracts from PEDECIBA, CSIC, CIDEA, and a grant to E.K. from NSF (IBN 0118368).

### Abbreviations.

PARP=Periaxoplasmic ribosomal plaques; DTT=dithiothreitol;  
EDTA=ethylenediamine-tetraacetic acid; EGTA=ethylene glycol bis( $\beta$ -  
aminoethyl ether) N,N,N',N'-tetraacetic acid; PMSF= phenylmethylsulfonyl  
fluoride.

### **REFERENCES**

Alvarez J, Giuditta A, Koenig E. 2000. Protein synthesis in axons and terminals: significance for maintenance, plasticity and regulation of phenotype. With a critique of slow transport theory. *Prog Neurobiol* 62: 1-62

Aronov S, Aranda G, Behar L, Ginzburg I. 2002. Visualization of translated tau protein in the axons of neuronal P19 cells and characterization of tau RNP granules. *J Cell Sci* 115: 3817-27.

Benech C, Sotelo JR Jr, Menendez J, Correa-Luna R. (1982) Autoradiographic study of RNA and protein synthesis in sectioned peripheral nerves. *Exp Neurol* 76:72-82.

Bridgman PC. 1999. Myosin Va movements in normal and dilute-lethal axons provide support for a dual filament motor complex. *J Cell Biol* 146:1045-60.

Brown JR, Simonetta KR, Sandberg LA, Stafford P, Langford GM. 2001. Recombinant globular tail fragment of myosin-V blocks vesicle transport in squid nerve cell extracts. *Biol Bull* 201: 240-1.

Brown JR, Peacock-Villada EM, Langford GM. 2002. Globular tail fragment of myosin-V displaces vesicle-associated motor and blocks vesicle transport in squid nerve cell extracts. *Biol Bull* 203: 210-1.

Calliari A, Sotelo-Silveira J, Costa MC, Nogueira J, Cameron LC, Kun A, Benech J, Sotelo JR. 2002. Myosin Va is locally synthesized following nerve injury. *Cell Motil Cytoskeleton* 51:169-76.

De Matteis, M.A. and Morrow, J.S. (1998) The role of ankyrin and spectrin in membrane-transport and domain formation. *Curr. Opin. Cell. Biol.* 10:542-549).

Espreafico EM, Cheney RE, Matteoli M, Nascimento AA, De Camilli PV, Larson RE, Mooseker MS. 1992. Primary structure and cellular localization of chicken brain myosin-V (p190), an unconventional myosin with calmodulin light chains. *J Cell Biol* 119(6):1541-57.

Espreafico EM, Coling DE, Tsakraklides V, Krogh K, Wolenski JS, Kalinec G, Kachar B. 1998. Localization of myosin-V in the centrosome. *Proc Natl Acad Sci U S A.* 95:8636-41.

Hirokawa N. 1998. Kinesin and dynein superfamily proteins and the mechanism of organelle transport. *Science*, 279: 519-26.

Huang JD, Brady ST, Richards BW, Stenolen D, Resau JH, Copeland NG, Jenkins NA. 1999. Direct interaction of microtubule- and actin-based transport motors. *Nature.* 397: 267-70.

Kanai Y, Okada Y, Tanaka Y, Harada A, Terada S, Hirokawa N. 2000. KIF5C, a novel neuronal kinesin enriched in motor neurons. *J Neurosci* 20:6374-84.

Koenig E. 1965. Synthetic mechanisms in the axon. II. RNA in myelin-free axons of the cat. *J. Neurochem.* 12:357-361.

Koenig E (1991) Evaluation of local synthesis of axonal proteins in the goldfish Mauthner cell axon and axons of dorsal and ventral roots of the rat in vitro. *Mol Cell Neurosci* 2:384–394.

Koenig E, Martin R. 1996. Cortical plaque-like structures identify ribosome-containing domains in the Mauthner cell axon. *J Neurosci* 16:1400-11.

Koenig E, Giuditta A. 1999. Protein-synthesizing machinery in the axon compartment. *Neuroscience* 89:5-15.

Koenig E, Martin R, Titmus M, Sotelo-Silveira JR. 2000. Cryptic peripheral ribosomal domains distributed intermittently along mammalian myelinated axons. *J Neurosci* 20: 8390-400.

Giuditta A, Kaplan BB, van Minnen J, Alvarez J, Koenig E. 2002. Axonal and presynaptic protein synthesis: new insights into the biology of the neuron. *Trends Neurosci* 25:400-4.

Goldstein LS, Yang Z. 2000. Microtubule-based transport systems in neurons: the roles of kinesins and dyneins. *Annu Rev Neurosci* 23:39-71.

Karcher RL, Deacon SW, Gelfand VI (2002). Motor-cargo interactions: the key to transport specificity. *Trends Cell Biol.* 12: 21-7.



Kruse C, Jaedicke A, Beaudouin J, Bohl F, Ferring D, Guttler T, Ellenberg J, Jansen RP. 2002. Ribonucleoprotein-dependent localization of the yeast class V myosin Myo4p. *J Cell Biol.* 159:971-82.

Langford GM. 2002. Myosin-v, a versatile motor for short-range vesicle transport. *Traffic* 3:859-65.

Lerner EA, Lerner MR, Janeway CA Jr, Steitz JA. 1981. Monoclonal antibodies to nucleic acid-containing cellular constituents: probes for molecular biology and autoimmune disease. *Proc Natl Acad Sci U S A* 78:2737-41.

Long RM, Singer RH, Meng XH, Gonzalez I, Nasmyth K, Jansen RP. 1997. Mating type switching in yeast controlled by asymmetric localization of ASH1 mRNA. *Science* 277: 383-387.

Miki H, Setou M, Kaneshiro K, Hirokawa N. 2001. All kinesin superfamily protein, KIF, genes in mouse and human. *Proc Natl Acad Sci U S A* 98:7004-11.

Muslimov IA, Titmus M, Koenig E, Tiedge H. 2002. Transport of Neuronal BC1 RNA in Mauthner Axons. *J Neurosci* 22:4293-301.

Palacios IM, St Johnston D (2001). Getting the message across: the intracellular localization of mRNAs in higher eukaryotes. *Annu Rev Cell Dev Biol.* 17:569-614.

Ohashi S, Koike K, Omori A, Ichinose S, Ohara S, Kobayashi S, Sato T, and Anzai K. 2002. Identification of mRNA/Protein (mRNP) Complexes Containing

Pur  $\alpha$ , mStaufen, Fragile X Protein, and Myosin Va and their Association with Rough Endoplasmic Reticulum Equipped with a Kinesin Motor. *J Biol Chem.* 40:37804–37810.

Rao MV, Engle LJ, Mohan PS, Yuan A, Qiu D, Cataldo A, Hassinger L, Jacobsen S, Lee VM, Andreadis A, Julien JP, Bridgman PC, Nixon RA. 2002. Myosin Va binding to neurofilaments is essential for correct myosin Va distribution and transport and neurofilament density. *J Cell Biol* 159:279-90.

Rogers SL, Gelfand VI. (2002) Membrane trafficking, organelle transport, and the cytoskeleton. *Curr Opin Cell Biol.* 12:57-62.

Sotelo JR, Benech CR, Kun A. (1992). Local radiolabeling of the 68 kDa neurofilament protein in rat sciatic nerves. *Neurosci Lett.* 144: 174-6.

Sotelo-Silveira JR, Koenig E 2000. Localization of beta-actin mRNA in cryptic ribosomal periaxoplasmic plaque domains of myelinated axons. *Mol Biol Cell* 11: 800 Suppl.

Sotelo-Silveira JR, Calliari A, Cardenas M, Koenig E, Sotelo JR (2002) Myosin V and Kinesin motor protein are enriched in ribosomal domains (periaxoplasmic plaques) of myelinated axons. *Mol Biol Cell* 13: 2678 Suppl.

Stafford P, Brown J, Langford GM. 2000. Interaction of actin- and microtubule-based motors in squid axoplasm probed with antibodies to myosin V and Kinesin. *Biol Bull* 199:203-5.

Tabb JS, Molyneaux BJ, Cohen DL, Kuznetsov SA, Langford GM. 1998. Transport of ER vesicles on actin filaments in neurons by myosin V. *J. Cell Sci.* 111: 3221-3234.

Tobias GS, Koenig E. (1975) Axonal protein synthesizing activity during the early outgrowth period following neurotomy. *Exp Neurol.* 49:221-34.

Vale RD. (2003) The molecular motor toolbox for intracellular transport. *Cell* 112:467-80.

## **Comentarios sobre artículos IV y V.**

Los trabajos presentados en el presente capítulo se centran en el análisis de la expresión de los motores moleculares miosina V y kinesina, en distintos tipos de axones.

El estudio de la distribución de la miosina V en el nervio ciático de la rata (trabajo IV) nos permitió caracterizar por primera vez la expresión de esta proteína en sistema nervioso periférico. A su vez, fue posible conocer la localización de dicha proteína en axones intactos y lesionados. Mediante inmunohistoquímica se observó que la myosina V se localizaba en la zona limítrofe entre la vaina de mielina y el axoplasma (Figura 2, trabajo IV). Dicha localización era esperable ya que el citoesqueleto de actina se encuentra en esa zona del axoplasma. En esta misma zona, hemos encontrado la proteína ribosomal S1 y el ARNm codificante para la subunidad menor de los neurofilamentos (figura 7, trabajo II). Esta colocalización nos llamó la atención ya que quizá pudiera existir una interacción física o funcional entre estos tres componentes en la zona cortical del axón.

Con respecto a la expresión de la proteína, se observó que esta era sintetizada localmente en el nervio ciático y se regulaba positivamente (mRNA y proteína) frente a una lesión del mismo (figura 4 y 5, trabajo IV). El origen de este aumento podía ser local o dependiente del soma neuronal. Dado que su ARNm se regula positivamente en el sitio de la lesión (figura 5, trabajo IV), nos inclinamos a pensar que el origen del incremento de la proteína neosintetizada es local (glial). Sin embargo, la posibilidad de que el ARNm pueda transportarse desde el soma neuronal y acumularse en el sitio de la lesión, sigue vigente ya que Todha y cols (2001) han detectado una

acumulación del ARNm codificante para el receptor VR1 en el extremo proximal del nervio lesionado, utilizando una metodología similar a la empleada en el trabajo IV. Los resultados de estos investigadores implican el transporte de dicho ARNm y su posterior acumulación, al interrumpir la continuidad axonal, como hemos constatado en nuestro modelo experimental.

La distribución axonal cortical de la proteína miosina V en las fibras del nervio ciático, nos motivó a realizar estudios más detallados de dicha región axonal. Para analizar, con mayor detalle, la relación entre las PARPs y los motores moleculares como la miosina Va, kinesina o dineína, se utilizó inmunohistoquímica sobre los axones *in toto*.

Los resultados presentados indican que la miosina Va y la kinesina Kif3a, se encuentran diferencialmente distribuidas en el axón. Estos estudios muestran que hay un enriquecimiento de las mismas en las zonas identificadas como placas ribosomales periaxoplásmicas. Es interesante destacar que esto no sucede con otras proteínas motoras. Cuando se utilizó un anticuerpo contra kinesina Kif5, se detectó únicamente reacción cruzada en pequeños partículas ubicadas homogéneamente en el axoplasma. Resultados similares fueron obtenidos cuando se buscó la proteína dineína. Ambos resultados son consistentes con las observaciones que relacionan a Kif5 y dineína, con el transporte de vesículas anterógrado y retrógrado, respectivamente (Goldstein y Yang, 2000).

Por otro lado, esto sugiere que las proteínas identificadas en las PARPs tienen una función específica con relación a este dominio. Esto estaría de acuerdo a su vez con la idea de que distintos grupos de proteínas

motoras, y sus isoformas correspondientes, poseen funciones de transporte determinadas. Otro componente esencial para lograr transporte de moléculas particulares dirigido a destinos celulares específicos, son las proteínas asociadas a los motores y a las especies transportadas, llamados adaptadores. Para profundizar en los mecanismos de transporte asociados a las PARPs, sería interesante identificar que tipos de adaptadores se encuentran presentes en las PARPs.

Con respecto a la miosina Va y kinesina se discutirá con profundidad su relación al transporte de ARN mensajero y componentes de la maquinaria traduccional en la discusión general.

Capítulo 4  
Discusión General y  
Perspectivas.

La célula neuronal presenta un alto grado de polaridad funcional y estructural. Diferentes dominios, con funciones específicas, se van determinando a lo largo de la diferenciación neuronal y se mantendrán durante la vida adulta. Para ello, esta célula posee diversos sistemas de transporte selectivo para componentes celulares que incluyen organelos (mitocondrias, vesículas), complejos proteicos, ribosomas y ARN mensajeros. La localización final de los componentes transportados dependerá de un sistema de etiquetado, transporte y anclaje en el destino. Entre los sitios posibles de destino se encuentran las dendritas, la post sinapsis, el cono de arranque axónico, los nodos de Ranvier, el axón y la pre-sinapsis. Para una buena parte de los componentes mencionados se comienza a conocer las rutas y códigos necesarios para obtener una localización específica de dichos elementos. Considerando en particular al aparato traduccional y al ARN mensajero, las observaciones referentes al transporte selectivo hacia las dendritas son numerosas (Steward, 2001). Nuestros estudios se centran en el análisis de la presencia y localización precisa de ribosomas y componentes del aparato traduccional en los axones de vertebrados.

El problema de la compartimentalización de los componentes moleculares y las funciones neuronales asociadas a ellas puede ser estudiado desde diferentes perspectivas. Por ejemplo, se puede observar como se clasifican y direccionan los diferentes componentes celulares en el soma neuronal, o se pueden estudiar los mecanismos que subyacen las diferentes modalidades de transporte. Pero también se puede analizar la estructura y función del dominio que va recibir los componentes clasificados y transportados selectivamente hacia dicho destino final. El presente trabajo de tesis analiza la estructura, localización y composición molecular de las placas



ribosomales periaxoplásmicas. Dichas estructuras se observan a intervalos regulares en la región cortical de los axones largos del sistema nervioso central o periférico de vertebrados. Las evidencias aquí presentadas apoyan la hipótesis de que estas estructuras podrían ser un sitio especializado en síntesis de proteínas axonales. Si es así, estas observaciones tienen que insertarse en un marco que integre la posible función de las placas ribosomales periaxoplásmicas en su entorno axonal y celular. Una forma sería considerarlas como un posible destino final de la maquinaria de transporte donde serían localizados ARNm y la maquinaria básica de traducción. Los productos de traducción serían en este caso sintetizados en ese lugar o sus inmediaciones y redistribuidos localmente en el entorno axoplásmico. A continuación se discutirá las principales observaciones obtenidas sobre la estructura y composición de las placas ribosomales periaxoplásmicas.

### **Estructura de las PARPs.**

En 1996, Koenig y Martin, describen las placas ribosomales periaxoplásmicas y realizan la primera descripción de estas estructuras, determinando tres importantes características de las mismas: a) alto contenido de ARN, b) localización cortical subaxolemal en intervalos discontinuos y c) presencias de partículas con un tamaño similar a un ribosoma. Estas observaciones que comenzaron en el axón gigante de Mauthner, postulaban a las PARPs como estructuras candidatas para la síntesis de proteínas en el territorio axoplásmico. Una pregunta importante, que surgió del hecho de encontrar las PARPs en un tipo particular de axones,

era si estas formaciones ricas en RNA podían encontrarse en otro tipo de axones y en otros grupos zoológicos. La presencia de dominios ribosomales en los axones fue investigada en diferentes modelos experimentales que incluyeron tanto invertebrados (calamar) así como diversos vertebrados (conejo, rata y ratón). Los axones estudiados fueron el axón gigante de calamar (Sotelo et al., 1999 y Bleher y Martin, 2000) y los axones de la raíces ventrales de las especies mencionadas (trabajos I, III y V). Los acúmulos ribosomales encontrados en invertebrados tienen características morfológicas y localización subcelular diferentes a los presentes en todos los vertebrados estudiados hasta el momento. En el axón gigante de calamar no se observa una localización preferentemente cortical y se encuentran distribuidos de manera uniforme en el espacio axoplásmico. Estos acúmulos se presentan en forma de esferas conteniendo un número pequeño de polisomas en estrecha proximidad entre sí y en algunos casos con relación al citoesqueleto. En cambio, los axones de mamíferos observados presentan una clara distribución en la zona cortical del axón y los acúmulos nos son esféricos sino alargados y de mayores dimensiones que los observados en calamar (trabajos I y V). Si se compara las dimensiones de las PARP en el axón de Mauthner con las de los axones de raíces ventrales, las segundas son de menor tamaño, más constantes en su morfología y sin ramificaciones importantes.

En el estado actual del conocimiento en el área, es difícil establecer si las diferencias mencionadas tienen consecuencias funcionales. Sin duda es interesante relacionarlas con las diferencias de complejidad funcional de los diferentes sistemas, así como con consideraciones de tipo hidrodinámicas y/o mecánicas. Respecto a esto último, el cambio de posición de agrupaciones

ribosomales desde zonas axónicas centrales a periféricas quizás refleje una optimización del tráfico intracelular ya que estas estructuras ocuparían una posición inestable en el centro del tráfico macromolecular del axón. A su vez, el localizarse inmediatamente por debajo de la membrana axónica puede significar una vinculación directa a señales extracelulares. Por otra parte, la presencia de acúmulos ribosomales en vertebrados superiores (mamíferos) sugiere que estas estructuras pueden tener un rol particular en todos los vertebrados. Hasta el momento, sigue siendo una incógnita si estas estructuras se presentan en axones cortos como los de interneuronas del sistema nervioso central. Es de destacar, sin embargo, que axones del sistema nervioso central como el axón de Mauthner o las fibras que se encuentran en sus proximidades en la médula espinal (Koenig & Martin, 1996) presentan placas ribosomales.

### **Localización intra-axonal y sub-axolemal de las PARPs.**

Los datos obtenidos sobre la morfología y localización de las PARPs provienen del estudio de las preparaciones *in toto* (“wholemout”) donde los axones son extraídos del tejido ya sin su vaina de mielina (trabajo I). Una vez identificadas y caracterizadas morfológicamente, se buscó si se podían identificar por técnicas *in situ*. Las PARPs fueron observadas en segmentos axonales que preservaban parte de su envoltura mielínica así como en secciones semi-finas de raíces ventrales (trabajo I, Figura 2G). En este último caso zonas axonales en íntimo contacto con la vaina de mielina presentaron regiones YOYO-1 positivas, similares a las dimensiones de PARPs descritas en la preparación *in toto* (trabajo I, Figura 2 H e I). Estos resultados coinciden

con que las señales obtenidas para el ARNm que codifica para NF-L en secciones transversales de nervio ciático lesionado se encuentran aproximadamente en la misma región (trabajo II, Figura 7). Twiss y colaboradores (2000) intentaron con cierto éxito la búsqueda de estas regiones utilizando el anticuerpo anti ARN ribosomal Y10B mediante microscopía láser confocal. Estos investigadores mostraron regiones donde existía co-localización de este anticuerpo anti ribosomas con marcadores axonales (tubulina, y neurofilamentos), confirmando la presencia cortical intra-axonal de estos dominios *in situ*.

La localización intra-axonal sub-axolemal de los ribosomas fue confirmada por los resultados obtenidos por Rainer Martin (trabajo I, figura 7 y 8) mediante microscopía electrónica combinada con el análisis espectral de emisión de energía de electrones (ESI). De esta forma se detectaron partículas tipo ribosomas en forma de acúmulos en diferentes regiones subyacentes a la membrana plasmática axonal. Estos resultados tienen mucha relevancia, no sólo porque confirman la presencia axoplásmica de estas estructuras, sino porque es la descripción más reciente de ribosomas en axones de mamíferos, luego de años de búsqueda y a 30 años de la comunicación pionera y controvertida de Zelena (1972). Los resultados obtenidos confirman que también existiría en las placas de mamíferos, una “matriz” donde los ribosomas estarían insertos. La caracterización de dicha matriz es un tema abierto ya que el análisis realizado mediante ESI, no es de utilidad para una caracterización morfológica precisa.

## **Los componentes de la maquinaria traduccional y el ARNm de la $\beta$ -actina se localizan en las PARPs.**

A pesar de las diferencias morfológicas entre los dominios ribosomales del axón de Mauthner y los dominios de axones de raíces ventrales, los análisis moleculares muestran elementos comunes. La presencia en los mismos de diferentes moléculas claves para la traducción de proteínas, fue estudiada mediante inmuno-histoquímica e hibridización *in situ*. La presencia de ribosomas fue estudiada mediante la búsqueda de ARN ribosomal y proteínas ribosomales. El primero fue demostrado utilizando un anticuerpo monoclonal, proveniente de enfermedades autoinmunes, que es capaz de reconocer el ARN ribosomal de la subunidad mayor de los ribosomas. Dicho anticuerpo, presentó reacción cruzada en las placas de ambas especies (trabajo I, figuras 4 y 5). A su vez presentó un alto grado de colocalización con la tinción para ácidos nucleicos YOYO-1, sin marcar las abundantes mitocondrias axonales. Esto corroboraba que las imágenes obtenidas por ESI, que indicaban no sólo la presencia de ribosomas, a su vez indicaban que el ARNr ocupaba la placa ribosomal casi en su totalidad. Esto fue analizado específicamente realizando morfometría de las placas ribosomales de las raíces ventrales de conejo (trabajo I. Tabla I). Esto, además, fue confirmado utilizando otro anticuerpo anti-ribosoma (llamado anti-P), disponible comercialmente, que reconoce 3 proteínas de la subunidad mayor. De esta forma, utilizando criterios ultraestructurales e inmunohistoquímicos, se comprueba que uno de los principales componentes moleculares de estas estructuras son los ribosomas. Un punto controversial es si los ribosomas encontrados pueden tener asociado o no retículo endoplásmico. En la figura 7

del trabajo I, se muestran perfiles membranosos intraaxonales que podrían pertenecer al retículo endoplásmico. Si esto fuera así, no sólo sería posible sintetizar proteínas cuyo destino sea el citosólico, sino también proteínas integrales de membrana. Esta posibilidad se ve apoyada por evidencias de que ciertos axones de mamífero, durante el crecimiento *in vivo*, son capaces de sintetizar e insertar en la membrana axoplásmica el receptor para efrinas (Brittis y cols., 2002, ver más adelante). Van Minen y colaboradores (Spencer y cols., 2000) demostraron claramente que axones adultos de moluscos eran capaces de sintetizar e integrar a la membrana axoplásmica un receptor para conopresina. Ambos grupos de evidencias apoyarían la idea de que cierto tipo de axones podrían sintetizar localmente proteínas de membrana.

Realizando experimentos de marcado *in vivo* de proteínas axonales, Koenig (1991), demostró que entre las proteínas axoplásmicas sintetizadas *de novo* se encontraba entre otras, la actina. En la mencionada comunicación, no se lograba identificar que estructura axónica era la responsable de la síntesis de esta proteína, pero a partir de la descripción de las placas ribosomales periaxoplásmicas, éstas pasaron a ser un buen candidato. Si dicha proteína citoesquelética es sintetizada en estas estructuras, el ARNm respectivo tendría que estar localizado preferencialmente en estos sitios. Utilizando hibridización *in situ* fluorescente y microscopia láser confocal (trabajo III) logramos demostrar que el ARNm codificante para la beta actina se encuentra localizado preferentemente en estos dominios. Utilizando RT-PCR de alta sensibilidad se confirmó la presencia de dicho ARNm en extractos de ARN total provenientes de axones de Mauthner. Tomando ambas observaciones en conjunto (Koenig, 1991 y trabajo III) existe alta probabilidad de que la beta actina sea sintetizada

localmente en el axón. Nuevamente, son los estudios realizados en cultivos neuronales los que indican que el ARNm codificante para la beta actina se transporta selectivamente hacia los axones y sus conos de crecimiento en cultivo (Bassell y cols 1998, Olink-Coux-Hollenbeck, 1996), traducándose localmente en esos lugares. Estos estudios han caracterizado que el extremo 3' no traducido de este ARNm posee un segmento de su secuencia que es el responsable del transporte dirigido del mensajero. También se demostró que es capaz de asociarse con una proteína necesaria para que dicho transporte ocurra. Esta secuencia se encuentra conservada en diferentes especies y es capaz de dirigir el tránsito específico de este ARNm en diferentes tipos celulares incluido la neurona (Oleinikov y Singer, 1998).

La localización subcelular de este ARNm en las PARPs no sólo implica su posible traducción localizada en estos dominios ribosomales, sino que también implica que dicho ARNm sea transportado hacia ese lugar. El origen de este mensajero probablemente sea somático y utilice la maquinaria de transporte rápido para lograr llegar intacto a los sitios distantes como las placas periaxoplásmicas. Los experimentos de micro inyección de ARN marcado radioactivamente sugieren que la maquinaria utilizada para el transporte sería en parte dependiente del citoesqueleto microtubular y en parte por aquel compuesto por microfilamentos (Muslimov y cols 2002). En este caso, el transporte axonal del ARN BC1 (transcrito de la polimerasa III, con funciones moduladoras de la traducción) es bloqueado por agentes depolimerizantes de los microtúbulos; mientras que el transporte radial, desde la red microtubular hacia la red cortical de actina, es bloqueado por agentes que depolimerizaban la red de actina. Como discutiremos más adelante, el

transporte y localización del ARNm antes mencionado sea mediado por sistemas clásicos de transporte axonal.

### **Estudios sobre el repertorio de ARN mensajeros axonales.**

La identidad del repertorio de ARN mensajeros localizados en el territorio axoplásmico o en los dominios ribosomales es un enigma interesante. Este punto aún no ha sido explorado en axones adultos de vertebrados. El grupo de Giuditta ha construido una genoteca de ADNc a partir de ARN extraído del axón gigante de calamar (Gioio y cols., 1994). Aunque las neuronas de invertebrados no presentan una gran polaridad morfológica en sus prolongaciones, si presentan una localización diferencial de los ARNm en las mismas. La complejidad de las moléculas (determinada mediante estudios de hibridización por  $R_{ot}$ ) de ARN axonal es mucho menor que la complejidad encontrada en los somas neuronales, indicando el transporte selectivo de un grupo de ARNm hacia el axón (Chun y cols, 1996). En el caso del calamar existen evidencias de que el sitio de origen de estos ARNm axonales puede ser tanto del soma neuronal como de la glía adaxonal (Cuttillo y cols., 1983). Para el caso de vertebrados superiores hemos constatado que la célula de Schwann es capaz de transcribir ARNm neuro-específicos como los que codifican para las tres subunidades de los neurofilamentos (trabajo II, figura 1 y 5) y que el ARNm codificante para la subunidad menor se encuentra en la zona limítrofe entre el mesaxón interno y la corteza axonal (trabajo II, figura 7). Aunque no existen pruebas de que exista transferencia de ARN entre estas dos células, quedan las



observaciones sobre la expresión de los neurofilamentos el nervio ciático (trabajo II y otros) como un hecho muy sugestivo sobre esta posibilidad.

Más allá del origen del ARNm axonal, es importante caracterizar la diversidad de los mismos. Para esto se diseñaron protocolos para aislar picogramos de ARN total a partir de axoplasmas aislados y se utilizó dicho ARN para realizar un proceso de amplificación aleatorio de ADNc que generara una población de "ESTs" que representan el extremo 3' de los ARNm de la población original. Con la mezcla de "ESTs" se generó una minibiblioteca de ADNc (aprox. 200 clonas) y se secuenciaron 30 clonas al azar por secuenciación automática. Uno de los posibles problemas con esta aproximación es el grado de pureza de los axones utilizados. Antes de realizar este tipo de experimentos se demostró que esta preparación (axones *in toto*) era adecuada para estudios inmunohistoquímicos tanto a nivel óptico como electrónico, pero para métodos de análisis por biología molecular de alta sensibilidad como la RT-PCR su utilidad se relativizó, debido a que se identificaron frecuentemente contaminantes de células adyacentes. Utilizando GFAP como marcador glial (Weiner y cols 1998 y trabajo III) se ha verificado que la mayoría de las muestras contenían dicho mensajero y solo en baja frecuencia se colectaban axones donde no se encontraba el ARNm de GFAP (trabajo III fig. 4). Esto le resta potencia a la generación de ESTs a partir de ARN extraído de axones de Mauthner, ya que parte de estas clonas podrían ser provenientes de la glía circundante a este axón.

De todas maneras, al analizar la secuencia de los ARN clonados de la forma descrita, se observan hechos bastante significativos. En primer lugar, 7 clonas de 21 correspondieron a ARN mitocondriales (ARNr y ARNm). Los ARN mitocondriales se encontraban entre los candidatos a ser encontrados

mediante este estudio, ya que extracciones de ARN total del axón incluirían el proveniente de la abundante población de mitocondrias presentes en el axoplasma. Esto sugiere de que de existir ARN en el axón, además del mitocondrial, esta técnica así como las otras empleadas (RT-PCR, HIS), serían capaces de detectarlo. Además, la detección de los mismos nos indica que logramos amplificar ARN intra-axonales ya que en la mielina compacta circundante al axón las mitocondrias son muy escasas. Por último, 12 de las 21 secuencias corresponden a ARNm codificantes para diferentes proteínas citoplásmicas, 6 de las cuales corresponden a ORFs que aún no han sido caracterizados. Para confirmar si estos ARNm se encuentran localizados específicamente en los dominios ribosomales o no, tendríamos que realizar hibridaciones in situ con los mismos sobre wholemount axonales.

Dentro de los ARNm encontrados se encuentran uno similar a la proteína motora miosina V, una proteína asociada a los microtúbulos y la proteína reguladora 14-3-3. El caso de la miosina V se discutirá más adelante. Uno de los hallazgos con características peculiares fue el de 3 clonas que contenían secuencias idénticas a ARNm codificantes para proteínas ribosomales. Dado que el ensamblaje de un ribosoma es un proceso de alta complejidad que ocurre en el nucleolo celular, es difícil explicar su presencia en un extracto axonal. Si tomamos estos resultados en cuenta, aunque claramente requieran confirmación, tendríamos varias formas de explicarlos. Una hipótesis que podría plantearse, aunque no hemos encontrado antecedentes que la apoyen, sería que un ribosoma ensamblado, pudiera realizar hasta cierto punto un recambio de sus proteínas. Por otro lado existen observaciones de que ciertas proteínas ribosomales (diferentes a las encontradas) poseen funciones extra ribosomales (Wool, 1996,

Zimmermann, 2003). Por último, estos podrían ser contaminantes de algún soma celular (glial o neuronal) cercano a las fibras de Mauthner que este aportando moléculas como estas. Esto último es bastante improbable dado que por la forma de preparar los axones, sería muy sencillo detectar contaminantes YOYO-1 positivos en la superficie de los mismos. Si fueran contaminaciones de la vaina glial, nos encontraríamos con el mismo problema logístico: ARNm ribosomales muy lejos del sitio de ensamblaje natural de estas proteínas, el nucleolo, siendo esta opción inconsistente con el funcionamiento de estas proteínas.

Sin duda, aunque estos resultados son preliminares, muestran que es posible caracterizar el repertorio de ARNm presentes en axones. En la actualidad estos experimentos se continúan mediante ensayos de amplificación de ARN con kits comerciales que son capaces de utilizar nanogramos de ARN como punto de partida para una amplificación lineal de tres ordenes de magnitud. El objetivo es lograr la suficiente cantidad de ARN para producir sondas con el fin de ser usadas para hibridizar con microarreglos de ADN. De esta forma se estaría investigando a una escala genómica la diversidad de ARNm que se pueden encontrar en el axón.

### **Etiquetado y transporte selectivo de la maquinaria traduccional.**

La localización axonal de los dominios ribosomales provoca una serie de preguntas muy atractivas. Una de ellas es, cual es el origen de los componentes de estas estructuras. Como discutimos previamente una de las fuentes de estos componentes es el soma neuronal. El transporte de ARN es un campo que ha avanzado de forma importante utilizando modelos distintos

a los neuronales, ya que en diversos sistemas se había constatado una distribución diferencial para varios ARNm específicos. La biología del desarrollo de las primeras etapas de la mosca *Drosophila melanogaster* presenta ejemplos singulares que ilustran un punto esencial para la siguiente discusión. Algunas proteínas de importancia para el desarrollo antero posterior del embrión como Bicoid dependen de la localización y cantidad de su ARN mensajero para lograr especificar diferentes regiones embrionarias. Este ARNm es de origen materno, sintetizado por células nodrizas y transportado hasta el citoplasma del huevo por canales citoplásmicos y luego depositado en dicho citoplasma en un gradiente de concentraciones antero-posterior. Hoy en día se conocen el tipo y calidad de información necesaria para que este proceso de transporte y localización ocurra. Las secuencias propias del ARNm, las proteínas motoras que lo transportan y los sistemas de anclaje en el sitio final son los actores esenciales en este proceso. En un principio se pensaba que estos mecanismos eran característicos de situaciones tan complejas como las primeras etapas del desarrollo embrionario. Un ejemplo que demostró que la localización del ARNm es un mecanismo utilizado por células eucariotas con dimensiones y morfología sencillas, fue el estudio de la localización de la beta actina en fibroblastos en cultivo realizado por el grupo de Singer (Oleinikov y Singer, 1998). Estos investigadores observaron que el ARNm codificante para la beta actina se localizaba preferentemente en las zonas cercanas a los lamelipodios y que se traducía preferencialmente en esa zona y no en una forma aleatoria en cualquier región de la célula. La localización específica era dependiente de una secuencia en su posición 3' no traducido, a la que llamaron "zip code" o código postal. La inhibición del transporte del ARNm en estos fibroblastos en

cultivo generaba una disminución de la capacidad de migración de estas células. El punto más importante, es que existe el transporte específico de ARN hacia regiones citoplásmicas especiales incluso en células que no presentan una gran complejidad morfológica como las células neuronales.

Para las neuronas ha sido claramente puesto en evidencia que existe un transporte selectivo de ARNm hacia las dendritas y síntesis local de proteínas en zonas como la post sinapsis (Steward y Worley, 2001). En cambio, transporte de la maquinaria traduccional hacia el territorio axoplásmico recién se comienza discutir con profundidad. Los dominios ribosomales periaxoplásmicos serían, de acuerdo con nuestros resultados, el destino final de los ribosomas y los ARNm y por lo tanto esto implica el transporte selectivo de dichas moléculas hacia los axones. Estudios pioneros (Bondy & Purdue, 1975) indicaron el transporte de ARN ribosomal hacia los axones. Los cultivos neuronales son hoy en día la principal fuente de datos sobre transporte de ARNm. El grupo de Bassell ha caracterizado el transporte del ARNm de la beta actina (Bassell y cols, 1998) y el grupo de Ginsburg se ha dedicado al ARNm de la proteína axónica Tau (Aronov y cols, 2000, 2001). En términos generales la velocidad con que el ARN sería transportado corresponde al componente de transporte axonal rápido, y que depende de señales tipo “zip codes” y proteínas de unión específicas a las mismas. El transporte ocurriría en forma de partículas ribonucleoprotéicas que luego serían desensambladas en condiciones propicias para la traducción (Krichevsky y Kosik, 2001).

Un aspecto mayor, relacionado al transporte selectivo de materiales a las placas, es el propio transporte de los ribosomas hacia estos dominios. Esto ha sido poco estudiado tanto para axones como para dendritas, pero se

dispone de mucha información en lo que respecta al transporte de ribosomas desde el nucleolo al citoplasma y desde allí hacia las membranas del retículo endoplásmico. Ambos procesos implican un alto grado de organización del etiquetado y transporte para lograr enviar los ribosomas hacia distintas regiones dentro del citoplasma de la célula.

Las subunidades ribosomales (40S y 60S) son ensambladas en el nucleolo y transportadas en forma independiente hacia el citoplasma a través del complejo del poro nuclear (Johnson y cols 2002). Este proceso involucra el reconocimiento de “señales de exportación nuclear” (NES, nuclear export signals) presentes en las subunidades ribosomales, por parte del receptor CMR1, perteneciente a la familia de las importinas tipo beta, y las proteínas RAN-GTP. Recientemente, se ha identificado que una proteína llamada Nmd3 es necesaria para que ocurra la interacción ribosoma-receptor CMR1. Esta proteína cumple funciones adaptadoras entre la señal NES y el receptor para exportación de esta subunidad. El transporte de la subunidad 40S utilizaría a los receptores CMR1 y Ran-GTP, pero esta interacción dependería de adaptadores aún no identificados.

Una vez transportadas hacia el citoplasma, las proteínas utilizadas para concretar la exportación de las subunidades son recicladas hacia el núcleo y su función en el transporte de los ribosomas termina en este momento. El siguiente paso que gobierna el transporte direccionado de los ribosomas depende de la proteína que estén sintetizando los mismos. Una proteína que contenga en su secuencia un “péptido señal” será reconocida por el complejo citoplásmico SRP (signal recognition particle), deteniendo la traducción, hasta que todo el complejo (SRP-péptido nascente-ribosoma) haga contacto con el receptor de SRP en las membranas del retículo

endoplásmico. En ese momento se reanuda la síntesis de esa proteína y se transloca a través de la membrana gracias a un poro proteico llamado translocón (Keenan y cols 2001). Para las proteínas mitocondriales el acoplamiento traducción-translocación recién mencionado existe, pero la interacción con el complejo de translocación TOM es mucho más débil, registrándose síntesis de poli-péptido mitocondriales en el citoplasma. Asimismo, para las proteínas a ser importadas a la mitocondria, se han descrito secuencias capaces de señalar el destino de las mismas, pero no se ha encontrado aún un complejo con una función tan clara como el complejo SRP (Beddoe & Lithgow, 2002).

¿Que es lo que sucede con proteínas cuyo destino diferente al retículo endoplásmico o mitocondrial?, ¿existen a este nivel otros mecanismos que indiquen compartimentalización de la maquinaria traduccional? Un candidato para afectar la distribución de la maquinaria traduccional y posiblemente modularla, es el complejo dimérico “Nascent-poli peptide asociated complex” o “NAC” (Rospert y cols, 2002). El NAC es un dímero que tiene la propiedad de unirse a las cadenas nacientes presentes en ribosomas activos, cuya función exacta no ha sido determinada aún. Se le ha involucrado en diversas tareas como: i) protección de los péptidos nacientes, ii) regulación negativa del transporte hacia el retículo endoplásmico y iii) regulador positivo del transporte de proteínas hacia la mitocondria.

Recientemente en *Drosophila*, se ha demostrado que la mutación *bicaudal* se localizaba en el gen codificante para una de las subunidades de NAC, la proteína beta-NAC. Esto tenía como consecuencia la localización ectópica del ARNm y proteína Nanos, generando embriones que carecen de cabeza y torax, con duplicación en espejo de las estructuras abdominales

(Markesich y cols, 2000). Ya que se demostró que el ARNm *nanos* se encuentra asociado a polisomas y solo se traduce en la región posterior del embrión, se propuso que el efecto de la mutación en beta-NAC (bicaudal) sobre la traducción de *nanos* es doble: por un lado se afecta la represión traduccional que es ejercida en regiones diferentes a la posterior y por otro lado se afecta la localización del ARNm. Aunque todavía es muy prematuro generalizar, esta sería la primera demostración (a parte de las mencionadas para SRP) de que la localización de polisomas se ve afectado por la actividad de una proteína de unión a cadenas polipeptídicas nacientes.

A la luz de los resultados obtenidos en esta tesis y las observaciones que conciernen al transporte de ribosomas en dendritas, es altamente probable que existan mecanismos adicionales a los mencionados para etiquetar y transportar los mismos hacia destinos diferentes al retículo endoplásmico o mitocondrial. Es posible, entonces, que los polisomas sean enviados hacia las dendritas o axones y placas periaxoplásmicas, gracias a la existencia de proteínas con funciones similares a NAC u otras proteínas adaptadoras capaces de etiquetar un ribosoma que se encuentre sintetizando determinado tipo de proteínas. El hallazgo de partículas ribonucleoprotéicas conteniendo ARNm, proteínas de unión al ARN, proteínas motoras y poliribosomas indicaría que estos últimos se empaquetan en estas estructuras para su transporte (Mallardo y cols, 2003, Krichevsky & Kosik, 2001). El paso de etiquetado previo a la formación de estas partículas debe ser estudiado con mayor profundidad, ya que quizás en ese punto se encuentren claves para entender como los ribosomas se transportan selectivamente a regiones alejadas del pericarion.



## **Sistemas de transporte subcelular asociados a las PARPs.**

Los motores moleculares responsables de los movimientos del ARNm (o los ribosomas), recién comienzan a conocerse. Es a partir de estudios realizados en levaduras, donde se comenzó a identificar cuales eran los motores que desplazaban ARN en el citoplasma. El ARNm ASH1, involucrado en los procesos de diferenciación en levaduras, es transportado selectivamente hacia la célula hija utilizando filamentos de actina. En una cepa que tiene el gen Myo2 mutado, un homólogo de la proteína motora Miosina V, este transporte no ocurre. Esta fue la primera evidencia de que un motor molecular se encontraba involucrado en el transporte de ARN mensajeros. Más adelante se demostró que esta relación no era directa, sino que era mediada por otras dos proteínas adaptadoras (She1p, She2p) que son realmente las que determinan el destino final de la miosina V. Este fue un punto de partida para buscar motores moleculares, en particular la miosina V, en axones de vertebrados superiores (trabajos, IV y V) como una forma de relacionar la actividad y localización de estos motores con respecto a las zonas ricas en ribosomas y ARN en la corteza axonal.

Mediante inmunohistoquímica en secciones de nervio ciático normal y lesionado, se observó que la distribución de la proteína miosina Va localizaba preferencialmente en la zona cortical del axón rica en citoesqueleto de actina (Fig. 2, trabajo IV). Dicha distribución no era idéntica en todos los axones observados coincidiendo con los resultados obtenidos al observar su distribución en wholemounds de axones aislados (figura 2 y 3, trabajo V). Tanto en peces como en rata, se constató la distribución cortical y discontinua, observándose un enriquecimiento de esta proteína en los

dominios ribosomales periaxoplásmicos. Se ha descrito igualmente que la proteína motora kinesina, específicamente la isoforma Kif3A se encuentra enriquecida en los dichos dominios (figura 4 y 5, trabajo V). Ambas proteínas motoras presentan una colocación muy importante con la marcación para YOYO-1 y entre sí mismas. Sin embargo, para otra proteína motora como la dineína no se encontró una distribución correlacionada con estos dominios (figura 6, trabajo V). La presencia de ciertas proteínas motoras y no de otras, así como ciertas isoformas de una de ellas y no todas, nos habla de que hacia estos dominios no convergen o se dirigen las proteínas motoras en forma masiva. Quizá esto dependa de procesos de transporte selectivo hacia este dominio o procesos de organización intrínsecos de esta zona en particular.

Existen en la literatura evidencias que brindan apoyo para elaborar por lo menos dos hipótesis sobre la función de estas proteínas motoras en las placas periaxoplásmicas. La primera hipótesis sería la del transporte selectivo del material propio de la placa ribosomal desde el soma neuronal utilizando un transportador con dependencia doble de microtúbulos y filamentos de actina en diferentes momentos. Se ha demostrado que este transportador “dual” puede existir mediante la asociación de la kinesina con la miosina V (Karcher y cols., 2002, Brown, 1999). La kinesina llevaría la carga en distancias largas, a velocidades del transporte axonal rápido, utilizando la red de microtúbulos. En este viaje, la miosina V sería llevada como parte de la carga, en un estado posiblemente inactivo, y sería utilizada en el momento necesario para transferir la carga hacia la red de actina y los dominios ribosomales. El enriquecimiento de ambas proteínas en el supuesto destino final, ha sido observado para la miosina en levaduras, donde no es posible

observar las partículas durante su tránsito pero si en su destino final (Kruse y cols., 2002). A su vez ambos motores se encontraron participando en procesos de transporte de ARN en varios sistemas diferentes, lo cual hace de esta hipótesis un buen candidato para explicar la distribución observada. Experimentos *in vivo* apoyan esta hipótesis, ya que el transporte axonal anterogrado del ARN BC1 necesita de la red microtubular para el movimiento de largo alcance y de la red de actina para transferirse a regiones axonales corticales (Muslimov y cols., 2002).

El hecho de que sean isoformas particulares y no varias de ellas a la vez, coincide con las observaciones que muestran la gran variedad de isoformas (14 subtipos para las miosinas y cerca de 10 subtipos para la kinesina) implicando una gran diversidad de funciones, selectividad en la carga a ser llevada y destino final de la misma (Hirokawa, 1998; Langford, 2002). Esta capacidad del sistema de transporte se ve incrementada porque las proteínas “adaptadoras” que interaccionan con la carga por un lado y con los motores por el otro, incrementan la variedad de destinos y especificidad del sistema de transporte. En consecuencia, no sería raro encontrar proteínas adaptadoras específicas de los dominios ribosomales, como sucede con She2p y el ARNm ASH1 en la gemas hijas de las levaduras.

La posibilidad de que estas proteínas motoras cumplan una función organizadora interna del dominio ribosomal, debe tomarse en cuenta. Como hemos visto, la información morfológica obtenida mediante diversas aproximaciones indican que estos dominios presentan cierto grado de complejidad estructural. Esto puede implicar la necesidad de un tráfico macromolecular intrínseco organizado, como sucede para organelos como el aparato de Golgi (Dematteis y Morrows, 1998), donde la dinámica

organizativa es gobernada por el tráfico vesicular proveniente del retículo endoplásmico o a través de la red trans-golgi hacia los diferentes destinos celulares. Para comprender mejor el funcionamiento de estas moléculas en este dominio axonal es preciso avanzar en la caracterización ultra estructural de los mismos. Esta sería una forma de descifrar las características de la “matriz” observada previamente (Koenig y Martín, 1996 y trabajo I).

### **Modelo del funcionamiento de las placas ribosomales periaxoplásmicas.**

Tomando en cuenta los datos obtenidos hasta el momento, existen elementos para construir un modelo sobre la función e interrelaciones de las placas ribosomales periaxoplásmicas en el territorio axonal (ver esquema en la siguiente página). Si nos centramos en el ARN (ribosomal o mensajero) en vez de las placas, éste, en primera instancia, se sintetizaría en el soma neuronal. En algún momento posterior a la síntesis, se ensamblaría en partículas compuestas por proteínas y ARNm, como ha sido observado en varios casos para células neuronales (Bassell y cols., 1998, Krishevsky y cols., 2000, Aronov y cols., 2000). No se ha estudiado aún en detalle cuáles son los mecanismos de transporte para los ribosomas. La partícula ribonucleoprotéica sería capaz de reclutar los motores moleculares responsables de su transporte axonal (Kruse y cols., 2002, Ohashi y cols., 2002). Uno de los candidatos capaz de transportar estas partículas por grandes distancias sería la isoforma KIF3A del transportador anterógrado kinesina (Aronov y cols., 2002 y trabajo V). De acuerdo con el modelo de transporte dual (Langford y cols., 2002) basado en la interacción entre la Miosina V y Kinesina, la primera sería llevada junto con la carga hacia el

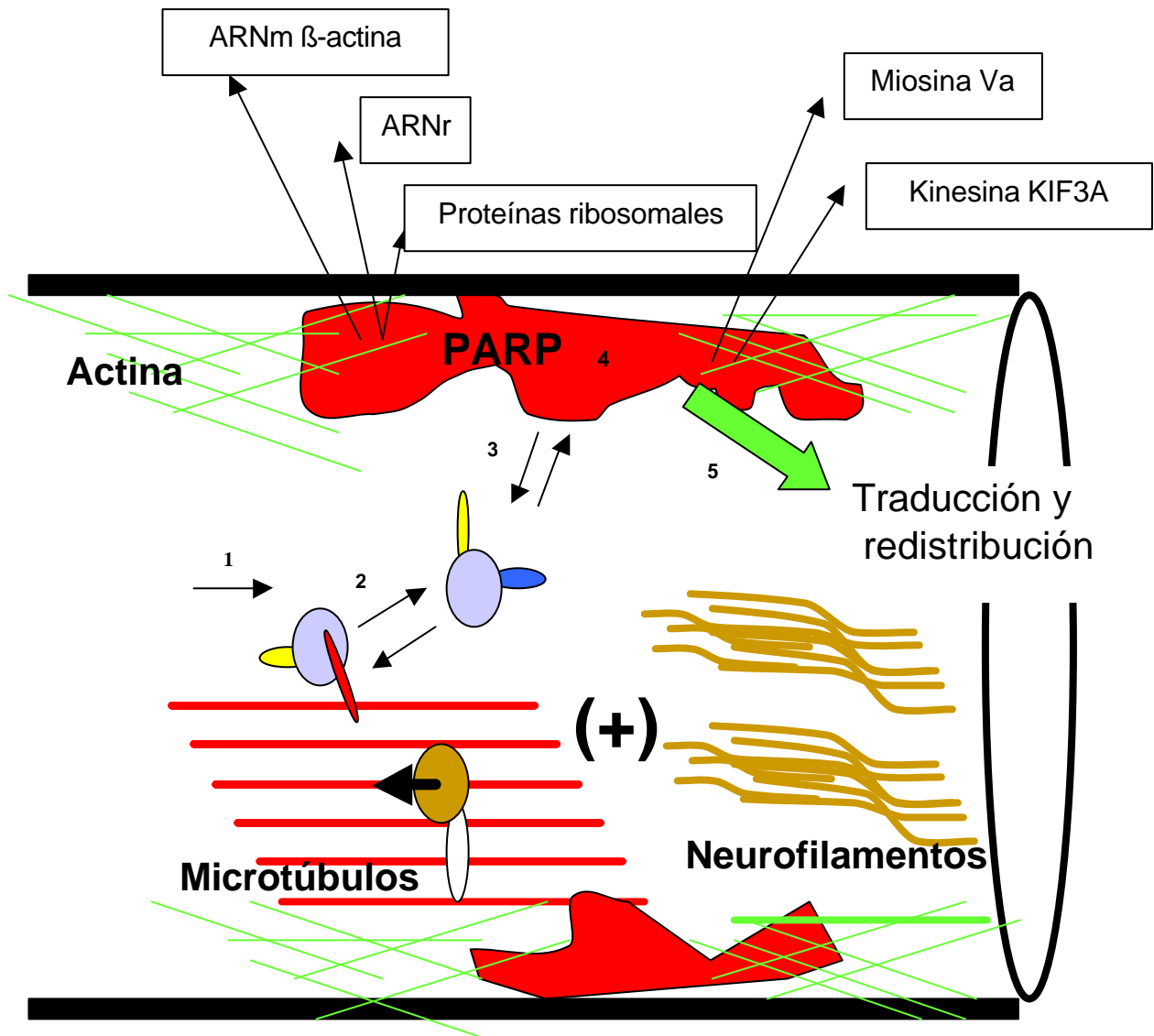
extremo más de los microtúbulos (indicado con 1 en el esquema). Ya que el transporte anterógrado rápido a través de la red de actina no ha sido demostrado, esto descartaría la posibilidad de que la miosina V fuera utilizada para las distancias largas. Tampoco está claro, como se realiza el cambio de un sistema de transporte (Kinesina/microtúbulos) a otro (Miosina/actina), pero este tipo de transiciones se ha registrado in vitro (Langford, 2002, indicado con 2 en el esquema). Ya que las placas ribosomales se encuentran en estrecha relación con el citoesqueleto de actina, el movimiento basado en la capacidad motora de la miosina podría ser la forma de trasladar la carga hacia estos dominios (indicado con 3 en el esquema). En este caso la kinesina sería transportada como carga. De acuerdo con la literatura, esta sería una forma de explicar los resultados obtenidos con respecto a la colocalización de los motores moleculares en los dominios ribosomales, pero sin duda se tratan de imágenes estáticas de un proceso que seguramente debe ser dinámico.




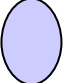
Los mecanismos discutidos podrían explicar como llegan los elementos constituyentes de las placas ribosomales periaxoplásmicas. A pesar de que hemos demostrado la presencia de ARNm, ARNr y proteínas ribosomales, la funcionalidad en si de estos dominios no se ha investigado. Según observaciones previas, el axón de Mauthner o las raíces ventrales de conejo tienen la capacidad de sintetizar proteínas, entre ellas posiblemente se encuentran los neurofilamentos, las tubulinas y la actina (Koenig, 1991). Si se toma en cuenta esto, y el hecho que los ribosomas colocalizan con el ARNm de la actina, las placas ribosomales serían el lugar de síntesis de esta proteína (indicado con 4 en el esquema). Las pruebas directas de que esto sucede todavía faltan. Para profundizar en el desarrollo de este punto se está

inyectando un ARNm híbrido que codifica para la proteína verde fluorescente, GFP y actina. De esta forma comprobaríamos que estos dominios son capaces de sintetizar una proteína en particular y podríamos seguir el destino de la misma luego de ser sintetizada.

Una vez que el ARNm es descargado en el dominio ribosomal este podría ser sustrato del aparato traduccional y luego ser redistribuido al axoplasma (indicado con 5 en el esquema), o quizás almacenado en partículas ribonucleoprotéicas para ser sintetizado a posteriori. Hoy en día no se conocen los mecanismos que regulan la traducción del ARNm que se encuentra empaquetado en partículas ribonucleoproteicas. Existen indicios de que un aumento en la cantidad de potasio intracelular cambiaría la organización de gránulos de ARN-proteína, teniendo como consecuencia que parte del ARNm transportado sea traducible en esos momentos (Krichevski y cols., 2002). Quizá una modulación de este tipo pueda estar operando en las placas ribosomales, cabe recordar que se encuentran muy cerca de la membrana plasmática y por consecuencia es una estructura que podría integrar las señales provenientes del medio exterior o las glía circundantes. Más allá de las especulaciones, es claro que luego de los hallazgos presentados a lo largo de esta tesis, es necesario avanzar hacia una caracterización funcional de estos dominios, y también comprender cual es el papel de estas estructuras en el mantenimiento axonal normal y patológico.

# Placas periaxoplásmicas: modelo de funcionamiento.



-  **Kinesina**
-  **Miosina V**
-  **Dineina**
-  **Partículas ribonucleoproteicas**

## **Perspectivas**

### **1. Ultraestructura y composición de las placas periaxoplásmicas.**

Los estudios estructurales de las PARPs se centraron en demostrar la presencia de ribosomas en estas zonas. Para hacerlo, se utilizó como técnica ultraestructural el ESI, con la que se obtienen imágenes que no aportan información estructural clásica. Es por eso que el estudio de la ultraestructura de estos dominios mediante microscopía electrónica de transmisión puede aportar observaciones de interés.

Una idea propuesta a partir de los estudios de ESI, fue que los ribosomas se encontraban unidos o incluidos en una matriz. Observaciones preliminares obtenidas recientemente por Koenig y nuestro grupo en Montevideo, indicarían que existe un enriquecimiento diferencial de actina y tubulina en las PARPS. Estudios estructurales utilizando MET podrían aportar datos sobre la organización del citoesqueleto en estos dominios. Combinando MET clásica con el uso de anticuerpos o sondas para detectar ARNm se puede lograr avances en la comprensión de la organización a nivel ultraestructural de las PARPs.

El repertorio de ARNm localizado en las placas sigue siendo una incógnita, pero las técnicas desarrolladas durante esta tesis, junto con los resultados preliminares obtenidos, indican caminos posibles para seguir trabajando. La generación de bibliotecas de EST, secuenciado de las mismas y localización subcelular mediante HIS, es un camino a seguir transitando. Otra opción es la comparación de distintos extractos de ARN provenientes de la vaina de mielina y axón, mediante el uso de microarrays. Para lograr dicho



objetivo se han explorado estrategias que utilizan sistemas de purificación de ARN y amplificación *in vitro* del mismo, para producir sondas que puedan ser utilizadas en ensayos de hibridación en microarrays. Los candidatos interesantes también deberán ser buscados mediante HIS sobre placas periaxoplásmicas.

## **2. Etiquetado y transporte de ARNm y ribosomas.**

El problema del etiquetado y transporte de ARNm, ribosomas y otros posibles componentes de las placas periaxoplásmicas recién comienza a ser estudiado. En lo que respecta a los motores moleculares, estos estudios generan varias preguntas interesantes. Entre ellas podemos destacar las siguientes: ¿existen otros motores diferentes a los encontrados en las PARPs?, ¿cuál es la carga específica de cada uno?, ¿cuáles son las señales que etiquetan las moléculas transportadas hacia estos dominios?, ¿cuáles son las moléculas adaptadores que median la interacción carga-motor y/o destino final?, ¿cuál es el grado de cooperación entre los sistemas de transporte basados en microtúbulos y actina?, ¿cuál es el papel de los motores moleculares en la organización interna de dichos dominios? ¿qué tipo de sistemas motores se utilizan para transportar los productos de las placas periaxoplásmicas?, ¿es posible que los motores moleculares se sinteticen en los dominios PARPs?.

Para responder algunas de estas preguntas se dispone de algunas alternativas. El modelo del axón de Mauthner ha sido utilizado para analizar el transporte axonal *in vivo*. Mediante la micro inyección de diferentes moléculas (ARNm o proteínas) marcadas diferencialmente (precursores radioactivos o

fluorescentes, o proteínas quiméricas fluorescentes) es posible trazar el camino de las mismas y si su localización se relaciona con las PARPs (Muslimov y cols., 2002). A su vez, se puede intentar interferir con los mecanismos de transporte operantes mediante el uso de anticuerpos específicos contra los posibles actores de estos procesos, así como tratamientos farmacológicos en particular.

Por otro lado, la inmunohistoquímica y la hibridación *in situ* sobre axones *in toto* o *in situ*, sigue siendo una opción viable para demostrar interrelaciones en los diferentes componentes observados en relación con las PARPs.

El transporte y etiquetado de la maquinaria traduccional constituye una materia pendiente de mucha importancia. ¿Cómo es que se logra enviar ribosomas hacia las prolongaciones axonales?, ¿de qué señales depende este proceso?, ¿cuál es la cadena de eventos que sucede para que se clasifiquen estas ribosomas?. Como se discutió en la sección precedente existen mecanismos que explican el transporte de las subunidades ribosomales desde el nucléolo hacia el citoplasma y desde el citoplasma hacia el retículo endoplásmico. A la luz de los resultados obtenidos en esta tesis y las observaciones que conciernen al transporte de ribosomas en dendritas, es altamente probable que existan mecanismos adicionales a los mencionados para clasificar y transportar los mismos hacia destinos diferentes del retículo endoplásmico. Para estudiar el transporte selectivo de proteínas ribosomales se ha comenzado a utilizar una construcción que codifica para una fusión entre la proteína verde fluorescente y dos proteínas ribosomales diferentes (L9 y L23, Chen y Huang, 2001) como forma de caracterizar el transporte y los destinos finales de estas proteínas al ser

transfectadas a neuronas en cultivo. Así mismo, se piensa inyectar los ARNm codificantes para estas proteínas de fusión en la célula de Mauthner, con el fin de poner en evidencia el tráfico selectivo de ribosomas hacia el axón y las placas periaxoplásmicas.

### **3. Función de las placas periaxoplásmicas**

La capacidad de síntesis de proteínas por parte de las PARPs tiene que ser demostrada directamente. Los resultados experimentales presentados indican que los componentes necesarios para sintetizar proteínas se encuentran localizados en estos dominios, pero todavía no conocemos cuáles son las proteínas sintetizadas por ellos. Para demostrar que estos dominios sintetizan proteínas pensamos realizar experimentos clásicos de “pulse-chase” y autoradiografía sobre axones *in toto*, como forma de correlacionar el sitio de incorporación de aminoácidos a proteínas con las placas periaxoplásmicas.

También disponemos de construcciones codificantes para híbridos entre GFP y actina (Bassell y cols., 1998). Pensamos utilizar los mismos para demostrar que estos dominios son capaces de traducir ARNm específicos exógenos dirigidos hacia esta estructura.

### **4. Regulación de la actividad de síntesis proteica en el dominio axonal.**

La expresión de proteínas en estas regiones axonales tiene que ser regulada de alguna forma. En condiciones fisiológicas, las señales moduladoras podrían llegar desde varias direcciones como el soma neuronal,

la sinapsis, el entorno axonal inmediato o desde el exterior celular, principalmente la glía circundante. Para resolver este tipo de incógnitas se debe mejorar de alguna manera el modelo de estudio, ya que las cantidades son, como se habrá notado, insuficientes para la mayoría de estudios bioquímicos.

Koenig posee resultados preliminares que relacionaban los niveles de AMP cíclicos con la capacidad de síntesis proteica axonal (comunicación personal). A su vez, se ha demostrado que la modulación de la actividad de síntesis de proteínas en axones en crecimiento regula la dirección y tamaño de dichas prolongaciones (Campbell y Holt, 2002). Por otro lado, en etapas embrionarias, axones que se encuentran en crecimiento activo traducen localmente el receptor de efrinas en respuesta a señales extracelulares de la placa del piso del tubo neural (Brittis y cols., 2002). Estas observaciones indican la posibilidad de estudiar mediante estos métodos u otros, la modulación de la actividad sintética de las placas periaxoplásmicas.

## **5. Formación de las placas periaxoplásmicas en el proceso de diferenciación neuronal.**

El hecho de que estas estructuras ha sido caracterizadas en animales adultos genera inmediatamente la pregunta que concierne al origen de las mismas. ¿En que momento del desarrollo y diferenciación de una neurona comienzan a organizarse?, ¿cuáles serían sus precursores? ¿cuál es la relación que guardan las partículas ribonucleoprotéicas encontradas en axones no diferenciados con estas estructuras?. Las aproximaciones a tomar para resolver estas preguntas tendrán que ver con observar la distribución de los ribosomas durante la diferenciación axonal. Para ello se tendrá que

perfeccionar los métodos de extracción de axones actualmente usados, ya que los mismos son buenos para extraer axones de calibre regular, pero son poco efectivos para axones delgados como los que recién comienzan a desarrollarse.

Una aproximación alternativa podría ser la microinyección de colorantes fluorescentes para ácidos nucleicos en neuronas en desarrollo para observar los acúmulos de ácidos nucleicos en distintos momentos del crecimiento axonal. Este tipo de aproximación ha sido muy útil para medir oscilaciones del ión calcio y crecimiento axonal *in vivo* en el pez zebra (Finley y cols., 2001; Fetcho y cols., 1998, Jontes y cols., 2000).

## **6. Futuro de la temática estudiada.**

Históricamente, los trabajos experimentales que apoyan la existencia de síntesis proteica axonal datan de la década de 1960, y han sido realizados principalmente por un grupo de investigadores que hoy en día han resumido sus hallazgos (incluyendo los obtenidos en la presente tesis) en revistas de alto impacto (Koenig and Giuditta 1999, Alvarez y cols., 2000, Giuditta y cols., 2002). Como consecuencia de la aceptación creciente de los mismos el núcleo de investigadores dedicados al tema se ha multiplicado en los últimos 5 a 10 años. Entre los más destacados se encuentran el grupo dirigido por Eric Kandel en Columbia (Martin, y cols., 1997), el grupo de Cristine Holt en Cambridge (Campbell y cols., 2001), el grupo de John Flanagan en Harvard (Britis & Flanagan, 2002), y el grupo de Mu Ming Poo en Berkeley (Zhang & Poo, 2001). Estos investigadores, utilizando diferentes modelos, han aportado nuevas evidencias sobre la existencia y significado funcional de la síntesis

proteica en los axones de invertebrados y vertebrados. Desde nuestro punto de vista todos estos aportes, comienzan a dar un nuevo impulso al tema y están generando un punto de inflexión en la opinión sobre la existencia de maquinaria traduccional en el territorio citoplásmico axonal. Nuevas generaciones considerarán la información hasta aquí generada desde un punto de vista diferente al que fue tomado en esta tesis, utilizando nuevos paradigmas de estudio o motivados por preguntas que provengan de distintas interrogantes sobre la biología de la neurona.

La presencia de maquinaria de síntesis de proteínas endógena en axones genera una nueva perspectiva para futuros estudios sobre la biología y patología de las neuronas. Como se sugiere en esta tesis y han observado otros investigadores, el crecimiento, la diferenciación, el mantenimiento, la plasticidad y patología de los axones debe ser observada en el contexto de mecanismos locales que permitan respuestas semi-autónomas frente a desafíos locales. Este nuevo marco de referencia abre puertas para diferentes aproximaciones experimentales que intenten mejorar el entendimiento de la biología celular neuronal.

Una de las preguntas más intrigantes concernientes a la síntesis de proteínas en territorio axonal se centra en los posibles mecanismos de regulación localizados de dicha actividad. Los mismos no estarán limitados únicamente al soma neuronal como fuente exclusiva de los ARN axonales, ya que las influencias extracelulares locales, proveniente de la interacción con glías o distintos tipos de contactos sinápticos, durante la vida de la neurona podría afectar la traducción local de distintos ARNm y a su vez interaccionar retrógradamente con el soma neuronal.

## REFERENCIAS GENERALES.

Alvarez J, Torres JC (1985) Slow axoplasmic transport: a fiction? *J. Theor. Biol.* 112: 627-51.

Alvarez, J. (1992) Maintenance of the axoplasm: can neurons accord with the accepted notions? *Neurosci. Lett.* 144: 1–3.

Alvarez, J. et al. (2000). Protein synthesis in axons and terminals: significance for maintenance, plasticity and regulation of phenotype. With a critique of slow transport theory. *Prog. Neurobiol.* 62, 1–62.

Aronov S, Aranda G, Behar L, Ginzburg I. (2002). Visualization of translated tau protein in the axons of neuronal P19 cells and characterization of tau RNP granules. *J. Cell. Sci.* 115: 3817-27.

Bassell GJ, Singer RH, Kosik KS. (1994). Association of poly(A) mRNA with microtubules in cultured neurons. *Neuron* 12: 571-82.

Bassell GJ, Zhang H, Byrd AL, Femino AM, Singer RH, Taneja KL, Lifshitz LM, Herman IM, Kosik KS. (1998). Sorting of beta-actin mRNA and protein to neurites and growth cones in culture. *J. Neurosci.* 18: 251-65.

Beaumont V, Zhong N, Fletcher R, Froemke RC, Zucker RS. (2001) Phosphorylation and local presynaptic protein synthesis in calcium- and calcineurin-dependent induction of crayfish long-term facilitation. *Neuron.* 32: 489-501.

Beddoe T and Lithgow T (2002). Delivery of nascent polypeptides to the mitochondrial surface. *Biochim. Biophys. Acta* 1592: 35– 39.

Benech C, Sotelo JR Jr, Menendez J, Correa-Luna R. (1982) Autoradiographic study of RNA and protein synthesis in sectioned peripheral nerves. *Exp. Neurol.* 76: 72-82.

Black MM, Lasek RJ. (1986). Slow components of axonal transport: two cytoskeletal networks. *J. Cell. Biol.* 86: 616-23.

Bleher R, Martin R. (2001) Ribosomes in the squid giant axon. *Neuroscience* 107: 527-34.

Bondy SC, Purdy JL. (1975) Migration of ribosomes along the axons of the chick visual pathway. *Biochim Biophys Acta.* 390: 332-41.

Brittis PA, Lu Q, Flanagan JG (2001). Axonal protein synthesis provides a mechanism for localized regulation at an intermediate target. *Cell* 110: 223-35.

Brown SS. (1999). Cooperation between microtubule- and actin-based motor proteins. *Annu. Rev. Cell Dev. Biol.* 15: 63-80.

Burack MA, Silverman MA, Banker G. (2000) The role of selective transport in neuronal protein sorting. *Neuron.* 26: 465-72.

Campbell DS, Holt CE. (2001) Chemotropic responses of retinal growth cones mediated by rapid local protein synthesis and degradation. *Neuron* 32:1013-26.

Casadio A, Martin KC, Giustetto M, Zhu H, Chen M, Bartsch D, Bailey CH, Kandel ER. (1999). A transient, neuron-wide form of CREB-mediated long-term facilitation can be stabilized at specific synapses by local protein synthesis. *Cell.* 99: 221-37.



Chen D, Huang S. (2001). Nucleolar components involved in ribosome biogenesis cycle between the nucleolus and nucleoplasm in interphase cells. *J Cell Biol.* 153: 169-76.

Chun JT, Gioio AE, Crispino M, Eyman M, Giuditta A, Kaplan BB. (1997). Molecular cloning and characterization of a novel mRNA present in the squid giant axon. *J. Neurosci. Res.* 49: 144-53.

Chun JT, Gioio AE, Crispino M, Giuditta A, Kaplan BB. (1996). Differential compartmentalization of mRNAs in squid giant axon. *J. Neurochem.* 67: 1806-12.

Chun JT, Gioio AE, Crispino M, Giuditta A, Kaplan BB. (1995) Characterization of squid enolase mRNA: sequence analysis, tissue distribution, and axonal localization. *Neurochem. Res.* 20: 923-30.

Cutillo V, Montagnese P, Gremo F, Casola L, Giuditta A. (1983). Origin of axoplasmic RNA in the squid giant fiber. *Neurochem. Res.* 8: 1621-34.

Dixon AK, Richardson PJ, Lee K, Carter NP, Freeman TC. (1998) Expression profiling of single cells using 3 prime end amplification (TPEA) PCR. *Nucleic Acids Res.* 26: 4426-31.

Edstrom A, Sjostrand J. (1969) Protein synthesis in the isolated Mauthner nerve fibre of goldfish. *J. Neurochem.* 16: 67-81.

Edstrom A, Edstrom JE, Hokfelt T. (1969) Sedimentation analysis of ribonucleic acid extracted from isolated Mauthner nerve fibre components. *J. Neurochem.* 16: 53-66.

Eng H, Lund K, Campenot RB. (1999). Synthesis of beta-tubulin, actin, and other proteins in axons of sympathetic neurons in compartmented cultures. *J. Neurosci.* 19: 1-9.

De Matteis MA, Morrow JS. (1998) The role of ankyrin and spectrin in membrane transport and domain formation. *Curr. Opin. Cell Biol.* 10: 542-9.

Fetcho JR, Cox KJ, O'Malley DM. (1998). Monitoring activity in neuronal populations with single-cell resolution in a behaving vertebrate. *Histochem. J.* 30: 153-67.

Finley KR, Davidson AE, Ekker SC. (2001) Three-color imaging using fluorescent proteins in living zebrafish embryos. *Biotechniques.* 31: 66-70, 72.

Forgue, S.T. and Dahl, J.L. (1978) The turnover of tubulin in rat brain. *J. Neurochem.* 31, 1289–1297.

Frankel RD, Koenig E. (1978). Identification of locally synthesized proteins in proximal stump axons of the neurotomized hypoglossal nerve. *Brain Res.* 141: 67-76.

Gaete J, Kameid G, Alvarez J. (1998). Regenerating axons of the rat require a local source of proteins. *Neurosci Lett.* 251: 197-200.

Gardiol A, Racca C, Triller A (1999). Dendritic and postsynaptic protein synthetic machinery. *J. Neurosci.* 19:168-79.

Geraerts WP, Giuditta A, Kaplan BB, van Minnen J. (2002) Protein synthesis in synaptosomes: a proteomics analysis. *J. Neurochem.* 81: 735-44.

Gioio AE, Chun JT, Crispino M, Capano CP, Giuditta A, Kaplan BB. (1994). Kinesin mRNA is present in the squid giant axon. *J. Neurochem.* 63: 13-8.

Giuditta A, Metafora S, Felsani A, Del Rio A. (1977). Factors for protein synthesis in the axoplasm of squid giant axons. *J. Neurochem.* 28: 1393-5.

Giuditta A, Cupello A, Lazzarini G. (1980). Ribosomal RNA in the axoplasm of the squid giant axon. *J. Neurochem.* 34: 1757-60.

Giuditta A, Menichini E, Perrone Capano C, Langella M, Martin R, Castigli E, Kaplan BB. (1991). Active polysomes in the axoplasm of the squid giant axon. *J. Neurosci. Res.* 28:18-28

Giuditta A, Kaplan BB, van Minnen J, Alvarez J, Koenig E. (2002) Axonal and presynaptic protein synthesis: new insights into the biology of the neuron. *Trends Neurosci.* 25: 400-4.

Goldstein LS, Yang Z. (2000) Microtubule-based transport systems in neurons: the roles of kinesins and dyneins. *Annu. Rev. Neurosci.* 23: 39-71.

Hemminki, K. (1973) Turnover of actin in rat brain. *Brain Res.* 57, 259–260

Hesketh JE, Pryme IF. (1991) Interaction between mRNA, ribosomes and the cytoskeleton. *Biochem. J.* 277: 1-10

Hirokawa N. (1998) Kinesin and dynein superfamily proteins and the mechanism of organelle transport. *Science* 279: 519-26.

Hovland R, Hesketh JE, Pryme IF (1996) The compartmentalization of protein synthesis: importance of cytoskeleton and role in mRNA targeting. *Int. J. Biochem. Cell Biol.* 28: 1089-105.

Ingoglia NA, Giuditta A, Zanakis MF, Babigian A, Tasaki I, Chakraborty G, Sturman JA. (1983). Incorporation of 3H-amino acids into proteins in a partially purified fraction of axoplasm: evidence for transfer RNA-mediated, post-translational protein modification in squid giant axons. *J. Neurosci.* 3: 2463-73.

Jontes JD, Buchanan J, Smith SJ. (2000) Growth cone and dendrite dynamics in zebrafish embryos: early events in synaptogenesis imaged in vivo. *Nat. Neurosci.* 3: 231-7.

Karcher RL, Deacon SW, Gelfand VI. (2002) Motor-cargo interactions: the key to transport specificity. *Trends Cell Biol.* 1: 21-27.

Keenan RJ, Freymann DM, Stroud RM, Walter P. (2001) The signal recognition particle. *Annu Rev Biochem.* 70: 755-75.

Koenig E. (1965) Synthetic mechanisms in the axon. I. RNA in myelin-free axons of the cat. *J. Neurochem.* 12: 357-61.

Koenig E. (1979) Ribosomal RNA in Mauthner axon: implications for a protein synthesizing machinery in the myelinated axon. *Brain Res.* 174: 95-107.

Koenig, E. (1984) Protein síntesis in axons. In *Handbook of Neurochemistry* (Vol. 7) (Lajtha, A. ed.), pp. 315–340. Plenum Press.

Koenig E, Repasky E. (1985). A regional analysis of alpha-spectrin in the isolated Mauthner neuron and in isolated axons of the goldfish and rabbit. *J. Neurosci.* 5: 705-14.

Koenig E. (1986) Isolation of native Mauthner cell axoplasm and an analysis of organelle movement in non-aqueous and aqueous media. *Brain Res.* 398: 288-97.

Koenig E. (1989). Cycloheximide-sensitive [<sup>35</sup>S]methionine labeling of proteins in goldfish retinal ganglion cell axons in vitro. *Brain Res.* 481: 119-23.

Koenig E (1991) Evaluation of local synthesis of axonal proteins in the goldfish Mauthner cell axon and axons of dorsal and ventral roots of the rat in vitro. *Mol. Cell Neurosci.* 2: 384–394.

Koenig E, Martin R. (1996). Cortical plaque-like structures identify ribosome-containing domains in the Mauthner cell axon. *J. Neurosci.* 16:1400-11

Koenig, E. and Giuditta, A. (1999) Protein synthesizing machinery in the axon compartment. *Neuroscience* 89, 5–15.

Krichevsky AM, Kosik KS (2001) Neuronal RNA Granules: A Link between RNA Localization and Stimulation-Dependent Translation. *Neuron*, 32: 683–696.

Kruse C, Jaedicke A, Beaudouin J, Bohl F, Ferring D, Guttler T, Ellenberg J, Jansen RP. 2002. Ribonucleoprotein-dependent localization of the yeast class V myosin Myo4p. *J. Cell Biol.* 159: 971-82.

Langford GM. (2002). Myosin-V, a versatile motor for short-range vesicle transport. *Traffic.* 3: 859-65.

Mallardo M, Deitinghoff A, Muller J, Goetze B, Macchi P, Peters C, Kiebler M. (2003). Isolation and characterization of Staufen-containing ribonucleoprotein particles from rat brain. *Proc. Natl. Acad. Sci.* 100: 2100–2105.

Markesich D. C., Gajewski K. M., Nazimiec M. E. and Beckingham K. (2000) bicaudal encodes the *Drosophila* beta NAC homolog, a component of the ribosomal translational machinery. *Development* 127: 559–572.

Martin KC, Casadio A, Zhu H, Yaping E, Rose JC, Chen M, Bailey CH, Kandel ER. (1997). Synapse-specific, long-term facilitation of aplysia sensory to motor synapses: a function for local protein synthesis in memory storage. *Cell.* 91: 927-38.

Martin R, Fritz W, Giuditta A. (1989) Visualization of polyribosomes in the postsynaptic area of the squid giant synapse by electron spectroscopic imaging. *J. Neurocytol.* 18: 11-8.

Mohr E, Fehr S, Richter D. (1991). Axonal transport of neuropeptide encoding mRNAs within the hypothalamo-hypophyseal tract of rats. *EMBO J.*10:2419-24.

Muslimov IA, Titmus M, Koenig E, Tiedge H. 2002. Transport of Neuronal BC1 RNA in Mauthner Axons. *J. Neurosci.* 22: 4293-301.

Nixon, R. (1998). The slow axonal transport of cytoskeletal proteins. *Curr. Opin. Cell Biol.* 10: 87–92.

Ohashi S, Koike K, Omori A, Ichinose S, Ohara S, Kobayashi S, Sato T, and Anzai K. (2002). Identification of mRNA/Protein (mRNP) Complexes Containing Pur  $\alpha$ , mStaufen, Fragile X Protein, and Myosin Va and their Association with Rough Endoplasmic Reticulum Equipped with a Kinesin Motor. *J. Biol. Chem.* 40: 37804–37810.

Olink-Coux M, Hollenbeck PJ. (1996). Localization and active transport of mRNA in axons of sympathetic neurons in culture. *J. Neurosci.* 16:1346-58

Oleynikov Y, Singer RH. (1998) RNA localization: different zipcodes, same postman? *Trends Cell Biol.* 10: 381-3.

Pannese, E. and Ledda, M. (1991) Ribosomes in myelinated axons of the rabbit spinal ganglion neurons. *J. Submicrosc. Cytol. Pathol.* 23, 33–38

Perrone-Capano C, Giuditta A, Castigli E, Kaplan BB. (1987). Occurrence and sequence complexity of polyadenylated RNA in squid axoplasm. *J. Neurochem.* 49: 698-704.

Rospert S, Dubaquier Y, Gautschi M. Nascent-polypeptide-associated complex. *Cell Mol Life Sci.* 59: 1632-1639.

Safaei R and Fischer I (1990). Turnover of cytoskeletal proteins in vivo. *Brain Research*, 533: 83-90.

Schacher S, Wu F. (2002). Synapse formation in the absence of cell bodies requires protein synthesis. *J. Neurosci.* 22: 1831-1839.

Sotelo JR, Benech CR, Kun A. (1992) Local radiolabeling of the 68 kDa neurofilament protein in rat sciatic nerves. *Neurosci Lett.* 144: 174-6.

Sotelo JR, Kun A, Benech JC, Giuditta A, Morillas J, Benech CR. (1999) Ribosomes and polyribosomes are present in the squid giant axon: an immunocytochemical study. *Neuroscience.* 90: 705-715.

Sotelo Silveira, JR (1998). Búsqueda de ARNm neuroespecíficos en axones de vertebrados. Tesis de Maestría, PEDECIBA.

Spencer GE, Syed NI, van Kesteren E, Lukowiak K, Geraerts WP, van Minnen J. (2000). Synthesis and functional integration of a neurotransmitter receptor in isolated invertebrate axons. *J. Neurobiol.* 44: 72-81.

Steward O, Worley PF. (2001) A cellular mechanism for targeting newly synthesized mRNAs to synaptic sites on dendrites. *Proc. Natl. Acad. Sci. U S A.* 98: 7062-7068.

Tobias GS, Koenig E. (1975) Axonal protein synthesizing activity during the early outgrowth period following neurotomy. *Exp Neurol.* 49: 221-234

Tohda C, Sasaki M, Konemura T, Sasamura T, Ito M, Kuraishi Y (2001). Axonal transport of VR1 capsaicin receptor mRNA in primary afferents and its participation in inflammation-induced increase in capsaicin sensitivity. *J. Neurochem* 76: 1628– 35.

van Minnen, J. (1994) RNA in the axonal domain: a new dimension in neuronal functioning? *Histochem. J.* 26: 377–391

Wang L, Ho CL, Sun D, Liem RK, Brown A. (2000) Rapid movement of axonal neurofilaments interrupted by prolonged pauses. *Nat Cell Biol.* 2: 137-41.

Weiner OD, Zorn AM, Krieg PA, Bittner GD. (1996). Medium weight neurofilament mRNA in goldfish Mauthner axoplasm. *Neurosci. Lett.* 213: 83-6.

Wool, I. (1996). Extraribosomal functions of ribosomal proteins. *Trends Biochem. Sci.* 21: 164–165.

Zelena J. (1972) Ribosomes in myelinated axons of dorsal root ganglia. *Z Zellforsch Mikrosk Anat.* 124: 217-29.

Zimmermann RA. (2003). The double life of ribosomal proteins. *Cell.* 115: 130-132.

Zheng JQ, Kelly TK, Chang B, Ryazantsev S, Rajasekaran AK, Martin KC, Twiss JL. (1999) A functional role for intra-axonal protein synthesis during axonal regeneration from adult sensory neurons. *J. Neurosci.* 21: 9291-9303.